10-9-2020 1:30 PM

Metabolic Syndrome Impairs Cerebrovascular Tone and Behaviour in Obese Zucker Rats

Brayden D. Halvorson, *The University of Western Ontario*

Supervisor: Frisbee, Jefferson C., *The University of Western Ontario*

A thesis submitted in partial fulfillment of the requirements for the Master of Science degree in Medical Biophysics

Abstract

Metabolic syndrome is associated with cerebrovascular disease and cognitive impairment. We determined vascular reactivity in middle cerebral arteries (MCA), and performed cognitive testing using an operant conditioning chamber (OCC) and Morris Water Maze (MWM). Male obese Zucker rats (OZR) were used to test the hypothesis that the pro-inflammatory environment present in the OZR impairs cerebrovascular tone regulation and is associated with neuroinflammation of the white matter and cognitive impairment. Dilation of MCA following challenge with acetylcholine was blunted, whereas constrictor responses were enhanced. Learning was impaired in the MWM and a shift in swim strategy towards increased allocentric navigation was observed. Few impairments were detected in the OCC tests or when white matter regions were examined for markers of neuroinflammation. These results suggest that the reactivity of MCA in OZR is altered with MetS, and that this impairment is associated with cognitive dysfunction in the absence of white matter inflammation.

Keywords

Metabolic syndrome, cerebral circulation, rat models of metabolic syndrome, vascular tone regulation, mild cognitive impairment

Summary for Lay Audience

Metabolic syndrome is a cluster of conditions including increased blood pressure, high blood sugar, excess body fat around the waist, and abnormal cholesterol or triglycerides. It is a prevalent public health concern associated with elevated cardiovascular disease risk throughout the body. Impairments associated with this disease are particularly problematic when they affect the brain and lead to problems such as stroke (a blockage in an artery that supplies blood to the brain). Even in the absence of an acute event such as stroke, metabolic syndrome is strongly associated with impaired cognitive function and decreased quality of life. The work presented in this thesis aims to describe some of the changes occurring to the ability of blood vessels in the brain to alter their diameter which has implications in regulating blood flow. It also investigated if these changes are associated with cognitive impairment and inflammation in the brain using a rodent model of metabolic syndrome. Understanding these risk factors allows for better implementation of targeted therapeutic strategies aimed at ameliorating the regulation of blood flow in the brain and has the potential to improve current negative outcomes associated with metabolic syndrome.

Co-Authorship Statement

This thesis partially integrated a published book chapter into the introductory chapter.

- Brayden Halvorson and Jefferson Frisbee (2020). Cerebral Vascular Tone Regulation: Integration and Impact of Disease, in Basic and Clinical Understanding of Microcirculation, Kaneez Fatima Shad, Seyed Soheil Saeedi Saravi and Nazar Luqman Bilgrami (Editors), IntechOpen, DOI: 10.5772/intechopen.90404. Available from: https://www.intechopen.com/books/basic-and-clinical-understanding-of-microcirculation/cerebral-vascular-tone-regulation-integration-and-impact-of-disease.

Acknowledgments

I would to thank my supervisor Dr. Jefferson Frisbee for taking me into the lab and allowing me to learn under your guidance. Your mentorship and support has been incredible and I especially admire the collaborative approach you promote with other laboratories which has allowed me to learn a wide variety of techniques. It has been an absolute pleasure to learn in the Vulnerable Brain Lab led by Dr. Shawn Whitehead and the lab of Dr. Krishna Singh. I am especially thankful for the technical support, and kindness from Dr. Lynn Wang as well as the students making up these labs that has made coming into work fun and memorable. Thank you to my advisory committee of Dr. John McGuire, Dr. Shawn Whitehead, and Dr. Krishna Singh for your guidance and enthusiasm towards research. Finally, the work in this thesis was supported by sources of funding from the Canadian Institute of Health Research (CIHR), Natural Sciences and Engineering Research Council (NSERC), and Western Graduate Research Scholarship.

Table of Contents

Abbreviations

AA: arachidonic acid
ACh: acetylcholine
AKt: protein kinase B
ANOVA: analysis of variance
Anxa5: annexin V
A_{2A}: adenosine A_{2A} receptor
A_{2B}: adenosine A_{2B} receptor
Bk_{Ca}: large conductance calcium-activated potassium channels
cAMP: cyclic adenosine monophosphate
cGMP: cyclic guanylyl cyclase
COX-2: cyclooxygenase-2 (aka PTGS2: prostaglandin-endoperoxide synthase 2)
CxCr5: CXC motif receptor
CxCl4:CXC motif ligand 4
EDHF: endothelium dependent hyperpolarizing factor
eNOS: nitric oxide synthase 3
ET: endothelin
5-HT: 5-hydroxytryptamine
GFAP: glial fibrillary acidic protein
GLUT4: glucose transporter type 4
HDL: high-density lipoproteins
H_2O_2: hydrogen peroxide
IHC: immunohistochemistry
K_{ATP}: ATP-sensitive potassium channel
K_{IR}: inward-rectifier potassium channel
L-NAME: L-N^G-Nitroarginine methyl ester
LZR: lean Zucker rat
MAP: mean arterial pressure
MCA: middle cerebral artery
MCI: mild cognitive impairment
MetS: metabolic syndrome
MHCII: major histocompatibility complex II
MWM: Morris water maze
NADPH: nicotinamide adenine dinucleotide phosphate
NO: nitric oxide
OCC: operant conditioning chamber
OLETE: Otsuka Long-Evans Tokushima fatty
OZR: obese Zucker rat
$PaCO_2$: arterial partial pressure of carbon dioxide
PCO_2: partial pressure of carbon dioxide

PCR: polymerase chain reaction
PFA: paraformaldehyde
PGI_2: prostacyclin
PO_2: partial pressure of oxygen
PSS: physiological salt solution
Ptgs2: prostaglandin-endoperoxide synthase 2 (aka COX-2: cyclooxygenase 2)
qPCR: quantitative real-time PCR
ROS: reactive oxygen species
sGC: soluble guanylyl cyclase
SNP: sodium nitroprusside
SVCC: supraventricular corpus callosum
TEMPOL: 4-hydroxy-TEMPO
TgAPP21: transgenic rat model of Alzheimer disease; Fischer 344 homozygous for pathogenic hAPP with Swedish and Indiana mutations
TIA: transient ischemic attack
Tnf-1: tumor necrosis factor receptor 1
TNF-α: tumor necrosis factor
T2DM: type II diabetes mellitus
20-HETE: 20-hydroxyeicosatetraenoic acid
VSMC: vascular smooth muscle cell
Xdh: xanthine dehydrogenase

List of Tables

List of Figures

List of Appendices

Chapter 1

1 General Introduction

This chapter will present a description of the local mechanisms involved in the regulation of cerebral vascular tone, their integration with one another, how they can be compromised in disease and the resultant functional impairments in cognition. Although impairments to the regulation of cerebral vascular tone are not limited to conditions associated with metabolic syndrome (MetS) the discussion will focus on the impact of MetS and its associated risk factors in contributing to cerebrovascular disease leading to cognitive impairment.

1.1 Overview

1.1.1 Microcirculation and Homeostasis

All living cells require a mechanism that allows for the delivery and removal of metabolic substrates. Large organisms have developed cardiovascular systems made up of the heart, blood, and network of blood vessels that facilitate this process. Although each of these components is critical to the maintenance of homeostasis the most dynamic changes occur at the level of the microcirculation (arterioles, capillaries, venules) by adjusting resistance to flow and surface area for diffusion of metabolic substrates in order to maintain homeostasis.

1.1.2 The Cerebral Circulation

The brain has a high metabolic rate and thus requires a highly disproportional amount of blood flow. Although its only 2% of body weight, the brain is supplied by 15-20% of cardiac output (Cipolla, 2010), making it one of the most highly perfused organs in the

human body. This high metabolic rate coupled with its limited capacity for energy storage (Brown & Ransom, 2007) necessitates heavy reliance on oxidative metabolism and thus requires constant blood flow to maintain nutrient and oxygen supply, remove waste products, and maintain a state of cerebral metabolic homeostasis. Severe under perfusion can quickly result in unconsciousness (Van Lieshout *et al.*, 2003) and if prolonged, death (Smith *et al.*, 2011); while chronic mild under perfusion is associated with cognitive decline (Ng *et al.*, 2016). In addition to its highly regulated and consistent perfusion and metabolic rate, the cerebral circulation faces a unique challenge of being enclosed in the skull. This rigid structure prevents the volume expansion of tissue and extracellular fluid. Swelling within the skull from vasogenic edema, extracellular accumulation of fluid from a disruption of the blood-brain barrier (Michinaga & Koyama, 2015), leads to an increase in intracranial pressure which in turn can lead to neurologic complications or in more extreme cases death (Cipolla, 2010). The unique challenges of the cerebral circulation, including intolerance to a restriction of blood flow (ischemia) and edema, coupled with the paramount importance of maintaining constant nutrient and oxygen supply to cerebral tissue for cognitive processes creates a need for precise regulation of cerebral blood flow and therefore, the presence of redundant intrinsic mechanisms for its regulation. The anatomy of the brain vasculature ensures multiple routes for blood and oxygen delivery potentially allowing for perfusion even in cases of a blocked blood vessel (Gebremedhin *et al.*, 2014); however, acute regulation of flow is done primary by altering the diameter of blood vessels, and thus the resistance to flow. The major mechanisms of local regulation of vascular tone intrinsic to the cerebral vasculature include myogenic, shear, and metabolic based regulation. Although each mechanism has a discrete effect on vascular

tone the integration of the different contributors to determine an appropriate level of tone is much more difficult to discern, especially in the cerebral circulation. These complex interactions not only allow for highly accurate control of cerebral blood flow in addition to protecting vulnerable downstream capillaries from high pressures and flow rates that could otherwise lead to edema, but also introduce several potential areas for failure. The intimate interactions of the various mechanisms of regulation of flow mean that the failure of one mechanism has the potential to initiate a cascade of events that results in inappropriate regulation of flow. As such abnormal execution of vascular tone regulation may form the basis of vascular pathologies (El-Yazbi & Abd-Elrahman, 2017).

1.1.3 Metabolic Syndrome

MetS is a pathology having a significant vascular component associated with impaired cerebral vascular tone regulation. The criteria for a clinical diagnosis of MetS as defined by the American Heart Association and National Heart, Lung, and Blood Institute is having any three of the following five criteria: elevated waist circumference (men ≥102 cm, women ≥88 cm), elevated triglycerides (≥150 mg/dL) reduced HDL cholesterol (men <40 mg/dL, women <50 mg/dL), elevated blood pressure (≥130/≥85 mmHg), and elevated fasting glucose (≥100 mg/dL). With the spreading of Western lifestyle across the globe, MetS has become a global problem and is contributing to decreased quality of life and increased economic burden (Boutayeb *et al.*, 2013; De Carvalho Vidigal *et al.*, 2013; Fu & Prasad, 2014). Thus an understanding of how it alters the cerebral circulation is crucial. MetS is categorized by a collection of metabolic risk factors including obesity, hypertension, atherogenic dyslipidemia, and impaired glycemic control creating a pro-oxidant pro-inflammatory environment that raises the risk of developing impaired vascular

structures and function (Shin *et al.*, 2013; Donley *et al.*, 2014; Ferdinand *et al.*, 2014; DeVallance *et al.*, 2015). These impairments are particularly problematic when they affect the cerebral circulation and lead to cerebrovascular pathologies such as stroke or transient ischemic attack (TIA) due to the detrimental consequences associated with such events. However, cognitive impairments are not limited to individuals that have experienced an acute ischemic event since even in their absence MetS is strongly associated with impaired cognitive function and decreased quality of life (Rosenberg, 2009; Yates *et al.*, 2012; Alfaro *et al.*, 2016; Tsai *et al.*, 2016). Therefore, preventing their occurrence by protecting the cerebrovasculature from functional and structural decline is paramount.

1.2 Cerebrovascular Tone Regulation

1.2.1 Myogenic Mechanism

The myogenic mechanism, which was first described by Bayliss, is an intrinsic property of the vascular smooth muscle to respond to changes in intravascular pressure which is independent of other mechanisms of tone regulation including neural, metabolic, and hormonal influences (Bayliss, 1902). The intrinsic nature of the myogenic response is supported by its existence in arteries and arterioles that have been sympathetically denervated and had their endothelium removed (Schubert *et al.*, 2002) thus leaving only the vessel itself to initiate and execute the response. The prototypical response of the vascular smooth muscle in response to an increase in intraluminal pressure is initial distension quickly followed by a constriction with the opposite occurring in situations of decreased intraluminal pressure and tension of the VSMC (Davis & Sikes, 1990). The myogenic response has several physiological roles including establishing and maintaining basal vascular tone (some degree of constriction) so that resistance may be increased or

decreased by vasoconstrictors or vasodilators respectively, in order to regulate tissue perfusion. The establishment and maintenance of this partially constricted state in a pressurized vessel is referred to as myogenic tone. Additionally, myogenic tone has a role in flow and pressure regulation. It functions by constricting to drop the pressure that reaches the downstream capillaries and protect them from edema or vascular remodeling associated with hypertension in the capillaries (Davis & Hill, 1999; Roman & Dokkum, 2014). Equally important as protecting from hypertension is the ability of the vasculature to promote flow during low pressure by dilating. This ability to alter diameter over a range of pressures is referred to as myogenic reactivity. Beyond the local implications for the regulation of vascular tone, resistance to flow also has implications for systemic blood pressure since mean arterial pressure (MAP) is the product of total peripheral resistance and cardiac output. This relationship illustrates the system-wide implications of accurate vascular tone regulation. While the myogenic response is present in a variety of vessels (arterioles, veins, lymphatic vessels) (Von der Weid, 2013) the aforementioned functions of the myogenic response are particularly important in the cerebral circulation due to the catastrophic outcomes associated with under or over perfusion including unconsciousness and edema respectively. The most prominent myogenic response is found in the cerebral circulation with arterioles (resistance vessels) having the most pronounced response (Cipolla, 2010). It should also be noted that the large arteries feeding the brain have a greater contribution in regulating vascular resistance in the cerebral circulation compared to other vascular beds, again providing evidence for the importance of regulating tone in the cerebral circulation. A phase model of arterial myogenic behaviour is commonly used to describe the response over a range of pressures (Figure 1). In the first phase, there is an

initial development of myogenic tone at approximately 40-60 mmHg with increasing pressure up to that point causing passive distension. There is then a phase of myogenic reactivity in the pressure range of ~60-140 mmHg. In this range of intralumenal pressure, where the myogenic tone has already been established, increases in pressure within this range leads to a stretch of VSMC that initiates, a combination of calcium-dependent and -independent intracellular signaling pathways that leads to cell shortening (Figure 2). Finally, there is a phase of forced dilation at transmural pressures greater than approximately 140 mmHg (Osol *et al.*, 2002). This process results in a loss of myogenic tone, and thus an increase in vessel diameter and a rapid increase in wall tension. Although the name implies a degree of passiveness in the process, forced dilation is likely an active vasodilation involving potassium channels, nitric oxide (NO), and or reactive oxygen species (ROS), which are activated to induced dilation in order to protect the arterial wall from damage associated with high intraluminal pressure (Jaggar *et al.*, 2000; Paterno *et al.*, 2000). For example hydrogen peroxide can induce dilation by hyperpolarizing vascular smooth muscle (Sato *et al.*, 2003). If the pressure is reduced to within the myogenic reactivity range reestablishment of tone is generally observed.

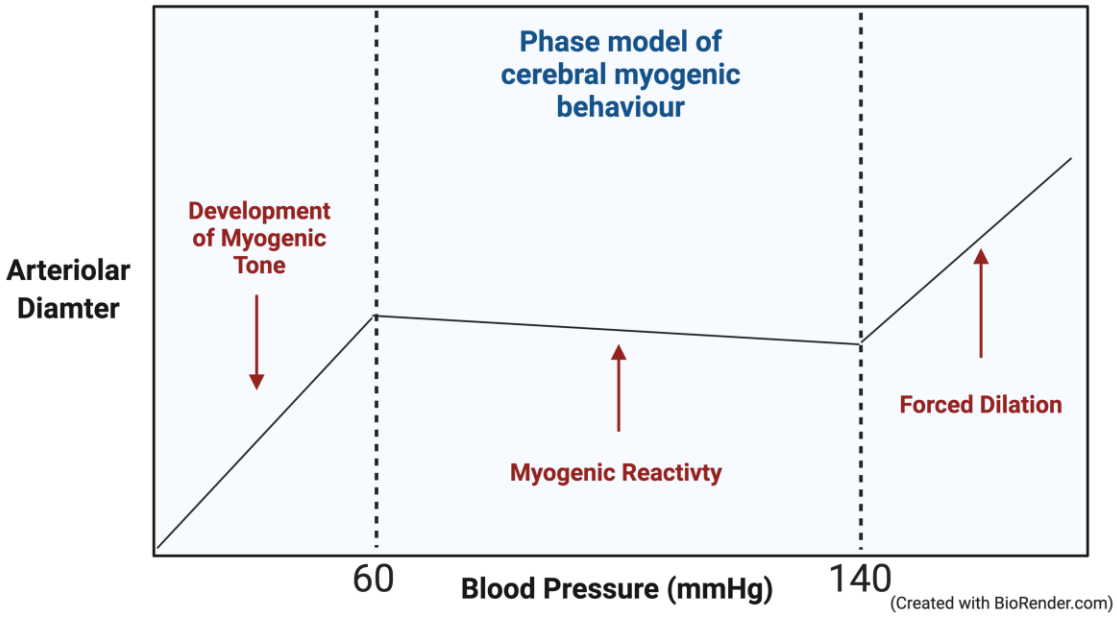

Figure 1: A phase model of cerebral myogenic behaviour.

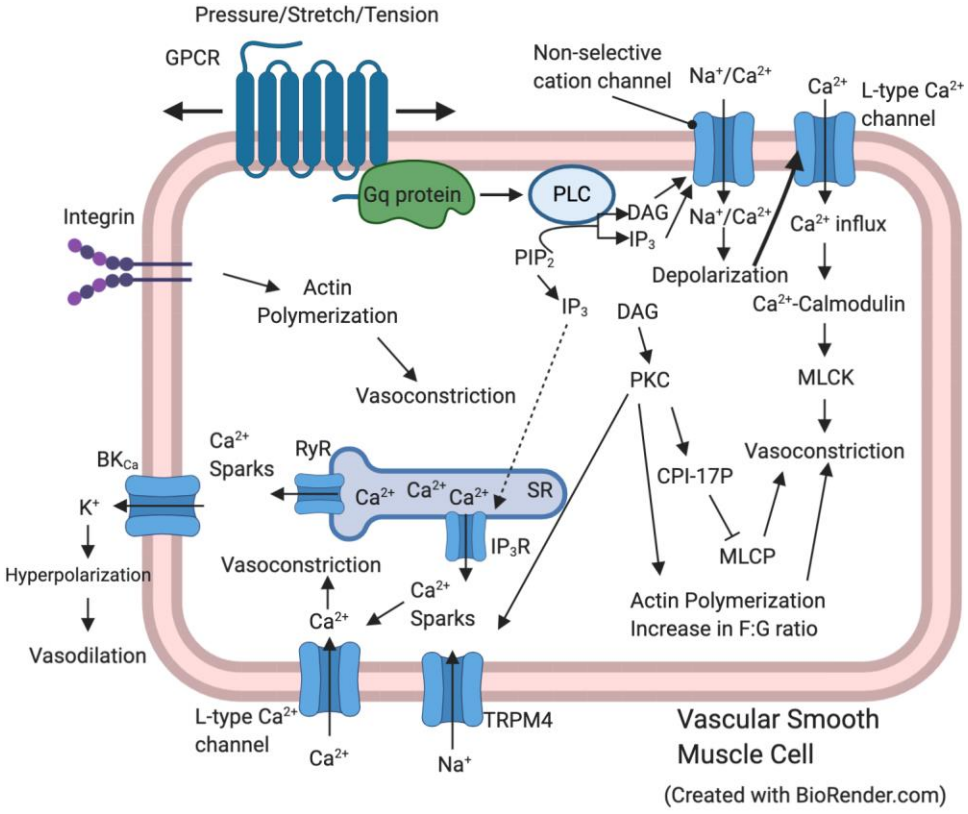

Figure 2: Molecular mechanisms of myogenic reactivity

Abbreviations: BK_{Ca}, large conductance Ca^{2+}-activated K^+ channel; CPI-17, 17-kDa protein kinase C-potentiated inhibitory protein; DAG, diacylglycerol; GPCR, G protein-coupled receptor; IP_3, inositol triphosphate; IP_3R, inositol triphosphate receptor; MLCK, myosin light chain kinase; MLCP, myosin light chain phosphatase; $MYPT_1$, myosin phosphate targeting subunit; PIP_2, phosphatidylinositol bisphosphate; PKC, protein kinase C; PLC, phospholipase C; RyR, ryanodine receptor, SR, sarcoplasmic reticulum; $TRPM_4$, transient receptor potential melastatin 4.

1.2.2 Response to Flow (Shear Stress)

An increase in flow leads to an increase in a frictional force known as shear that is detected

by the endothelial cells lining the vessel lumen. As such, the magnitude of the shear force is proportional to blood flow. Shear stimulates physiologically important responses in the cerebral vasculature such as encouraging reperfusion after ischemia, aiding in the hyperemic response to increased metabolic demand, and perhaps protection of downstream capillaries from edema and structural damage. The endothelium which can sense changes in shear, has been reported to release constrictor, and dilator factors that act on the adjacent layers of vascular smooth muscle cells (VSMC) to produce a level of tone accounting for opposing processes (if any). It is generally accepted that in the peripheral circulation flow leads to dilation; however, in the cerebral circulation, the response is more controversial with both constriction and dilation being reported. These opposing observations may be because of a variety of factors including the area of the brain studied, the preparation used, or because of interactions with other mechanisms affecting cerebral vascular tone. Within the cerebral circulation, the vertebrobasilar systems appear to elicit flow-mediated dilation, as measured in rats and mice (Koller & Toth, 2012) and humans (Fujii *et al.*, 1991). The increase in flow is sensed by the endothelium, which initiates a negative feedback mechanism in an attempt to decrease the shear stress by dilating. Shear-induced dilation is largely endothelium-dependent and is at least partially mediated by nitric oxide (NO) (Thorin-Trescases & Bevan, 1998). In endothelial cells, NO is synthesized by the enzyme nitric oxide synthase 3 (eNOS) which catalyzes the reaction L-arginine + O_2 + NADPH → L-citrulline + NO. NO production by the endothelium can also be induced by other stimuli other than shear stress, such as acetylcholine (ACh) or bradykinin. Both increase endothelial cell intracellular Ca^{2+} since eNOS is Ca^{2+}-dependent, and principally activated by Ca^{2+}-dependent binding of calmodulin. NO diffuses from endothelial cells to

neighboring VSMC where it binds to and activates soluble guanylyl cyclase (sGC), leading to increased accumulation of guanosine 3',5'-cyclic monophosphate (cGMP), which leads to relaxation of VSMC (Figure 3).

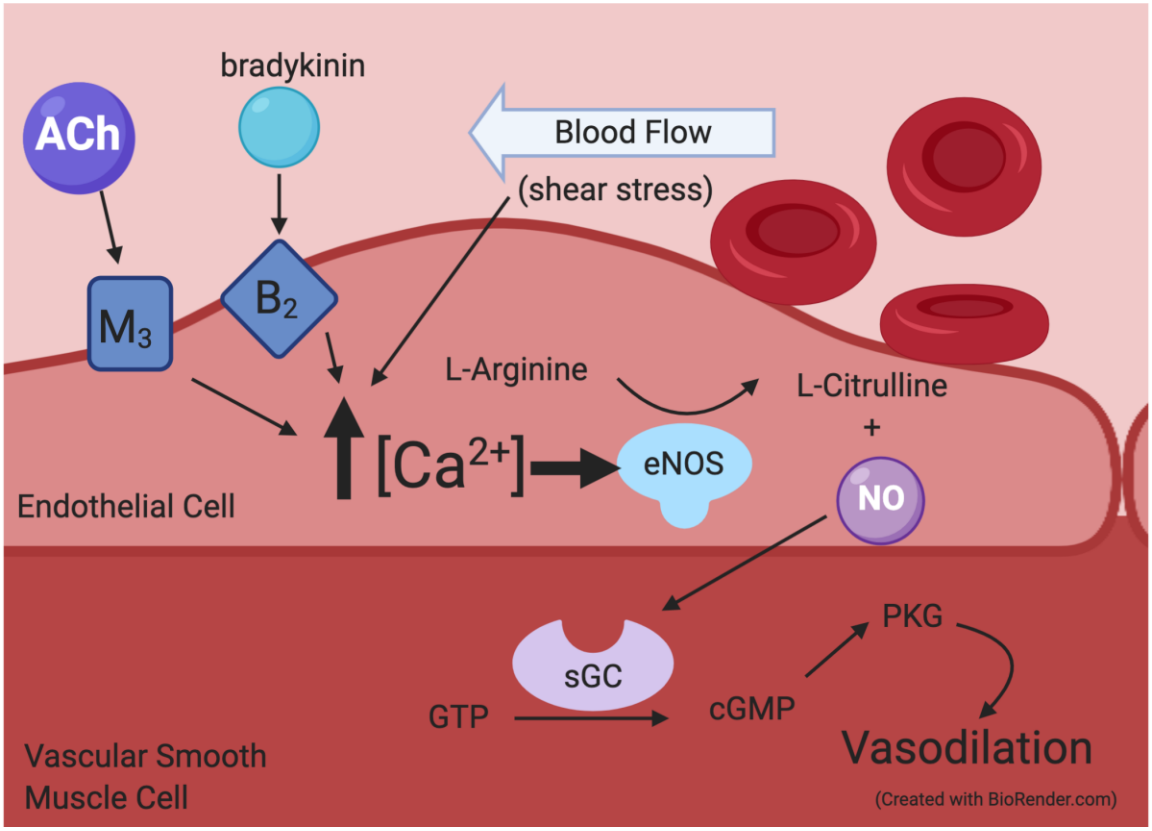

Figure 3: Endothelial nitric oxide production.

Abbreviations: ACh, acetylcholine; B_2, bradykinin receptor B_2; cGMP, cyclic guanosine monophosphate; eNOS, nitric oxide synthase 3; GTP, guanosine triphosphate; M, muscarinic acetylcholine receptor; NO, nitric oxide; PKG, protein kinase G, sGC, soluble guanylate cyclase.

1.2.3 Flow and Pressure

In a physiological setting multiple inputs are being processed by the cerebral vasculature leading to the generation of a certain level of tone. Pressure and shear stress exerted by flowing blood are two mechanical stimuli that have been described to play a major role in

the regulation of vascular tone (Burnstock, 1985; Jones *et al.*, 1993). It is, therefore, important to consider their interaction when determining the resultant effect on vascular tone. At high pressures (approximately >80 mmHg) cerebral vessels tend to constrict in response to flow (Reich & Rusinek, 1989; Garcia-Roldan & Bevan, 1990, 1991; de Wit *et al.*, 1997). This biphasic response is further supported by findings from Garcia-Roldan and Bevan in isolated rabbit pial arterioles that constricted with flow rates from 0 to 20 uL/min at 90 mmHg but did not with the same flow at 60 mmHg (Garcia-Roldan & Bevan, 1991).

1.2.4 Metabolic Control

The mechanical stimuli of pressure and flow are generally thought to be important in setting the basal vascular tone so that metabolic influences are able to cause dilation or constriction depending on the needs of the cerebral tissue (Davis & Hill, 1999). Metabolic control of vascular resistance is of particular importance in the cerebral circulation since cerebral tissue is extremely intolerant to ischemia (Peterson *et al.*, 2011). As such, the cerebral circulation has a precise and highly localized coupling between the metabolic requirements of cerebral tissue and the magnitude of blood flow by controlling vascular resistance. There are numerous vasoactive metabolites that contribute to the control of cerebral vascular tone including adenosine, CO_2, O_2, and adenosine. Increasing concentrations of adenosine, and CO_2, along with decreased concentration of O_2 result in relaxation of VSM and dilation of cerebral resistance vessels. Each metabolite is associated with a cascade of events that ultimately either alters intracellular Ca^{2+} concentration or Ca^{2+} sensitivity of the VSMC and results in a change in vessel diameter. Although the effects of each metabolite have been well characterized, the relative importance of each along with their interaction with each other and other parameters of tone remains an area of further

investigation.

1.2.4.1 Adenosine

Adenosine is a naturally occurring nucleoside produced as a byproduct of ATP metabolism; thus, its accumulation signals a need for increased blood flow to match the metabolic activity. This relationship with metabolism has widely implicated adenosine in local regulation of cerebral vascular tone during functional hyperemia, ischemia, or whenever the partial pressure of oxygen becomes limited (Berne *et al.*, 1981; Bari *et al.*, 1998). Adenosine has direct effects on the vasculature (Ramkumar *et al.*, 2001; Tabrizchi & Bedi, 2001) that can both vasodilate and hyperpolarize VSMC (Ohta *et al.*, 2013). There are four distinct subtypes of adenosine receptors; however, the A_2 receptors, a member of the G protein-coupled receptor family appears to be of high importance in mediating vasodilation (Kusano *et al.*, 2010). Adenosine causes dilation in a concentration-dependent manner (Ngai & Winn, 1993) once bound to the A_2 receptors (particularly the A_{2A} subtype) by activation of adenylate cyclase (Anand-Srivastava *et al.*, 1982) and therefore, cyclic adenosine monophosphate (cAMP) (de Jong *et al.*, 2000) which reduces cytosolic calcium and leads to vasodilation. The opening of ATP-sensitive potassium channels (K_{ATP}) also occurs secondary to the increase in cAMP levels as a result of adenosine binding to its receptors on the cell membrane (Li & Puro, 2001). The contribution of opening K_{ATP} channels to dilation is likely substantial since during blockade of K_{ATP} channels with glibenclamide, adenosine-induced dilation was reduced by approximately 50% (Carter & Kanagy, 2002). Adenosine may also lead to endothelium-dependent dilation since A_{2A} receptors located on the endothelium mediate the release of NO. However, the contribution of the NO and the endothelium to adenosine-induced dilation is relatively minor, compared

to ACh-induced dilation for example, since the dose-response curve to adenosine had only a relatively small shift to the right after incubation with L-NAME or in the absence of endothelium (Prentice & Hourani, 2000). In addition to dilating the cerebral vasculature adenosine may also block vasoconstrictive signals in the parenchyma as evidenced by *in vitro* data from Gordon *et al*. (Gordon *et al.*, 2008). When adenosine receptors were blocked with theophylline, dilation was attenuated in response to arterial hypoxia (Morii *et al.*, 1987). Similarly, the competitive adenosine receptor antagonist aminophylline causes a 20-30% decrease in CBF and cerebral oxygen delivery in normoxia (Willie *et al.*, 2014*b*).

1.2.4.2 Carbon Dioxide

Similar to adenosine CO_2 tends to increase under conditions of increased metabolism without adequate flow to eliminate it from the area of production and thus its accumulation leads to dilation of the vasculature. High sensitivity to the partial pressure of CO_2 (PCO_2) is unique to the cerebral circulation (Ainslie *et al.*, 2005) causing approximately 3-6% increase and 1-3% decrease in flow *per* mmHg change in arterial PCO_2 above or below eupnoeic PCO_2 respectively. This high sensitivity is seen throughout the arterial side of the vascular network including the large arteries in the neck (Willie *et al.*, 2012) and large intracranial arteries (Wilson *et al.*, 2011; Willie *et al.*, 2014*a*) to the smallest pial arterioles and parenchymal vessels (Binks *et al.*, 2008; Mandell *et al.*, 2008; Nöth *et al.*, 2008; Piechnik *et al.*, 2008).

1.2.4.3 Oxygen

The effects of oxygen are unique in that its availability is required for aerobic metabolism rather than being a byproduct of it like some of the metabolic factors discussed. Therefore,

it is not surprising that its abundance leads to vasoconstriction and its relative shortage leads to dilation. Although its availability is tightly linked to that of PCO_2 and H^+ and other metabolic byproducts in a physiological setting, studies have been able to discern its independent effect in the presence of otherwise constant conditions. There are various mediators of hypoxic dilation including endothelial-derived NO (Frisbee *et al.*, 2002*a*; Lynch *et al.*, 2006), prostanoids (Messina *et al.*, 1992; Frisbee *et al.*, 2002*a*), 20-HETE (Frisbee *et al.*, 2002*a*) and EDHF (Liu & Flavahan, 1997); however, the contribution of each factor appears to be dependent on the severity of hypoxia (Frisbee *et al.*, 2002*a*). In all cases, there appears to be significant involvement by the endothelium to mediate the dilation, which is further supported by a reduction in hypoxic dilation when isolated vessels were exposed to indomethacin, an inhibitor of arachidonic acid (AA) metabolism, and thus the production of prostacyclin (PGI_2) (Busse *et al.*, 1983, 1984; Halvorson *et al.*, 2019) and to a lesser degree by L-NAME (an inhibitor of NO production from NOS) (Halvorson *et al.*, 2019). Therefore, PGI_2 is likely a substantial contributor to hypoxic dilation with a lesser but likely still significant role for NO.

1.3 Effects of Metabolic Syndrome

1.3.1 Cerebrovascular Tone Regulation with Metabolic Syndrome

Each component implicated in the regulation of tone has a multitude of signals being produced that are intended to alter the vasomotor response from the VSMC. Signals from myogenic, shear, metabolic, and neurovascular influences may be additive or opposing in their effect on VSMC and further combine with one another creating intricate and precise regulation of cerebral vascular tone. This complexity also introduces many possible steps in the pathway for an abnormal response to occur. Accordingly, changes to the regulation

of tone may form the basis of several pathologies. MetS and its contributing risk factors tend to alter the regulation of cerebral vascular tone by inducing changes in both the structure and function of the vessels. These risk factors include hypertension, type 2 diabetes mellitus (T2DM), and obesity which promote a pro-inflammatory pro-oxidant state. Functionally, MetS is associated with increased smooth muscle activation and endothelial dysfunction which has important implications for the ability of a vessel to dilate in response to a multitude of stimuli previously discussed including hypotension, shear, hypoxia, and other metabolic stimuli. Increased myogenic properties are consistently overserved in MetS in multiple vascular beds (Frisbee *et al.*, 2002*b*; Hayashi *et al.*, 2002) including in the cerebral circulation (Phillips *et al.*, 2005; Jarajapu *et al.*, 2008; Brooks *et al.*, 2015). This increase in constriction may be due to both a decrease in buffering capacity from endothelial dysfunction and alterations in the vascular smooth muscle itself (Baumbach *et al.*, 1994; Brooks *et al.*, 2015). The chronic inflammatory state seen in MetS likely contributes to the reduction in NO bioavailability due to increased scavenging to the produced NO by reactive oxygen species (ROS) converting the NO to peroxynitrate before the NO may induce dilation (Kazuyama *et al.*, 2009). Other theories suggest an uncoupling of the enzymatic reaction, converting eNOS into a superoxide producing enzyme, which leads to less NO production (Li & Förstermann, 2013). Reduced NO bioavailability is consistently reported to evolve in parallel with oxidant stress and the development of a chronic inflammatory state (Barbato *et al.*, 2005; Dandona *et al.*, 2005). This is supported by improved dilation of the middle cerebral artery (MCA) with the pretreatment of the cell-permeable superoxide dismutase mimetic TEMPOL in a model of T2DM (Halvorson *et al.*, 2019). Interestingly some studies have actually shown an increase in eNOS expression

which may be an attempt to compensate for the increased scavenging; however, they too continue to find reduced dilator reactivity (Kazuyama *et al.*, 2009).

Aside from reduced NO bioavailability, a shift in arachidonic acid metabolism (AA) towards the production of constrictors and away from dilators that are highly responsible for hypoxic dilation has been demonstrated in a previous study (Halvorson *et al.*, 2019). PGI_2 and TxA_2 are two notable opposing vasoactive end products of AA metabolism, causing vasodilation and vasoconstriction respectively whose production is altered in MetS. The cascade of AA metabolism is described in further detail in the following figure (Figure 4). A change in sensitivity to various metabolites in addition to their differential production may contribute to impaired vasomotor responses. For example, in studies using sodium nitroprusside (SNP), an exogenous NO donor, while blocking endogenous NO production by eNOS using L-NAME, found less relaxation of the MCA in spontaneously hypertensive rats which was attributed to a decreased expression of sGC (López-Farré *et al.*, 2002; González *et al.*, 2008). In a model of T2DM decreased sensitivity of MCA to the PGI_2 analog iloprost was also found suggesting that decrease sensitivity (and production as mention previously) of dilators may be contributing to the impaired dilation of the cerebral circulation in MetS (Halvorson *et al.*, 2019).

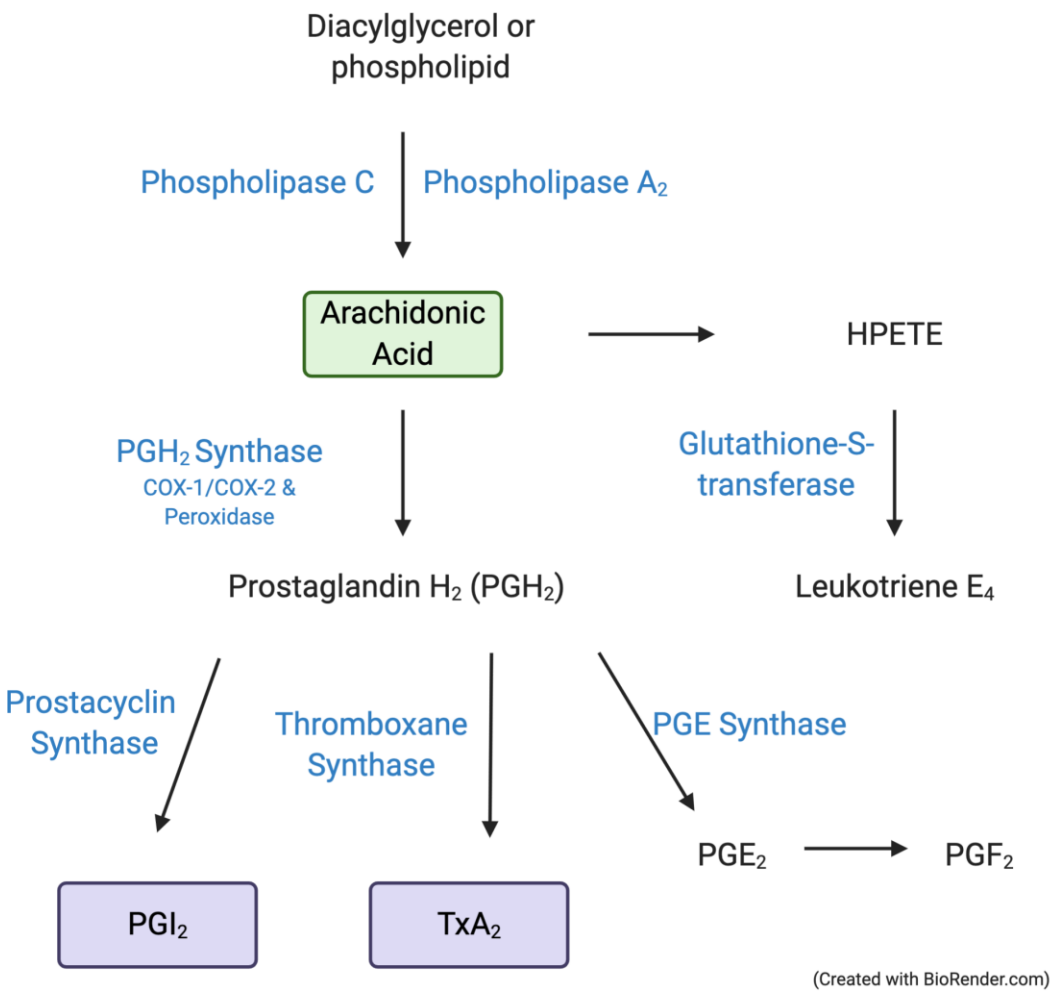

Figure 4: Arachidonic acid metabolism cascade.

Abbreviations: COX-1, cyclooxygenase-1; COX-2, cyclooxygenase-2; PGE_2, prostaglandin E2; PGF_2, prostaglandin F2alpha; PGI_2, prostacyclin; TxA_2, thromboxane A2.

Impaired dilation in response to exogenous dilator metabolites may also be due to vascular remodeling. Structural changes are an important consideration since even if the smooth muscle of a cerebral vessel is able to relax due to metabolic influences resulting in

hyperpolarization, remodeling may prevent an increase in lumen diameter which is ultimately the major contributor to acute changes in resistance and thus the regulator of flow. Hypertension is largely implicated in the thickening of the vascular smooth muscle as well as increasing the ratio of collagen to elastin in the vessel which increases its stiffness. High intralumenal pressure increases the shear stress exerted on the vascular endothelium which normally could be restored to baseline by NO-induced vasodilation; however, in a disease state with impaired NO production, there is a reduced ability to dilate resulting in endothelial damage and upregulation of atherogenic genes (Humphrey, 2008; Davies, 2009). As a means of protection from chronically increased shear stress and wall tension that may lead to downstream edema cerebral vessels tend to hypertrophy with chronic hypertension, but this protective hypertrophy is also detrimental (Cipolla *et al.*, 2018). Since wall tension is equal to the product of intraluminal pressure and radius, and wall stress is the quotient of wall tension and wall thickness, hypertension-induced hypertrophy and inward remodeling resulting in a decrease in radius and increase wall thickness can normalize both the wall tension and wall stress (Cipolla *et al.*, 2018). Although this remodeling may be protective in regard to increases in pressures and protecting the downstream capillaries from edema it increases the cerebrovascular resistance and limits the dilation reserve during hypotension and therefore, presents itself as a right-shift in the autoregulatory range (Heistad & Baumbach, 1992; Iadecola & Davisson, 2008). The development of myogenic tone at higher pressure implies an increased lower limit of autoregulation. This predisposes cerebral tissue to reduced blood flow during hypotension. When pressure drops below the lower limit flow becomes dependent on the passive diameter of the vessel. Not only does an impaired lower limit

predispose hypertensive individuals to ischemia but the reduced passive diameter from vascular remodeling further compromises flow to cerebral tissue resulting in hypoxic areas (Pires *et al.*, 2013).

In addition to hypertrophy and inward remodeling, there is substantial arterial stiffening commonly seen in MetS. Arterial stiffening is a natural process of aging; however, many of the cardiovascular risk factors involved in MetS have individually and synergistically been shown to expedite this process. Stiffening vessels favor both increased blood pressure and increased blood flow pulsations to reach further down the vascular network into the microcirculation of peripheral organs including the brain (Chantler & Larkin, 2020). The pro-oxidant stress of ROS may interact with components of the perivascular matrix and initiate collagen cross-linking and deposition as well as the breakdown of elastin making the vessel less distensible (Chantler & Frisbee, 2015). This is measured by a left shift in the stress-strain curve of isolated cerebral vessels under passive conditions achieved by using a Ca^{2+}-free solution preventing the development of tone (Brooks *et al.*, 2015). The stiffening vessels from increased collagen to elastin ratio is made worse by the thickening of vessel walls previously discussed. In a model of T2DM with hypertension significant collagen deposition in addition to medial hypertrophy, increasing the wall the lumen ratio and stiffness of the rats MCA, (Harris *et al.*, 2005) was demonstrated while T2DM in the absence of hypertension does not appear to induce structural changes to the cerebral vasculature (Halvorson *et al.*, 2019). This along with data that suggest the increase in arterial stiffness seems to follow a time course similar to that of the onset of hypertension suggests a strong relationship between hypertension and vascular remodeling (Payne *et al.*, 2010). Chronic uncontrolled hyperglycemia and inflammation do tend to lead to the

development of hypertension and thus contribute to changes in the composition of cerebral vessels and it is likely the combination of both, as seen in MetS, that increases the degree to which remodeling occurs.

1.3.2 Cognitive Impairment Associated with Metabolic Syndrome

With these impairments to cerebrovascular tone regulation and thus blood flow regulation the brain becomes susceptible to ischemia leading to tissue damage, inflammation and cognitive impairment. However, cognitive impairments are not limited to individuals that have experienced an acute ischemic event. Since even in their absence both epidemiological and clinical studies strongly suggest the presence of an interaction between MetS and cognitive impairment (Rosenberg, 2009; Yates *et al.*, 2012; Alfaro *et al.*, 2016; Tsai *et al.*, 2016). Vascular cognitive impairment (VCI) is a term used to describe cognitive impairment that is caused or associated with vascular factors (Hachinski *et al.*, 2006). One brain structure that may be particularly susceptible to chronic mild under perfusion is the white matter, which are areas of the central nervous system that are mainly made up of myelinated axons. White matter has the general role of transferring information within neural networks (Filley, 2005) by acting as a relay mechanism in coordinating communication between the different brain regions. Therefore, the preservation of its structure is essential for cognitive processes. White matter forms the majority of the deep brain and because of this anatomical positioning along with its precarious blood supply from terminal arterioles that have limited anastomosis and collateralization it is particularly vulnerable to dysfunction or occlusion of the vasculature associated with MetS leading to white matter damage and neuroinflammation (Iadecola & Gottesman, 2019). As such white matter inflammation is an event associated with both cognitive decline and MetS which

has been suggested to be one of the shared mechanisms contributing to the association of these two conditions (Misiak *et al.*, 2012). Although microglia are not the only cell type responsible for the inflammatory response in the brain, their activation is a strong indicator of a proinflammatory environment (Harry & Kraft, 2008) and reducing their activation has been shown to improve white matter function in a model of cerebral vascular disease (Manso *et al.*, 2018). Therefore, their activation will be used as an outcome measure of neuroinflammation with particular attention being paid to microglia activation in white matter. Activation of astrocytes in inflammatory environments may also promote the growth and activation of microglia (Von Bernhardi & Eugenín, 2004) and is used as a secondary measure of neuroinflammation in this thesis. VCI can affect all cognitive domains; however, the susceptibility of the white matter to vascular dysfunction and its importance with executive function means VCI frequently results in executive dysfunction (Smith, 2017). Executive function encompasses the cognitive domain that enables functional independence. These subdomains include inhibitory control such as ignoring stimuli that is not associated with goal-directed behaviour, working memory (holding and manipulating information that is not perceptually present) and cognitive flexibility (the ability to change goals) (Diamond, 2013). Many individuals with MetS may be diagnosed with understated deficits of VCI including cognitive slowing, inattention, and executive dysfunction (Kozora & Filley, 2011). Much of the changes to behaviour in rodent models of MetS has focused on hippocampal dependent cognitive impairments such as memory and spatial learning (Winocur & Gagnon, 1998) and the resultant hippocampal neuroinflammation (Gomez-Smith *et al.*, 2016) with limited investigation into examining particular subdomains of executive function. Therefore, the implementation of a rodent

model of MetS known to exhibit cerebrovascular dysfunction is needed to investigate these subdomains of executive function and their association with white matter inflammation.

1.3.3 The Obese Zucker Rat as a Model of Metabolic Syndrome

The obese Zucker rat (OZR) provides an appropriate model for the study of MetS based on the recessive dysfunctional leptin receptor gene mutation leads to an impaired satiety reflex, and thus a chronic elevation in food intake (Bray, 1977; Kurtz *et al.*, 1989). This leads to the rapid development of extensive obesity characterized by both hypertrophy and hyperplasia of adipocytes and the development of associated disease states including insulin resistance and hypertriglyceridemia (Bray, 1977). Additionally, OZR develops clinically relevant hypertension best characterized as mild to moderate (Toblli *et al.*, 2004; Frisbee, 2005; Johnson *et al.*, 2006) as well as a pro-inflammatory pro-thrombotic environment (Vaziri *et al.*, 2005). The parallel development of metabolic risk factors to clinically relevant degrees coupled with the prolonged period of hypertriglyceridemia and insulin resistance prior to overt T2DM supports the use of OZR as an appropriate model for studying the origin, outcomes, and potential treatment for MetS in humans. The OZR has demonstrated both depressive and anxious behaviour (Brooks *et al.*, 2018*b*) but little work has been done using more comprehensive tests to investigate executive dysfunction that could be related to impaired cerebrovascular tone regulation and white matter pathology. Therefore, gaining an understanding of the cognitive deficits potentially brought on by impairments in vascular tone regulation in a model of MetS is of interest.

1.4 Summary

In summary, the regulation of vascular tone involves a complex set of pathways with

myogenic, shear, and metabolic control. The mechanical influences of pressure and flow serve as a stimulus for the myogenic and shear responses to set a basal level of tone over a wide range so that metabolic factors have room to produce vasoactive responses on the vasculature. Due to the paramount importance of precise cerebral blood flow control these mechanisms are particularly pronounced and redundant in the cerebral circulation allowing for greater protection against insufficient perfusion or edema and capillary damage in situations of hypotension and hypertension respectively. However, due to the complexity of these homeostatic blood flow mechanisms there is the potential for the development of a pathological state. MetS presents a constellation of cardiovascular risk factors that are highly linked to the development of such cerebrovascular pathologies increasing the risk of stroke, TIA, and vascular dementia. The metabolic and inflammatory changes in MetS, such as increased oxygen stress and the pro-inflammatory state likely contribute to a shift in cerebral vascular tone regulation towards a constricted state. This occurs through mechanisms including vascular remodeling, which decreases the lumen size and increases stiffness, and when paired with endothelial dysfunction and increased activation of the vascular smooth muscle it promotes increased cerebrovascular resistance. This right shift to the autoregulatory zone of myogenic regulation allows for enhanced protection from hypertension but leaves cerebral tissue, the white matter in particular, vulnerable to under-perfusion and the development of neuroinflammation.

1.5 Hypothesis

The pro-inflammatory and high oxidative stress environment present in the OZR will alter vascular reactivity through mechanisms related to endothelial cell dysfunction. These

changes will present in conjunction with markers of white matter inflammation and evidence of executive dysfunction.

1.6 Specific Aims

1. To determine whether alterations to the structure and function of small resistance vessels including myogenic tone regulation, endothelial function, or wall mechanics exist in a model of metabolic syndrome and to determine the mechanistic contributors to changes in this response between the OZR and control lean Zucker rat (LZR). These experiments employ pressure myography of the middle cerebral artery with specific mechanical and pharmacological challenges to determine vasomotor diameter and mechanical responses in MetS. Pressure myography allows for precise measurement of the vasomotor responses in a controlled environment under near physiological conditions while being able to easily manipulate variables including intralumenal pressure, and agonist concentration. Information into the mechanistic changes occurring in Mets was achieved by probing of dozens of genes related to endothelial cell biology simultaneously by using a PCR array to provide an efficient workflow into the up/down regulation of endothelial genes in MetS.
2. Determine if the impairments in cerebrovascular regulation present in conjunction with impaired cognition. These experiments involved the use of two established cognitive tests: an operant-chamber-based test of extradimensional set shifting (Brady and Floresco, 2015) and the Morris water maze (MWM) which allows for examination of subdomains of executive functioning previously linked to white matter inflammation and allows for comparison of previous findings

related to hippocampal dependent function by testing spatial learning, memory, and working memory.

3. To determine if the impairments associated with metabolic syndrome are associated with markers of neuroinflammation. These experiments use immunohistochemistry to visualize key cellular components of the inflammatory response, microglia and astrocytes, in the white matter areas of the brain and the hippocampus. Activated microglia were identified by OX6 primary antibody for major histocompatibility complex II (MHCII) and glial fibrillary acidic protein (GFAP) primary antibody was used to identify reactive astrocytes.

Chapter 2

2 Materials and Methods

2.1 Vascular Reactivity

2.1.1 Animals

Male lean Zucker rats (LZR) and obese Zucker rats (OZR) (Harlan/Envigo) were purchased at ~10 weeks of age and were maintained on standard chow and tap water *ad libitum* until the time of final usage. Animals were housed in the animal care facility at the Schulich School of Medicine and Dentistry at the University of Western Ontario and all protocols received prior Institutional Animal Care and Use Committee approval (Appendix 5).

2.1.2 Experimental Design

At ~18 weeks of age, each rat was weighed, anesthetized with injections of sodium pentobarbital (50 $mg \bullet kg^{-1}$ i.p.) and received tracheal intubation to facilitate the maintenance of a patent airway. A carotid artery and an external jugular vein were cannulated for determination of arterial pressure using the BP-1 pressure monitor (World Precision Instruments Inc., Sarasota, FL) and for infusion of additional anesthetic, respectively, as necessary. Blood glucose was taken using a Contour glucose meter (Bayer, Toronto, ON) on blood collected from a tail vein prick. While deeply anesthetized, each rat was euthanized by decapitation, after which the brain was removed from the skull case and placed in cold physiological salt solution (PSS; 4ºC). Subsequently, MCA were dissected from their origin at the Circle of Willis. Each MCA was doubly cannulated with glass micropipettes (100-125 μm tip diameter) in a heated chamber (37°C) that allowed the lumen and exterior of the vessel to be perfused and superfused, respectively, with PSS (pH 7.4) from separate reservoirs (Living Systems Inc., Burlington, MA). The PSS had the following composition

(mM): 130 NaCl, 4 KCl, 1.2 $MgSO_4$, 4 $NaHCO_3$, 1.8 $CaCl_2$, 1.8 HEPES, 1.18 KH_2PO_4, 0.03 EDTA, and 6 glucose. Any side branches were ligated using a single strand teased from 6-0 suture. Vessel diameter was measured using television microscopy and an on-screen video micrometer (Butcher *et al.*, 2012).

2.1.3 Measurements of Vascular Reactivity in *Ex Vivo* Middle Cerebral Arteries

Following cannulation, MCAs were extended to their *in situ* length and equilibrated at 80% of the animal's mean arterial pressure (MAP) to approximate *in vivo* perfusion pressure (Lombard *et al.*, 1999). Any vessel that did not demonstrate significant active tone at the equilibration pressure was discarded. Active tone at the equilibration pressure was calculated as $(\Delta D/D_{max})\bullet 100$, where ΔD is the diameter increase from rest in response to Ca^{2+}-free PSS, and D_{max} is the maximum diameter measured at the equilibration pressure in Ca^{2+}-free PSS. The active tone for vessels in the present study averaged 33.1% in LZR and 39.2% in OZR. Following equilibration, the myogenic activation was assessed in MCA over the range of 5, 20-160 mmHg, in 20 mmHg increments. Pressure was changed non-sequentially, and vessels were allowed 5 minutes to equilibrate at each pressure before arterial inner and outer diameters were recorded. Within each vessel, vascular reactivity curves were determined in response to increasing bath concentrations of acetylcholine (ACh) (10^{-10} M–10^{-6} M), 5-hydroxytryptamine (5-HT) (10^{-10} M–10^{-6} M), or adenosine (10^{-8} M–10^{-4} M). Agonists were added directly to the 10 mL bath surrounding the MCA and were allowed 5 minutes to equilibrate. Additionally, myogenic activation was repeatedly assessed over the same range of pressures (5, 20-160 mmHg) with a concentration of agonist 10^{-6} M bath concentration for acetylcholine and 5-HT, and 10^{-4} M for adenosine.

2.1.4 Data and Statistical Analysis

Mechanical responses following challenge with logarithmically increasing dosages of acetylcholine or adenosine were fit with the three-parameter sigmoidal equation:

$$y = \frac{a}{1 + e^{-(\frac{x - x_0}{b})}}$$

where y represents the vessel diameter and x is the agonist concentration. As a result of this approach, the upper bound represents that statistically determined asymptote for the concentration-response relationship and does not assume that the vascular response at the highest utilized concentration of the agonist represents the maximum possible response. Rather, the sigmodal relationship of best fit to the data will predict the statistical upper bound of the response given the data points entered into the model. As such, the upper bound is frequently slightly different than the dilator response of the vessel at the highest concentration of the agonist. Mechanical responses following challenge with logarithmically increasing dosages of 5-HT were analyzed by a repeated measure ANOVA since the sigmoidal equation did not fit the response. The myogenic properties of MCA from each experimental group was plotted as mean diameter at each intraluminal pressure from 60 to 140 mmHg as this is frequently regarded as the myogenic reactivity range (Osol *et al.*, 2002; Butcher *et al.*, 2013) and fitted with a linear regression

$$y = \alpha_0 + \beta x$$

where the slope coefficient β represents the degree of myogenic activation (Δdiameter/ Δpressure). Increasingly negative values of β therefore, represent a greater degree of

myogenic activation in response to changes in intralumenal pressure. Data fitting was performed using Sigma Plot, version 13.0 (Systat Software Inc.), and statistical analysis were performed using SPSS, version 26 (IBM). All data are presented as mean ± SEM. Differences in all slope coefficients or descriptive characteristics between LZR and OZR groups were assessed using the Welch's t-test (two-tailed) for comparison of means of 2 groups and multiplicity of comparisons was corrected using the Holm-Sidak method. A repeated measured mixed analysis of variance (ANOVA) was used to determine the effect of group, agonist, and group-agonist interaction followed by Sidak's post hoc tests. In all cases, $P<0.05$ was taken to reflect statistical significance.

2.2 PCR Array

Immediately following dissection of the MCA 6 LZR and 6 OZR brains from 18 weeks old rats were flash-frozen on a metal bar over dry ice. RNA was extracted with a monophasic solution of TRIzol (Invitrogen, Carlsbad Calif) following the manufacturer's instructions. Chloroform was added and each sample was separated into three phases (top aqueous phase solution containing RNA, and middle interphase and lower organic phase containing excess lipid, DNA and protein). The RNA was collected from the aqueous upper phase and isolated after incubation with isopropanol, washed in ethanol and resuspended in RNAse free water. The quality and quantity of the RNA were quantified by optical density ratio at 260-280 nm using a Nanodrop. 1 μg of RNA was used to synthesize cDNA following the RT^2 First Strand Kit (SA Biosciences, Hilden, Germany). Quantitative real-time PCR (qPCR) reactions were performed in 25μL of final volume with RT^2 SYBR Green ROX qPCR Mastermixes in a QuantStudio™ 3 Real-Time PCR system (Applied biosystems, Foster City, Calif). The amplification protocol included: 95 °C for 10 min and 40 cycles of

95 °C for 15 s and 60 °C for 1 min. Gene expression profiles were then generated with 96-well arrays containing endothelial-related genes (PAHS; 084, SA Biosciences) using the rat endothelial cell biology RT^2 profiler^{TM} PCR array (SA biosciences) containing 84 endothelial-related genes in accordance with the manufacturer's instructions. Data were analyzed with the RT^2 Profiler software (version 3.4; SA Biosciences). The relative gene expression was normalized with multiple control genes and the fold change in gene expression within OZR samples compared with the control LZR samples. Genes that had undergone significant upregulation or downregulation were identified. Data are presented as means ± SD for the number of samples (n=4 per group). qPCR primers for significantly up/down-regulated genes were then designed and optimized for validation of the PCR array results with n=6 rats per group. The amplification specificity was verified by an analysis of the melting curves. To quantify gene expression, the comparative Ct method ($2^{-\Delta\Delta Ct}$) was applied. The student *t*-test was applied for comparison of means of 2 groups.

2.3 Cognitive Testing

2.3.1 Animals

A separate cohort of Male LZR and OZR (Harlan/Envigo) (n=8 per group) were purchased at ~10 weeks of age and were maintained on standard chow and tap water *ad libitum* until 16 weeks of age, to allow for testing to be completed by 18 weeks of age and coincide with the age of animals used for vascular reactivity and qPCR experiments.

2.3.2 Set Shift and Reversal

At 16 weeks of age they began the set shifting protocol, which included side bias determination (Levit *et al.*, 2017). Rats were fasted overnight and maintained on food

restriction for the duration of the set shifting protocol in order to ensure motivation for 45 mg sucrose pellets (Dustless precision pellets, Bio-Serv) as behavioural reinforcement in the sound-attenuated operant conditioning chamber, cleaned with 70% ethanol (Med Associates). Correct lever presses were reinforced with the sucrose pellets using a fixed-ratio 1 schedule. After habituation to the chamber rats began lever- pressing training where they were required to lever press on at least 85 of 90 trials of alternating sides lever presentations before progressing to visual cue discrimination. 24 h after initial training, rats were trained on visual cue discrimination which involved both levers extending with only one lever paired with the light cue for 100 trials pseudorandomly alternating sides. Pressing the lever associated with the light cue was a correct response and a sucrose pellet reward was given (Figure 5A). A passing criterion of 8 correct consecutive responses was used for completion. 24 h later a retrieval session of 20 trials was performed to evaluate retention of the visual cue discrimination task immediately followed by 120 trials of response discrimination termed set shift. In this task only one lever (either left or right whichever was opposite to a previously determined side bias) would yield a food reward, even though the light continued to illuminate on alternating sides (Figure 5B). The passing criterion for response discrimination was also 8 correct consecutive responses. Again a 24 h delayed 20-trial retrieval test was given for response discrimination immediately followed by a 120-trial reversal session. In this task, the opposite lever yielded a reward and again the cue light continued to pseudorandomly alternate during the reversal trials (Figure 5C). During all tasks (visual cue, response, reversal), a 10 s response period was used during which the chamber was illuminated. If the correct lever was pressed, the chamber remained illuminated for 4 s so that rats could retrieve the sucrose pellet reward. This was followed

by a dark inter-trial period making the entire single-trial last 30 s. Cue lights were presented 3 s before lever extension and extinguished upon lever press or the end of the 10 s response period.

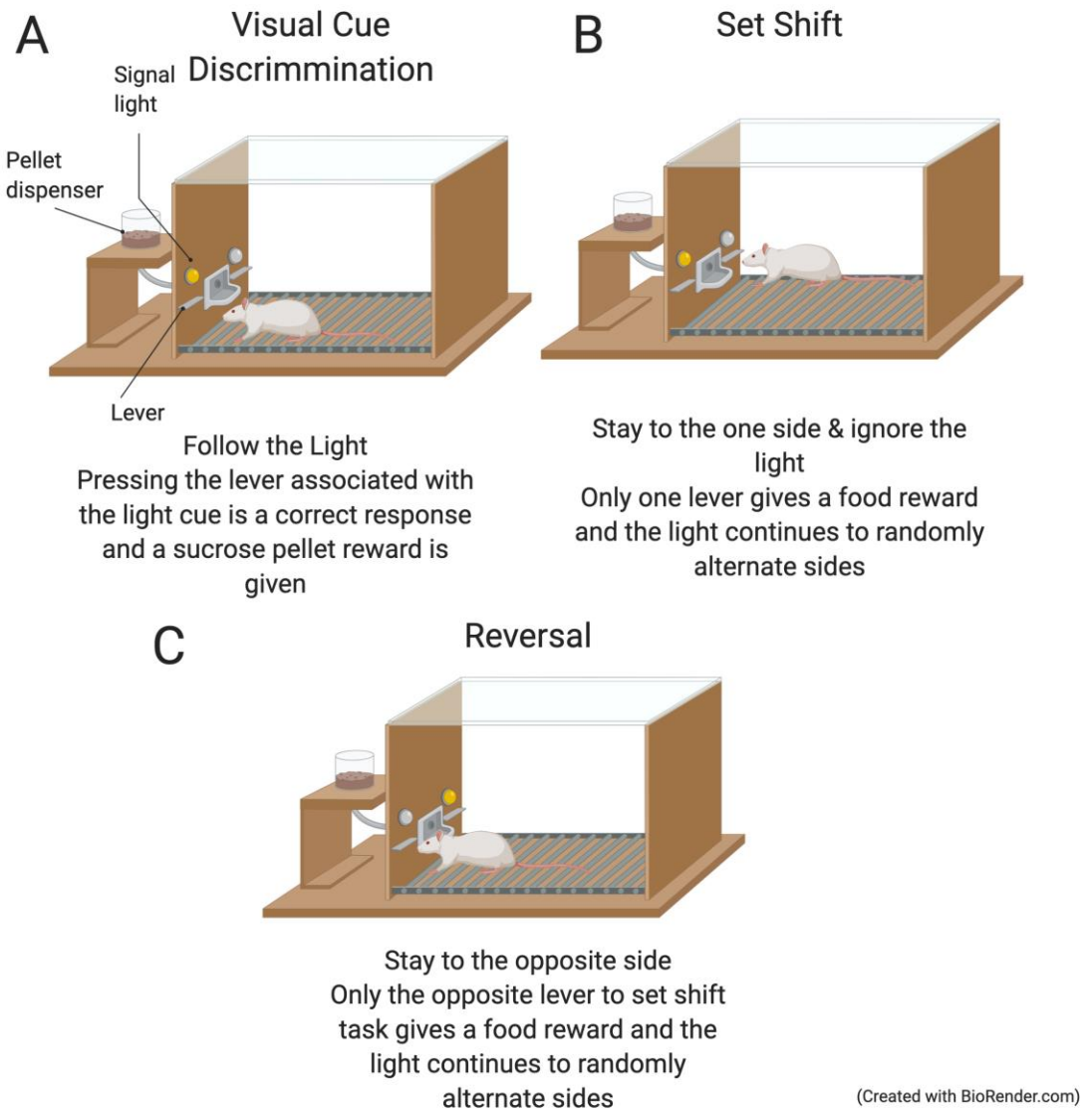

Figure 5: Operant conditioning chamber tasks

2.3.3 Morris Water Maze

One week following set shifting rats were tested in the MWM. A 144 cm diameter water tank filled with room temperature water dyed black with non-toxic acrylic paint was used in a dimly lit room. A target platform of 12 cm diameter was submerged 3 cm below the water surface. Rats were placed in the water from a fixed starting position and were given 90 s to locate the hidden platform in order to be removed from the water tank. Six learning trials were performed 1 h apart as has been previously adapted from a MWM protocol (Levit *et al.*, 2019). 24 h after the learning trials the rats were placed in the water tank with no platform and their swim path was recorded. In addition to tracking the rat's location over time, swim strategies were analyzed according to swim time in different set regions (Figure 6). Swim time in the annulus, a 27 cm wide ring, was used to represent the use of egocentric navigation based on distance from the wall (Rogers *et al.*, 2017). This egocentric navigation (navigating by internal cues) (Vorhees & Williams, 2014) was also measured in the annulus outside of the target quadrant in order to determine if this egocentric strategy was used in the rest of the maze and not merely in the target quadrant. Thigmotactic behaviour (motion in response to touch stimuli) was represented by time in the thigmotactic region defined as a 10 cm wide ring along the perimeter of the water maze. Finally, allocentric navigation (characterized by navigation using distal cues) (Vorhees & Williams, 2014) was approximated by a subjective measure of the time that the rat was directed at the platform location (Rogers *et al.*, 2017). After the probe tests, potentially confounding differences in visual perception or swim speed, perhaps due to body weight differences, were evaluated on 4 cued trials wherein the location of the platform was visibly marked. All swim paths were tracked using ANYmaze tracking software, version 6.33

(Stoelting Company), with a top-view webcam (C525, Logitech). The experimenter was not visible to the rats during testing.

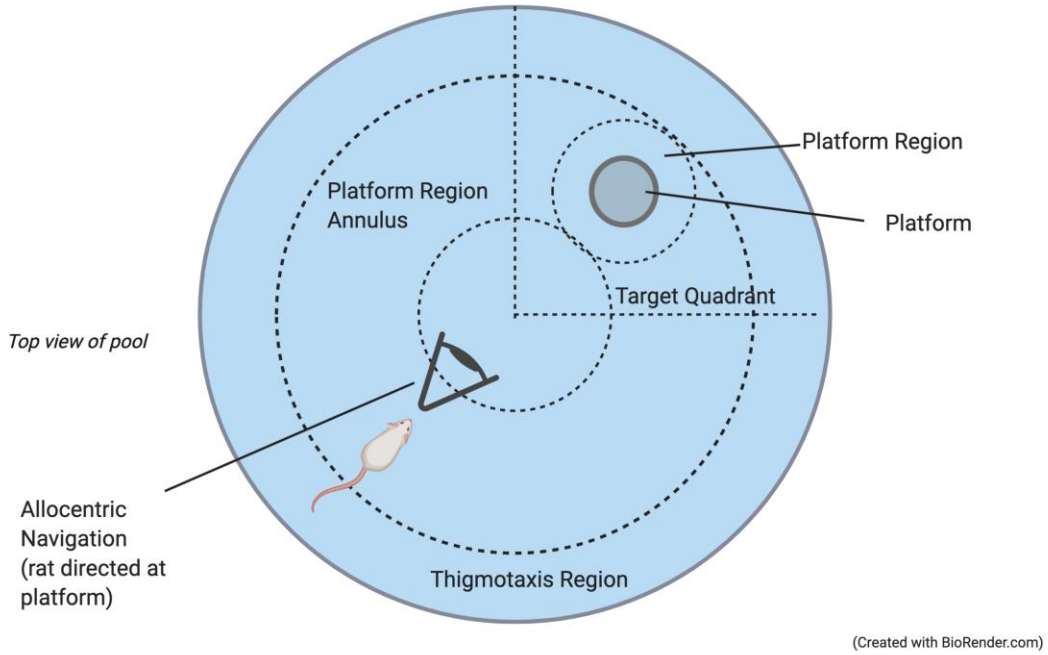

Figure 6: Areas used to approximate swim strategies during the 90 s probe test Morris Water Maze.

2.4 Immunohistochemistry and Image Processing

After all behavioural testing was complete, rats were euthanized by intraperitoneal injection of sodium pentobarbital. Rats (n=6 per group) were subsequently perfused transcardially with 200 mL of 0.01 M phosphate buffer saline followed by 200 mL of 4% paraformaldehyde (PFA). Once perfused the brains were removed from the skull and placed in 4% PFA for 24 h then transferred into a 30% sucrose solution until saturated. 35 μm coronal sections were prepared using a cryostat (CryoStar NX50, Thermo Fischer Scientific) and stored in

cryoprotectant at -20 °C until all tissue was available for immunohistochemistry (IHC). Standard protocols were followed for DAB-mediated IHC of free-floating sections, using an ABC-HRP kit (Thermo Fischer Scientific #32020). A 1:1000 concentration of OX6 primary antibody for MHC II was used to identify activated microglia (Lue *et al.*, 2010) (BD Pharmingen #554926), along with a 1:2000 concentration of GFAP primary antibody to identify the number of astrocytes indicative of reactive astrocytes (Sofroniew & Vinters, 2010) (Sigma-Aldrich #G3893). Stained brain sections were mounted onto slides and allowed to air-dry overnight. They were then dehydrated in baths of progressive concentrations of ethanol and xylene, and finally cover-slipped with DePex mounting medium (BDH Chemicals).

A 10x objective lens on an upright microscope (Nikon Eclipse Ni-E, Nikon DS Fi2 colour camera, NIS Elements Imaging) was used to create stitched micrographs of coronal sections. Prior to each scan, white balance was automated using an off-tissue reference point and a focus plane was programmed for the micrograph. For all images, the light source intensity, exposure, aperture, and diaphragm parameters were fixed. Anatomical regions of interest (cingulum, corpus callosum, internal capsule, hippocampus) were captured at the coronal sections of Bregma +2.00 mm, +0.00 mm, −3.00 mm, and −5.50 mm with each rat having a single section analyzed at each of the coronal planes. The subset of the corpus callosum, the supraventricular corpus callosum (SVCC), was outlined on the anterior two coronal planes of the corpus callosum, which excluded the portion of the corpus callosum that was medial to the lateral ventricles. Micrographs were processed and analyzed using ImageJ (version 1.53) where regions of interest were outlined using the polygon tool. Images were then converted to 8-bit, processed using the subtract background

command, and thresholded with a fixed grayscale cut-off value of 237. Area coverage (%) was recorded for each region of interest and used for statistical analysis using a repeated measures mixed ANOVA. For anatomical regions that spanned multiple coronal sections (corpus callosum, cingulum, hippocampus), a weighted average area coverage was calculated.

Chapter 3

3 Results

3.1 Baseline Characteristics

Table 1 presents body mass, MAP, and blood glucose, for both the OZR and LZR control at ~18 wk of age. The OZR exhibited characteristics of MetS compared to the age matched LZR control including obesity, hypertension and insulin resistance.

	LZR	OZR
Mass, g	414 ± 7	645 ± 14*
MAP, mmHg	106 ± 1	126 ± 1*
Glucose, mmol/L	7.6 ± 0.3	12.1 ± 0.5*

Table 1: Baseline characteristics

Values are means ± SEM; All animals were male ~18 wk of age (n = 21 per group). Mean arterial pressure (MAP) was measured at the carotid artery while under anesthesia with sodium pentobarbital. Glucose was measured from a drop of blood collected from the tail vein. *P< 0.05 vs LZR using Welch's t-test.

3.2 Responses from *Ex Vivo* Middle Cerebral Arteries

Dilator responses of *ex vivo* MCA from OZR were impaired compared to LZR in response to challenge with increasing concentrations of ACh (Figure 7A) but not adenosine (Figure 7B). The constrictor responses of isolated MCA in OZR were enhanced compared to LZR as measured by the response to increasing concentrations of 5-HT (Fig 8A) and by

myogenic activation with increasing intraluminal pressure (Fig 8B). Responses of *ex vivo* MCA for both slope of myogenic activation and average lumen diameter from LZR and OZR in response to increased intraluminal pressure and concentration of agonists, ACh (10^{-6} M) (Figure 9A), adenosine (10^{-4} M) (Figure 9B), and 5-HT (10^{-6} M) (Figure 9C) were determined across the intraluminal pressure range 60-140 mm. Pre-treatment with either ACh or adenosine increased the slope of myogenic activation and average arteriolar diameter. While 5-HT significantly decreased arteriolar diameter. The effect of group (LZR vs OZR) was not significant in the response to ACh and pressure but was in response to either adenosine or 5-HT and pressure. No difference in group by agonist interaction was observed. To determine whether there was evidence of remodeling in OZR the mechanical characteristics of *ex vivo* MCA under Ca^{2+}-free, passive conditions in response to increasing intraluminal pressure were determined. The inner diameter of the MCA (Figure 10A) and incremental distensibility (Figure 10B) of the MCA were not different between LZR and OZR at any level of intraluminal pressure.

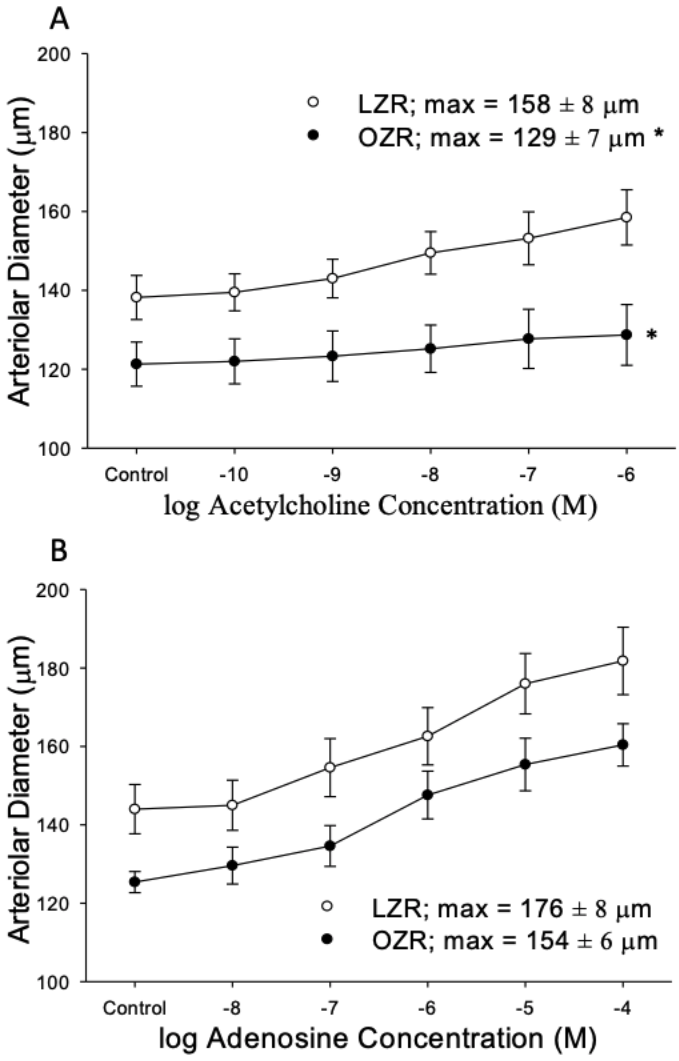

Figure 7: Dilation of *ex vivo* middle cerebral arteries

The dilation of isolated middle cerebral arteries at 80% mean arterial pressure from lean Zucker rat (LZR) and obese Zucker rat (OZR) in response to increasing bath concentrations of (A) acetylcholine (n=6 per group) and (B) adenosine (n=6 per group). Data are presented as mean ± SEM. * $P < 0.05$ vs statistically determined asymptote of the response in LZR using Welch's t-test.

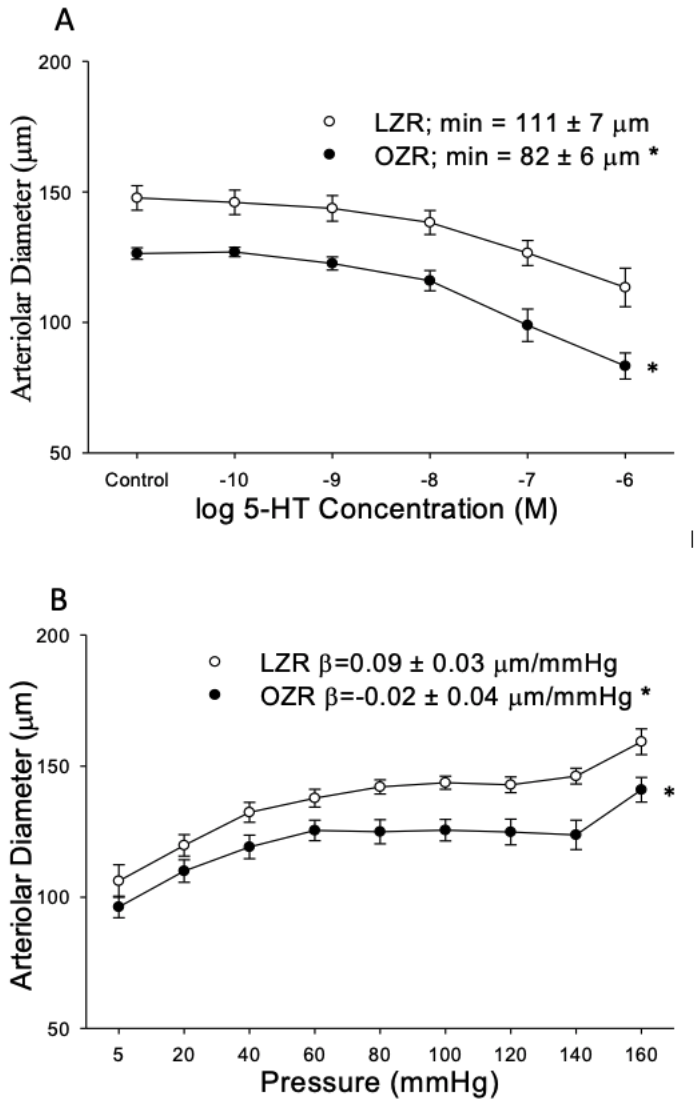

Figure 8: Constriction of *ex vivo* middle cerebral arteries

The constriction of isolated middle cerebral arteries from lean Zucker rats (LZR) and obese Zucker rats (OZR) in response to increasing (A) bath concentrations of 5-hydroxytryptamine at 80% mean arterial pressure (n=7) and (B) intraluminal pressure (n=13). Data are presented as mean ± SEM. *P< 0.05 vs response in LZR using (A) repeated measured mixed ANOVA and (B) Welch's t-test comparing the slope, β, of the linear regression performed between 60-140 mmHg.

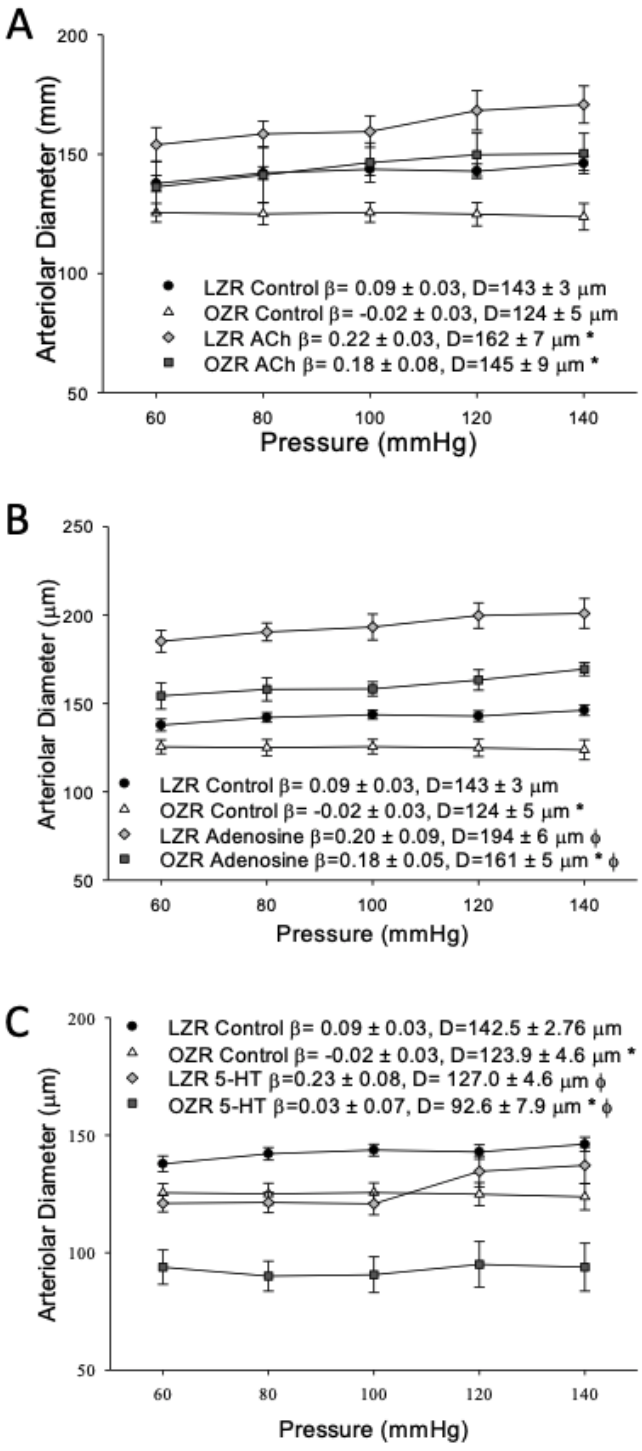

Figure 9: Myogenic response of *ex vivo* middle cerebral arteries challenged with ACh, adenosine, or 5-HT

The response of middle cerebral arteries from lean Zucker rats (LZR) and obese Zucker rats (OZR) in response to increasing intraluminal pressure. Data presented as mean ± SEM, are presented for vessels under control conditions following challenge with (A) acetylcholine (10^{-6} bath concentration) (n=4 per group), (B) adenosine (10^{-4} M bath concentrations) (n=4 per group), and (C) 5-hydroxytryptamine (10^{-6} M bath concentrations) (n=5 per group). The slope, β, of the linear regression performed between 60-140 mmHg and average middle cerebral artery lumen diameter, D, across the same pressure range are presented in the inset legend. *P< 0.05 vs LZR diameter (significant group effect in repeated measures mixed ANOVA) ϕP< 0.05 vs control diameter (significant agonist effect in repeated measures mixed ANOVA).

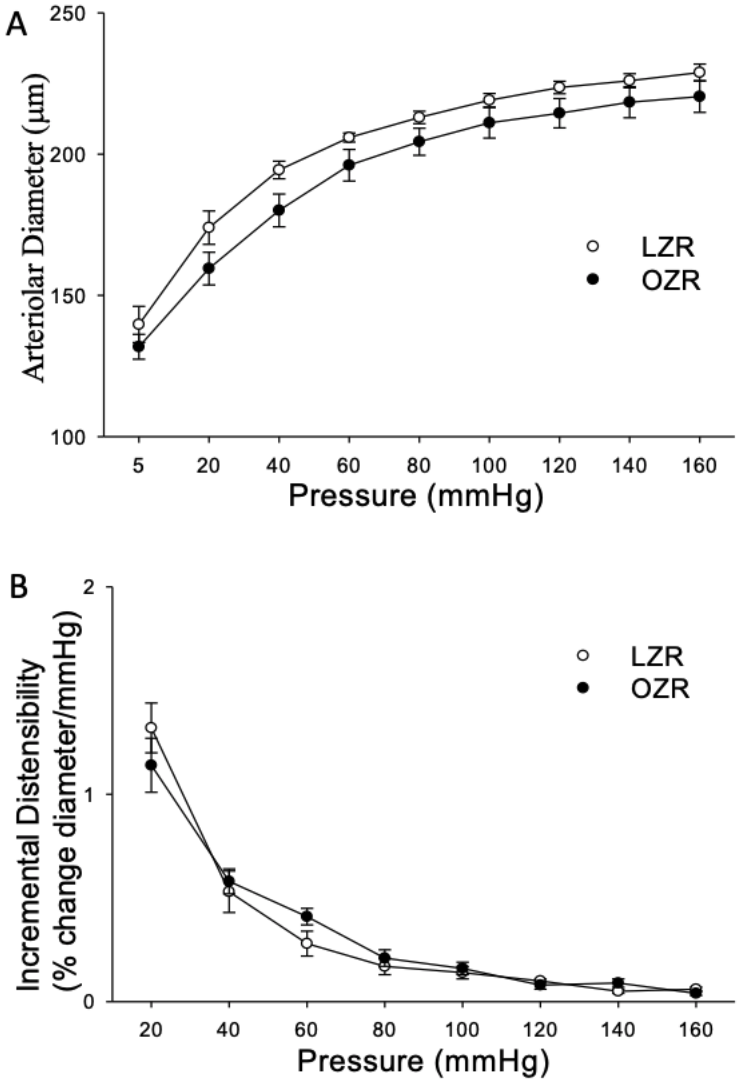

Figure 10: Passive mechanical response of *ex vivo* middle cerebral arteries under Ca^{2+}-free conditions.

The mechanical biophysical properties of the wall of isolated middle cerebral arteries from lean Zucker rats (LZR) and obese Zucker rats (OZR) (n=7 per group) under Ca^{2+} -free conditions following increasing intraluminal pressure. Mean ± SEM are presented for (A) arteriolar lumen diameter, and (B) incremental distensibility of the vessel wall.

No significant differences were determined between LZR and OZR using repeated measures mixed ANOVA.

3.3 Altered Expression of Endothelial Cell Function Genes

Six of 84 total endothelial cell function related genes examined with the Rat Endothelial Cell Biology RT^2 Profiler PCR Array demonstrated significant up/down regulation in expression (Table 2A). Genes related to thrombosis, oxygen stress, and chronic inflammation including Cxcl4, Cxcr5, and Xdh were found to be significantly upregulated in OZR, and genes related to COX-2 expression including Ptgs2, Tnf-1, and Anxa5 were found to be significantly downregulated. IL-3 was the most up-regulated gene identified in OZR in the PCR array but the changes were not significant. Validation qPCR for 6 significantly differentially expressed genes in PCR array demonstrated similar significant changes in expression of Cxcl4, Cxr5, Xdh, and Tnf-1 using 6 rats per group (Table 2B).

A

Gene Symbol	Fold Increase	P-value
Cxcl4/Pf4	2.06	0.01
Cxcr5	1.67	< 0.01
Xdh	1.59	0.04

B

Gene Symbol	Fold Decrease	P-value
Ptgs-2	1.82	0.02
Tnf	1.48	<0.01
Anxa5	1.12	0.04

Table 2: Select endothelial cell function related genes either upregulated or downregulated in PCR array

Selected endothelial cell function related genes either upregulated (Table 2A) or downregulated (Table 2B) in PCR array; n=4/group Abbreviations: Cxcl4, CXC motif ligand 4; Pf4, platlet factor 4; Cxcr5, CXC motif receptor 5; Xdh, xanthine dehydrogenase, Ptgs2, prostaglandin-endoperoxide synthase 2; tnf, tumor necrosis factor; Anxa5, Annexin V.

A

Gene Symbol	Fold Increase	P-value
Cxcl4/Pf4	2.06	< 0.01
Cxcr5	1.14	0.03
Xdh	2.07	< 0.01

B

Gene Symbol	Fold Decrease	P-value
Tnf	1.63	<0.01

Table 3: Select endothelial cell function related genes either upregulated or downregulated in PCR validation

Select endothelial cell function related genes either up regulated (Table 3A) or downregulated (Table 3B) in validation qPCR (Table 2B; n = 6/group). Abbreviations Cxcl4, CXC motif ligand 4; Pf4, platlet factor 4; Cxcr5, CXC motif receptor 5; Xdh, xanthine dehydrogenase, tnf, tumor necrosis factor.

3.4 Morris Water Maze

To test for spatial learning capacity, rats were trained on a MWM protocol with six learning trials at 1 h intervals to learn the location of a hidden platform. OZR demonstrated impaired spatial learning capacity as measured by an increase average time to reach the platform in

trials 2-6 (Figure 11A). In the probe test, performed 24 h later where the platform was removed, and the rats' memory of the platform location during 90 s probe test was inferred by preference for the target quadrant in which the platform was previously located during the learning trials. The OZR group showed a significant preference for the target quadrant compared to LZR (Figure 11B). Swim strategies for proportion of swim time in thigmotaxis, annulus, annulus outside target quadrant, and allocentric navigation were compared between groups (Figure 11C). Only the proportion of time spent in allocentric navigation as estimated by a subjective measure of when the rat was swimming toward the platform area was significantly greater in OZR. To determine if there were potentially confounding differences in visual perception or swim speed these variables were evaluated on 4 cued trials with a visible platform after all MWM testing was complete. No differences were observed in swim time to platform or swim speed in these trials.

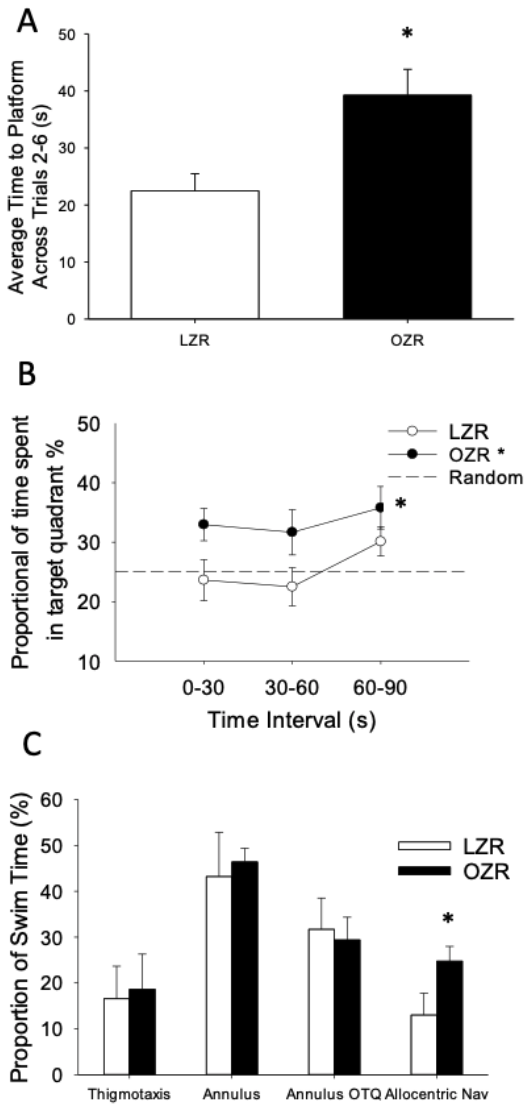

Figure 11: Morris Water Maze

Data presented as mean ± SEM describing the Morris Water Maze (A) learning represented by the average time to locate the platform across learning trials 2-6 for lean Zucker rats (LZR) compared to obese Zucker rats (OZR) (n=8 per group). Response during the 90 s probe test for (B) the proportion of time spent in the target quadrant (C) and swim strategies used. Refer to figure 6 for areas used to quantify swim strategies. *P< 0.05 vs LZR using

repeated measures mixed ANOVA for (A) and (B) showing a significant effect for group and (C) Welch's t-test. Abbreviations: OTQ, outside target quadrant; Nav, navigation.

3.5 Operant Conditioning Chamber Tasks

In the visual cue discrimination task the number of trials needed to reach the training criterion of 8 consecutive correct lever presses was not different suggesting that learning was not different in this task (Figure 12A). The next day in a 20-trials retrieval test for memory of the visual cue discrimination task demonstrated no impairment in visual cue memory in OZR (Figure 12C). Directly following the visual cue retrieval task attentional set shifting was evaluated over 120 trials where the rats were to ignore the cue light and learn a spatial strategy where only pressing one of the levers (either left or right) would produce a food reward. Again, no differences in the number of trials to reach 8 consecutive correct lever presses were found (Figure 13A) and in the 20-trial retrieval test no impairments in memory were detected (Figure 13C). Directly following set shift retrieval, the reversal task was evaluated over 120 trials again with no differences detected in the number of trials to reach criterion (Figure 14A). Error types were then categorized as perseverative, regressive, or never-reinforced as have been previously described (Levit *et al.*, 2017), along with the number of omissions, for visual cue discrimination (Figure 12B), set shift (Figure 13B), and reversal (Figure 14B) tasks. Perseverative errors are those that follow the previously reinforced visual cue, which tend to occur most often in the early trials before the new spatial cue is learned. Regressive errors were defined as errors following the previous cue that occur after the rat has learned the newly rewarded spatial strategy. Specifically, once <75% of responses follow the previously learned strategy subsequent errors are considered regressive. Never-reinforced errors are those that follow

neither the previous visual cue nor the newly rewarding spatial strategy. No differences were observed in types of errors committed; however, OZR had significantly more omissions in the visual cue discrimination task when compared to LZR.

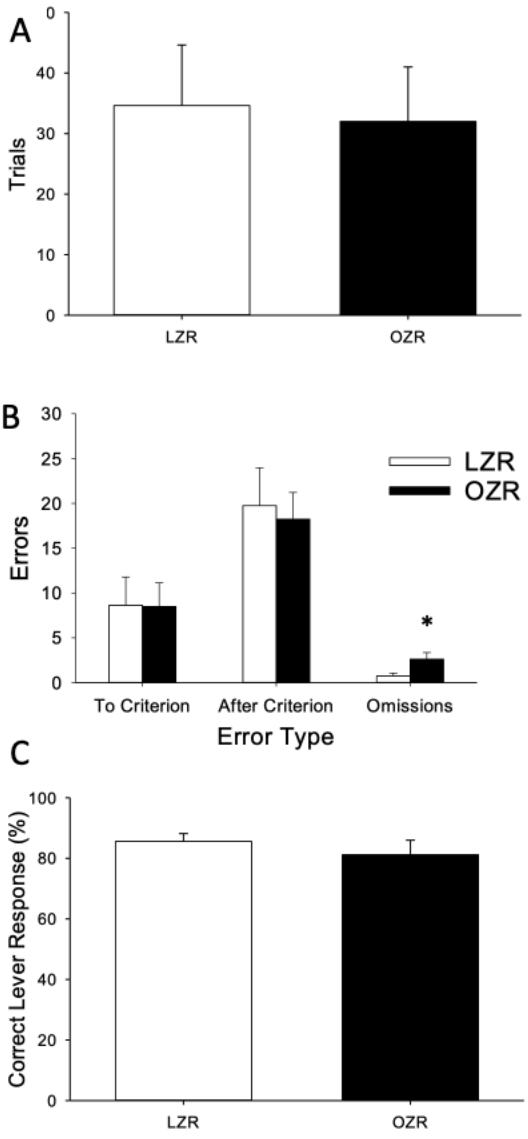

Figure 12: Visual discrimination task

The response of visual cue discrimination task, mean ± SEM, for lean Zucker rats (LZR) and obese Zucker rats (OZR) (n=8 per group) for (A) number of trials required to achieve 8 correct consecutive responses, (B) the types of errors committed during the 120 trials, and (C) the percentage of correct responses in 20 trials after a 24 h delay. *P< 0.05 vs response of LZR using Welch's t-test.

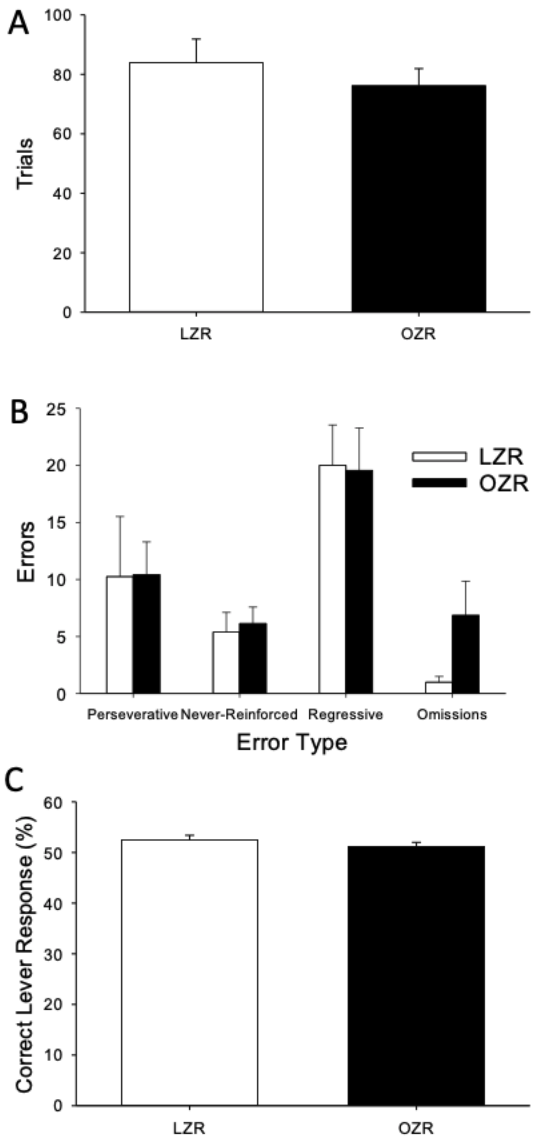

Figure 13: Set shift task

The response of set shift task, mean ± SEM, for lean Zucker rats (LZR) and obese Zucker rats (OZR) (n=8 per group) for (A) number of trials to achieve 8 correct consecutive responses, (B) the types of errors committed during the 120 trials, and (C) the percentage of correct responses after a 24 h delay. No significant differences were determined between LZR and OZR using Welch's t-test.

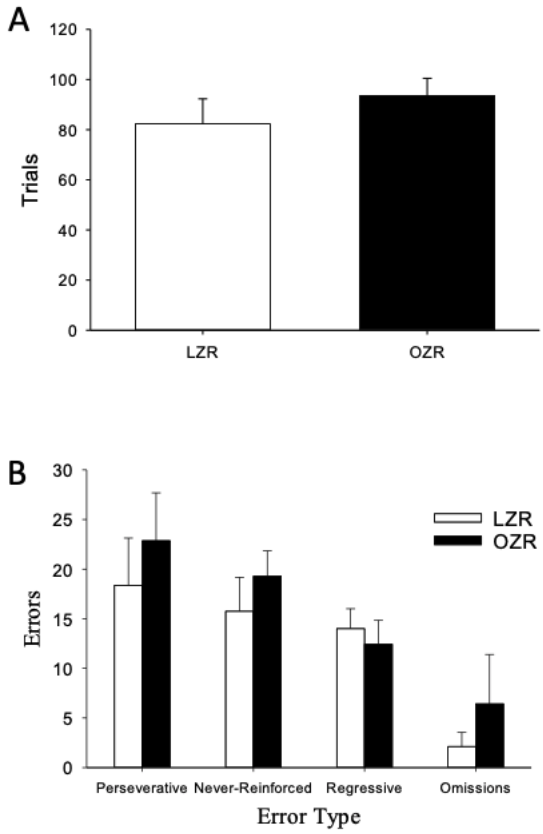

Figure 14: Reversal task

The response of reversal task, mean ± SEM, for lean Zucker rats (LZR) and obese Zucker rats (OZR) (n=8 per group) for (A) number of trials required to achieve 8 correct consecutive responses, and (B) the types of errors committed during the 120 trials. No significant differences were determined between LZR and OZR using Welch's t-test.

3.6 Immunohistochemistry

In order to examine for the presence of increased neuroinflammation the % area coverage of OX6-positive microglia and GFAP-positive astrocytes were used as a biomarker of activated microglia and reactive astrocytes in LZR versus OZR. Digital image analyses

showed that the % area coverage by OX6-positive microglia was not affected by group in all anatomical regions of interests (corpus callosum, supraventricular corpus callosum, hippocampus, and internal capsule) (Figure 15A). No group differences in area coverage by activated reactive GFAP-positive astrocytes were observed (Figure 15C).

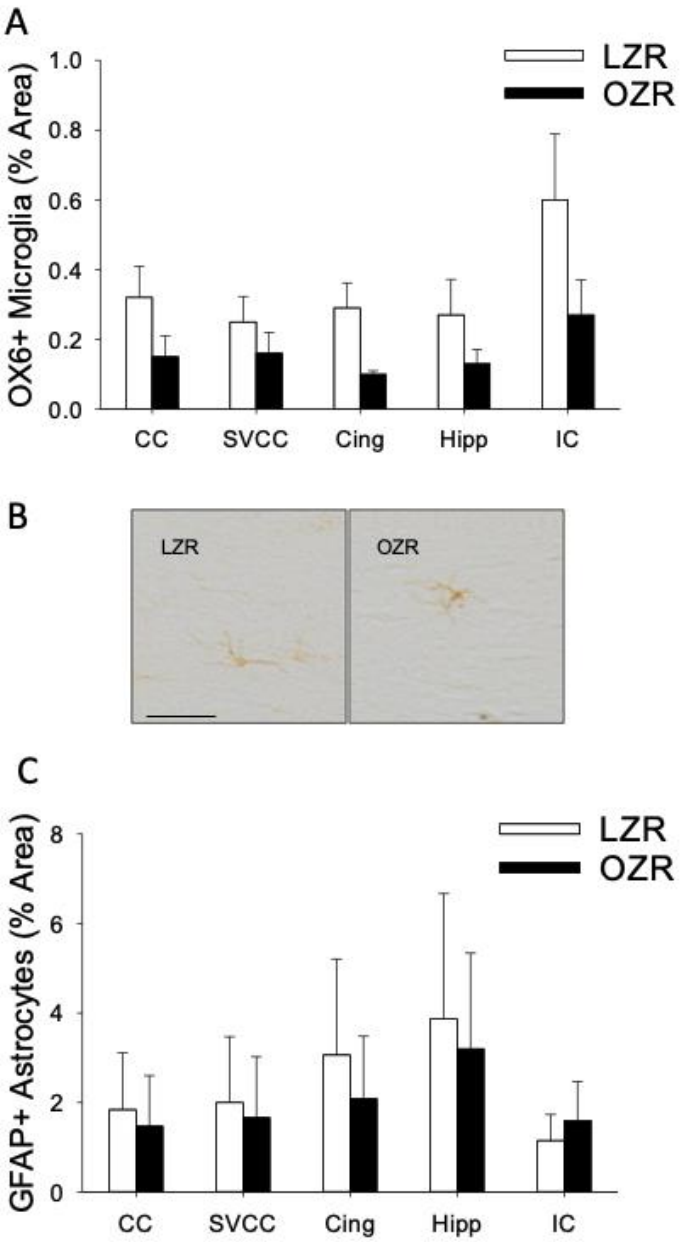

Figure 15: Markers of neuroinflammation in white matter regions and the hippocampus

Cross sectional % area coverage, mean ± SEM, by (A) OX6-positive microglial and (C) GFAP-positive astrocytes in the CC: corpus callosum, SVCC: supraventricular corpus callosum, Cing: cingulum, Hipp: hippocampus, and IC: internal capsule of lean Zucker rats (LZR) and obese Zucker rats (OZR) (n=6 per group). No significant effect of group

(LZR vs OZR) was observed using a repeated measured mixed ANOVA. (B) Representative micrographs of OX6-positive microglia area coverage in the corpus callosum, scale bar = 100 μm.

Chapter 4

4 Discussion

MetS is a chronic disease that can lead to long-term elevations in cardiovascular and cerebrovascular disease which may manifest in the form of stroke, TIA, or inappropriate cerebral perfusion (Chen *et al.*, 2017). Precise control of cerebral vascular tone is a crucial contributor to these poor outcomes that involves the integration of various signals from the endothelium, vascular smooth muscle and others to determine an appropriate level of tone. The MCA is a vessel of particular interest because of its significant role in cerebral blood flow regulation and because it is a frequent site of occlusion/stroke (Yu *et al.*, 2018). Therefore, changes to the reactivity of MCA associated with the development of MetS provide insights into how altered aspects of disease development can impact the control of blood flow within the brain. In general the vascular reactivity experiments revealed two overarching changes to the regulation of cerebral vascular tone to the OZR at this age enhanced myogenic tone and endothelial dysfunction.

4.1 Vascular Reactivity

This study observed impaired endothelial function in OZR as measured by impaired dilation to ACh, which has been consistently demonstrated in OZR (Brooks *et al.*, 2015, 2018*a*, 2018*b*) and is considered a hallmark of MetS. Dilation of the MCA in response to ACh is both endothelium and NOS dependent as evidenced by a severely blunted response in endothelium denudated vessels or in the presence of the NOS inhibitor L-NAME (Sylvester *et al.*, 2002). The impaired dilation is likely due to a combination of decreased NO bioavailability with the potential for some contribution of altered arachidonic acid metabolism brought on by the presence of ROS and inflammation. The pro-oxidant

environment in OZR leads to increased scavenging by ROS decreasing the NO bioavailability and limiting its ability to hyperpolarize VSMC thus impairing dilation. This decrease in NO bioavailability is supported by measurements from pooled arteries in previous studies showing both decreased NO and an increase in the ROS, H_2O_2 (Brooks *et al.*, 2015, 2018*b*). TEMPOL, a superoxide dismutase mimetic, is frequently used to assess the contributions of reactive oxygen species in altering vascular reactivity (Phillips *et al.*, 2005; Halvorson *et al.*, 2019) which has been shown to improve endothelial function in environments of increased oxygen stress. This includes the cerebral circulation and other vascular beds, in multiple models of metabolic disease (goto-kakizaki, OZR) while having no significant effect on healthy controls (Phillips *et al.*, 2005). Although outside the scope of this thesis, pervious work on the OZR has demonstrated increased plasma cytokines, chemokines, and other biomarkers associated with ROS and inflammation including N-tyrosine, TNF-a, and MCP-1 (Brooks *et al.*, 2015). The gene expression data in this thesis support the evidence in the literature citing increased markers of inflammation and oxygen stress as here xanthine oxidase expression, and although not statistically significant interleukin-3 (Il-3) expression were increased. Xanthine oxidase has been implicated in endothelial injury and hypoxia as a major generator of ROS in numerous studies by acting as a catalyst in the formation of uric acid from xanthine releasing ROS (Berry & Hare, 2004; Cai, 2005). Its overexpression can induce a cycle of ROS leading to impaired dilation and thus hypoxia which has been well demonstrated to further induce xanthine oxidase activation (Kayyali *et al.*, 2001; Sohn *et al.*, 2003). Although the observed increased expression of IL-3 in this study was not significant largely due to extremely low expression in LZR, since an approximately 9.5-fold increase was observed it should be noted that IL-

3 has been proposed as a marker of chronic inflammation (Dougan *et al.*, 2019) and thus likely contributes to the pro-inflammatory environment in OZR.

A shift in AA metabolism towards constrictor metabolites and away from dilators, would also contribute to impaired dilation and has been previously measured using pooled arteries. Previous work has found a decrease in NO bioavailability and PGI_2 along with increased TxA_2 and H_2O_2 (Halvorson *et al.*, 2019). COX-2 is a major contributor to the generation of PGI_2 in the endothelium of the MCA (Flavahan, 2007; Funk & FitzGerald, 2007). Therefore, the reduced expression of COX-2 in OZR in this thesis further supports that there are alterations in arachidonic acid metabolism in OZR. However, it is difficult to draw conclusions from the PCR data alone since COX-2 catalyzes the synthesis of prostaglandin H_2 which may then be used to form either the dilator PGI_2 or constrictor TxA_2 catalyzed by prostacyclin synthase or thromboxane synthase respectively. Although it's difficult to discern the implications of down regulation of COX-2, its importance in health is supported by disastrous results in its absence including the death of 30-40% of knockout mice pups within 48 h of birth from patent ductus arteriosus (Loftin *et al.*, 2001), with surviving mice having significantly shorter life spans than wild-type (Morham *et al.*, 1995). Murine models of cardiovascular disease have also established the negative consequences of COX-2 inhibitors on decreasing protection from thrombogenesis, hypertension, and atherogenesis *in vivo* (Tilo *et al.*, 2006). These inhibitors were disastrous in their clinical outcomes enhancing the probability of coronary atherothrombosis, heart failure, and increasing long-term cardiovascular risk (Patrono, 2016).

The reactivity to adenosine was also investigated due to its involvement with metabolic control and to provide a secondary stimulus for dilation with a different mechanistic action than ACh. In contrast to ACh, OZR did not demonstrate significant changes to adenosine sensitivity suggesting there is a different sensitivity to MetS for different mechanisms of vasodilation. Compared to ACh the involvement of NO in adenosine-mediated dilation is much less pronounced (Prentice & Hourani, 2000; Murrant *et al.*, 2014). Impairment in dilation to adenosine is more indicative of K^+ channels along with structural changes than NO bioavailability because of the direct hyperpolarizing effects of adenosine on the vasculature (Paisansathan *et al.*, 2010). No difference in adenosine reactivity has been shown in both gracilis and cremaster muscle arterioles of diabetic rats (Frisbee *et al.*, 2019), as well as in gracilis arterioles and middle cerebral arteries of OZR at this age but impairments could develop if tested at a later timepoint with more pronounced vascular remodeling (Butcher *et al.*, 2013). Although there is strong evidence for the presence of endothelial dysfunction leading to impaired dilator reactivity, the impaired dilator reactivity could also be a result of an increase in vascular tone from myogenic activation, or constrictor reactivity.

In this study both an increase in resting tone and constrictor reactivity in response to 5-HT was observed in OZR as had been previously demonstrated (Phillips *et al.*, 2005). The previously discussed endothelial dysfunction likely contributes to the hyperreactivity to constrictor stimuli by decreasing the buffering effect of endothelium-derived hyperpolarizing factors. However, since vascular hyper-reactivity associated with hyperglycemia and hypertension has been shown to be mediated by increased activation of

voltage-gated Ca^{2+} channels and protein kinase C in arteriolar smooth muscle, even in endothelium-denuded vessels, there are also likely other mechanisms at play (Ungvari *et al.*, 1999; Wendler *et al.*, 2001). Patients with T2DM had significantly higher 5-HT induced constriction on both the arterial and venous sides (internal thoracic artery and saphenous vein) (Matsuo *et al.*, 2011; Yokota *et al.*, 2016) due to higher level of $5\text{-}HT_{2A}$ receptors. Similar results were found by Liu and colleagues (Liu & Folz, 2004) who found enhanced 5-HT-induced constriction in intrapulmonary arteries of similar diameter to MCA after removal of the endothelium or treatment with L-NAME. Interestingly they also showed increased constrictor response with xanthine and xanthine oxidase treatment, an enzyme the current study found to be overexpressed in OZR (Liu & Folz, 2004). Increased expression of xanthine oxidase may be contributing to the observed enhanced vasoconstriction by increasing superoxide levels which has been shown to modulate vasoconstriction through various mechanisms both by acting directly on the vascular smooth muscle or by disrupting endothelium-derived relaxing or contracting factor (Kasemsri & Armstead, 1997; Liu & Folz, 2004).

This study also demonstrated an increase in myogenic activation and agrees with several others demonstrating increased myogenic activation with MetS in OZR (Phillips *et al.*, 2005). The increase in myogenic activation may be due to a loss of endothelium-dependent buffering of constrictor responses. Blunted production of metabolites involved in dilation such as NO or PGI_2, would result in increased constriction in response to higher intralumenal pressure; therefore, endothelial dysfunction may also be contributing to an increase in myogenic activation. This is supported by a decrease in myogenic activation in

the MCA of OZR with acute treatment of TEMPOL (Phillips *et al.*, 2005). Although this reduced the discrepancy between OZR and LZR, increased myogenic activation was still observed compared to the lean counterpart and that increased myogenic tone is elevated in endothelium-denuded vessels suggests there are other factors at play. The greatest risk factor associated with increased myogenic activation is hypertension (Baumbach & Heistad, 1989; Baumbach & Hajdu, 1993). Increased tone is observed in animal models of hypertension and is usually absent in models lacking hypertensive stimuli (Halvorson *et al.*, 2019). It is thought that increased myogenic activation may be a protective mechanism for hypertension in order to limit the potential for edema caused by high pressures in the microcirculation and may represent a chronic contributor to blood flow autoregulation. This study demonstrated mild non-significant remodeling of the MCA as measured by lumen diameter and incremental wall distensibility across a range of pressures under Ca^{2+}-free conditions. Greater remodeling can be expected as these animals age leading to more pronounced effects, as seen by Harris and colleagues (Harris *et al.*, 2005) in diabetic and hypertensive rats, characterized by increased wall-to-lumen ratio from medial hypertrophy and collagen deposition. However, at this age, it is possible that the change in wall mechanics was limited because of the presence of new collagen deposition rather than mature collagen, which has less impact on the distensibility of vessels. Interestingly, hyperglycemia has also been implicated in changes to myogenic tone with both decreased and increased myogenic tone being observed. In the mesenteric arteries of GK rats, the reduced myogenic activation was improved by glycemic control with metformin (Sachidanandam *et al.*, 2009*a*); however, they also suggested that hyperglycemia can activate endothelin receptors enhancing myogenic tone (Sachidanandam *et al.*, 2009*b*).

Taken together these data on the vascular reactivity of the MCA in OZR suggest endothelial dysfunction with increased activation of the VSMC.

Most studies of cerebrovascular reactivity investigate the response to a single stimulus because the simpler interpretations of mechanistic changes; however, in a physiological setting, the cerebral vasculature is constantly responding to a multitude of inputs which must be processed in order to determine a certain level of tone. In addition to testing the response to individual stimuli this study integrated either dilator (ACh, adenosine) stimuli or the constrictor 5-HT with the myogenic response. Integration of multiple stimuli may provide more physiologically relevant insights into the impairments occurring in MetS and is therefore, of interest. These results follow similar trends to the individual responses discussed and demonstrates that in a physiological setting the individual impairments in blunted dilation and hyper-constriction leads to a decreased ability to promote flow.

4.2 Cognitive Testing

This limited ability of the MCA to promote flow in OZR may lead to instances of hypoperfusion in cerebral tissue which has the potential to result in cognitive impairment. The documented interaction of cerebrovascular disease and cognitive impairment in Mets as well as the presence of both depressive and anxious symptoms in the OZR (Brooks *et al.*, 2018*b*) encouraged an investigation into the cognitive outcomes associated with the OZR. The MWM demonstrated impaired spatial learning in OZR as measured by increased average latency to reach the platform in learning trials two to six. Impaired spatial memory has previously been demonstrated in a similar model of MetS, also based on hyperphagia,

named the Otsuka Long-Evans Tokushima fatty (OLETE) rats. They have impaired spatial memory in both the MWM (Li *et al.*, 2002) and radial arm maze (Nomoto *et al.*, 1999) which were partially attributed to impaired vasoreactivity to insulin without changes to bulk blood flow. Also of note is an increased proportion of time spent in the target quadrant during the probe trial, suggesting the potential for either decreased behaviour flexibility or better memory. However, since improved memory was not demonstrated in set shifting tasks this is unlikely. The interpretation of enhanced memory in OZR would also go against some previous work in 4 month old OZR performing a go/no-go delayed alternation task where they performed worse when long intervals between trials were used, suggesting a memory impairment (Winocur *et al.*, 2005) which they attributed to reduced plasma membrane association of glucose transporter type 4 (GLUT4) although no learning impairment was found.

The cognitive impairments to OZR and other similar models appear to be task dependent. No changes were observed in the Barnes maze with OLETE rats at 40 weeks of age or in Sprague-Dawley rats on an ultra-processed diet termed the cafeteria diet at 4 months of age, or in learning go/no-go task in OZR (Gomez-Smith *et al.*, 2016; Olver *et al.*, 2017) just as the present study found no difference in set shift task learning, memory, or behavioural flexibility. Interestingly in the operant conditioning tasks OZR had significantly more omissions in the visual cue discrimination task and trended towards increased omissions over the lean controls in the other two tasks. Generally, omissions are associated with task motivation and so it is interesting that the OZR, a model of MetS based on hyperphagia, would demonstrate lower motivation for a task that involves a food reward. Loss of motivation has been shown in rats on a refined foods diet associated with

obesity and diabetes in an operant conditioning chamber task (Blaisdell *et al.*, 2017). Since this refined foods diet model has been associated with depression and previous work in the OZR has demonstrated the presence of depressive symptoms through increased coat score, latency to begin consumption in novelty supressed feeding, and latency to begin grooming after a sucrose spray (Brooks *et al.*, 2018*b*), the increased omissions in the operant conditioning chamber tasks could be a reflection of depressive symptoms and warrants further investigation.

4.3 Neuroinflammation

These mild cognitive impairments do not appear to be related to inflammation in the white matter or hippocampus at this age since neither showed increased OX6 positive microglia or GFAP positive astrocytes in OZR. These results go against the clinical findings that lesions in the white matter, which has been shown to be highly susceptible to pathological changes particularly vascular disruption (Li *et al.*, 2016; Wang *et al.*, 2016), tend to be present well before symptoms of cognitive impairment start to appear (Brickman *et al.*, 2015; Lee *et al.*, 2016). In a study investigating the comorbidity of MetS and dementia, the TgAPP21 rat model of Alzheimer's disease was fed a hypercaloric diet high in fat and simple sugars. The transgenic rats displayed both increased microglial activation and astrogliosis located primarily in the white matter; however, the hypercaloric diet alone was not sufficient to result in any inflammatory changes between wild type rats.

The high fat diet used to induce MetS was associated with an inability to improve path efficiency in a 16 trials MWM protocol performed over 4 days, although all other behaviour measures were unchanged (Ivanova *et al.*, 2020). Also of note is that the rats in that study

were significantly older (9 months compared to 18 weeks) then the rats used in this thesis. This likely contributes to the absence of any significant neuroinflammation found in these rats since 18 weeks is significantly younger than the equivalent of mid-life in humans where these risk factors being to appear (Andreollo *et al.*, 2012). This may explain why this thesis did not find the mild cognitive impairments to be associated with any significant neuroinflammation.

4.4 General Discussion and Conclusions

This study describes some of the impairment to cerebrovascular tone regulation that develop in the OZR model of MetS related to both vascular reactivity and endothelial cell function related gene expression. Endothelial dysfunction was present in the MCA of OZR demonstrated by blunted dilation in response to ACh, while an enhanced constrictor response to 5-HT and pressure was also demonstrated. These changes to cerebrovascular tone regulation are the results of the genesis of a proinflammatory and prooxidant environment in the OZR. Given the demonstrated altered cerebrovascular reactivity with evidence of mild cognitive dysfunction, this study provides a framework for additional investigation into mechanistic pathways and potential therapeutics for restoring function in the cerebral circulation and improving current negative outcomes associated with MetS including vascular cognitive impairment.

References

Ainslie PN, Ashmead JC, Ide K, Morgan BJ & Poulin MJ (2005). Differential responses to CO2 and sympathetic stimulation in the cerebral and femoral circulations in humans. *J Physiol* **566,** 613–624.

Alfaro FJ, Lioutas V-A, Pimentel DA, Chung C-C, Bedoya F, Yoo W-K & Novak V (2016). Cognitive decline in metabolic syndrome is linked to microstructural white matter abnormalities. *J Neurol* **263,** 2505–2514.

Anand-Srivastava MB, Franks DJ, Cantin M & Genest J (1982). Presence of "Ra" and "P"-site receptors for adenosine coupled to adenylate cyclase in cultured vascular smooth muscle cells. *Biochem Biophys Res Commun* **108,** 213–219.

Andreollo NA, Santos EF dos, Araújo MR & Lopes LR (2012). Rat's age versus human's age: what is the relationship? *Arq Bras Cir Dig* **25,** 49–51.

Barbato JE, Zuckerbraun BS, Overhaus M, Raman KG & Tzeng E (2005). Nitric oxide modulates vascular inflammation and intimal hyperplasia in insulin resistance and the metabolic syndrome. *Am J Physiol Hear Circ Physiol* **289,** H228–H236.

Bari F, Louis TM & Busija DW (1998). Effects of Ischemia on Cerebral Arteriolar Dilation to Arterial Hypoxia in Piglets. *Stroke* **29,** 222–228.

Baumbach GL, Faraci FM & Heistad DD (1994). Effects of local reduction in pressure on endothelium-dependent responses of cerebral arterioles. *Stroke* **25,** 1456–1462.

Baumbach GL & Hajdu MA (1993). Mechanics and composition of cerebral arterioles in renal and spontaneously hypertensive rats. *Hypertens (Dallas, Tex 1979)* **21,** 816–826.

Baumbach GL & Heistad DD (1989). Remodeling of Cerebral Arterioles in Chronic Hypertension. *Hypertension* **13,** 968–972.

Bayliss WM (1902). On the local reactions of the arterial wall to changes of internal pressure. *J Physiol* **28,** 220–231.

Berne RM, Richard Winn H & Rubio R (1981). The local regulation of cerebral blood flow. *Prog Cardiovasc Dis* **24,** 243–260.

Von Bernhardi R & Eugenín J (2004). Microglial reactivity to β-amyloid is modulated by astrocytes and proinflammatory factors. *Brain Res* **1025,** 186–193.

Berry CE & Hare JM (2004). Xanthine oxidoreductase and cardiovascular disease: Molecular mechanisms and pathophysiological implications. *J Physiol* **555,** 589–606.

Binks AP, Cunningham VJ, Adams L & Banzett RB (2008). Gray matter blood flow change is unevenly distributed during moderate isocapnic hypoxia in humans. *J Appl Physiol* **104,** 212–217.

Blaisdell AP, Biedermann T, Sosa E, Abuchaei A, Youssef N & Bradesi S (2017). An obesogenic refined low-fat diet disrupts attentional and behavioral control processes in a vigilance task in rats. *Behav Processes* **138,** 142–151.

Boutayeb A, Boutayeb S & Boutayeb W (2013). Multi-morbidity of non communicable diseases and equity in WHO Eastern Mediterranean countries. *Int J Equity Health* **12,** 60.

Bray GA (1977). The Zucker fatty rat: a review. *Fed Proc* **36,** 148–153.

Brickman AM, Zahodne LB, Guzman VA, Narkhede A, Meier IB, Griffith EY, Provenzano FA, Schupf N, Manly JJ, Stern Y, Luchsinger JA & Mayeux R (2015). Reconsidering harbingers of dementia: Progression of parietal lobe white matter hyperintensities predicts Alzheimer's disease incidence. *Neurobiol Aging* **36,** 27–32.

Brooks S, Brnayan KW, DeVallance E, Skinner R, Lemaster K, Sheets JW, Pitzer CR, Asano S, Bryner RW, Olfert IM, Frisbee JC & Chantler PD (2018*a*). Psychological stress-induced cerebrovascular dysfunction: the role of metabolic syndrome and exercise. *Exp Physiol* **103,** 761–776.

Brooks SD, DeVallance E, D'Audiffret AC, Frisbee SJ, Tabone LE, Shrader CD, Frisbee JC & Chantler PD (2015). Metabolic syndrome impairs reactivity and wall mechanics of cerebral resistance arteries in obese Zucker rats. *Am J Physiol - Hear Circ Physiol* **309,** H1846–H1859.

Brooks SD, Hileman SM, Chantler PD, Milde SA, Lemaster KA, Frisbee SJ, Shoemaker JK, Jackson DN & Frisbee JC (2018*b*). Protection from chronic stress-and depressive symptom-induced vascular endothelial dysfunction in female rats is abolished by preexisting metabolic disease. *Am J Physiol Hear Circ Physiol* **314,** 1085–1097.

Brown AM & Ransom BR (2007). Astrocyte glycogen and brain energy metabolism. *Glia* **55,** 1263–1271. Available at: www.interscience.wiley. [Accessed August 14, 2018].

Burnstock G (1985). Neurogenic Control of Cerebral Circulation. *Cephalalgia* **2,** 25–33.

Busse R, Förstermann U, Matsuda H & Pohp U (1984). The role of prostaglandins in the endothelium-mediated vasodilatory response to hypoxia*. *Pflugers Arch* **401,** 77–83.

Busse R, Pohl U, Kellner C & Klemm U (1983). Endothelial Cells are Involved in the Vasodilatory Response to Hypoxia*. *Pflugers Arch* **397,** 78–80.

Butcher JT, Goodwill AG & Frisbee JC (2012). The ex vivo Isolated Skeletal Microvessel Preparation for Investigation of Vascular Reactivity. *J Vis Exp* **62,** e3674.

Butcher JT, Goodwill AG, Stanley SC & Frisbee JC (2013). Differential impact of dilator stimuli on increased myogenic activation of cerebral and skeletal muscle resistance arterioles in obese zucker rats. *Microcirculation* **20,** 579–589.

Cai H (2005). Hydrogen peroxide regulation of endothelial function: Origins, mechanisms, and consequences. *Cardiovasc Res* **68,** 26–36.

Carter RW & Kanagy NL (2002). Tyrosine kinases regulate intracellular calcium during 2-adrenergic contraction in rat aorta. *Am J Physiol Hear Circ Physiol* **283,** H1673–H1680.

De Carvalho Vidigal F, Bressan J, Babio N & Salas-Salvadó J (2013). Prevalence of metabolic syndrome in Brazilian adults: A systematic review. *BMC Public Health* **13,** 1198.

Chantler PD & Frisbee JC (2015). Arterial Function in Cardio-Metabolic Diseases: From the Microcirculation to the Large Conduits. *Prog Cardiovasc Dis* **57,** 489–496.

Chantler PD & Larkin KT (2020). *Cardiovascular Implications of Stress and Depression*.

Chen W et al. (2017). Recurrent stroke in minor ischemic stroke or transient ischemic attack with metabolic syndrome and/or diabetes mellitus. *J Am Heart Assoc* **6,** 1–12.

Cipolla MJ (2010). *The Cerebral Circulation*. Morgan & Claypool Life Sciences.

Cipolla MJ, Liebeskind DS & Chan SL (2018). The importance of comorbidities in ischemic stroke: Impact of hypertension on the cerebral circulation. *J Cereb Blood Flow Metab* **38,** 2129–2149.

Dandona P, Aljada A, Chaudhuri A, Mohanty P & Garg R (2005). Metabolic Syndrome A Comprehensive Perspective Based on Interactions Between Obesity, Diabetes, and Inflammation. *Circulation* **111,** 1448–1454.

Davies PF (2009). Hemodynamic shear stress and the endothelium in cardiovascular pathophysiology. *Nat Clin Pract Cardiovasc Med* **6,** 16–26.

Davis MJ & Hill MA (1999). Signaling Mechanisms Underlying the Vascular Myogenic Response. *Physiol Rev* **79,** 387–423.

Davis MJ & Sikes PJ (1990). Myogenic responses of isolated arterioles: test for a rate-sensitive mechanism Myogenic re-sponses of isolated arterioles: test for a rate-sensitive mechanism. *Am J Physiol Hear Circ Physiol* **28,** H1890–H1900.

DeVallance E, Fournier SB, Donley DA, Bonner DE, Lee K, Frisbee JC & Chantler PD (2015). Is obesity predictive of cardiovascular dysfunction independent of cardiovascular risk factors? *Int J Obes* **39,** 244–253.

Diamond A (2013). Executive functions. *Annu Rev Psychol* **64,** 135–168.

Donley DA, Fournier SB, Reger BL, DeVallance E, Bonner DE, Olfert IM, Frisbee JC & Chantler PD (2014). Aerobic exercise training reduces arterial stiffness in metabolic syndrome. *J Appl Physiol* **116,** 1396–1404.

Dougan M, Dranoff G & Dougan SK (2019). GM-CSF, IL-3, and IL-5 Family of Cytokines: Regulators of Inflammation. *Immunity* **50,** 796–811.

El-Yazbi AF & Abd-Elrahman KS (2017). ROK and arteriolar myogenic tone generation: Molecular evidence in health and disease. *Front Pharmacol* **8,** 1–10.

Ferdinand KC, Rodriguez F, Nasser SA, Caballero AE, Puckrein GA, Zangeneh F, Mansour M, Foody JM, Pemu PE & Ofili EO (2014). Cardiorenal metabolic syndrome and cardiometabolic risks in minority populations. *CardioRenal Med* **4,** 1–11.

Filley CM (2005). White matter and behavioral neurology. *Ann N Y Acad Sci* **1064,** 162–183.

Flavahan NA (2007). Balancing prostanoid activity in the human vascular system. *Trends Pharmacol Sci* **28,** 106–110.

Frisbee JC (2005). Hypertension-independent microvascular rarefaction in the obese Zucker rat model of the metabolic syndrome. *Microcirculation* **12,** 383–392.

Frisbee JC, Lewis MT, Kasper JD, Chantler PD & Wiseman RW (2019). Type 2 diabetes mellitus in the Goto-Kakizaki rat impairs microvascular function and contributes to premature skeletal muscle fatigue. *J Appl Physiol* **126,** 626–637.

Frisbee JC, Maier KG, Falck JR, Roman RJ & Lombard JH (2002*a*). Integration of hypoxic dilation signaling pathways for skeletal muscle resistance arteries. *Am J Physiol Regul Integr Comp Physiol* **283,** R309–R319.

Frisbee JC, Maier KG & Stepp DW (2002*b*). Oxidant stress-induced increase in myogenic activation of skeletal muscle resistance arteries in obese Zucker rats. *Am J Physiol - Hear Circ Physiol* **283,** H2160–H2168.

Fu J & Prasad HC (2014). Changing epidemiology of metabolic syndrome and type 2 diabetes in Chinese youth. *Curr Diab Rep* **14,** 447.

Fujii K, Heistad DD & Faraci FM (1991). Flow-Mediated Dilatation of the Basilar Artery In Vivo. *Circ Res* **69,** 697–705.

Funk CD & FitzGerald GA (2007). COX-2 inhibitors and cardiovascular risk. *J Cardiovasc Pharmacol* **50,** 470–479.

Garcia-Roldan J-L & Bevan JA (1991). Augmentation of Endothelium-Independent Flow Constriction in Pial Arteries at High Intravascular Pressures. *Hypertension* **17,** 870–874.

Garcia-Roldan JL & Bevan JA (1990). Flow-induced constriction and dilation of cerebral resistance arteries. *Circ Res* **66,** 1445–1448.

Gebremedhin D, Gopalakrishnan S & Harder DR (2014). Endogenous events modulating myogenic regulation of cerebrovascular function. *Curr Vasc Pharmacol* **12,** 810–817.

Gomez-Smith M, Karthikeyan S, Jeffers MS, Janik R, Thomason LA, Stefanovic B & Corbett D (2016). A physiological characterization of the Cafeteria diet model of metabolic syndrome in the rat. *Physiol Behav* **167,** 382–391.

González JM, Beatriz S, Conde MV, Fernández-Alfonso MS, González MC & Arribas SM (2008). Hypertension increases middle cerebral artery resting tone in spontaneously hypertensive rats: role of tonic vasoactive factor availability. *Clin Sci* **114,** 651–659.

Gordon GRJ, Choi HB, Ellis-Davies GCR & Macvicar BA (2008). Brain metabolic state dictates the polarity of astrocyte control over the cerebrovasculature. *Nature* **456,** 745–749.

Hachinski V, Iadecola C, Petersen RC, Breteler MM, Nyenhuis DL, Black SE, Powers WJ, DeCarli C, Merino JG, Kalaria RN, Vinters H V., Holtzman DM, Rosenberg GA, Dichgans M, Marler JR & Leblanc GG (2006). National Institute of

Neurological Disorders and Stroke-Canadian Stroke Network vascular cognitive impairment harmonization standards. *Stroke* **37,** 2220–2241.

Halvorson BD, Whitehead SN, Mcguire JJ, Wiseman RW & Frisbee JC (2019). Endothelium-dependent impairments to cerebral vascular reactivity with type 2 diabetes mellitus in the Goto-Kakizaki rat. *J Physiol Regul Integr Comp Physiol* **317,** R149–R159.

Harris AK, Hutchinson JR, Sachidanandam K, Johnson MH, Dorrance AM, Stepp DW, Fagan SC & Ergul A (2005). Type 2 Diabetes Causes Remodeling of Cerebrovasculature via Differential Regulation of Matrix Metalloproteinases and Collagen Synthesis Role of Endothelin-1. *Diabetes* **54,** 2638–2644.

Harry GJ & Kraft AD (2008). Neuroinflammation and microglia: Considerations and approaches for neurotoxicity assessment. *Expert Opin Drug Metab Toxicol* **4,** 1265–1277.

Hayashi K, Kanda T, Homma K, Tokuyama H, Okubo K, Takamatsu I, Tatematsu S, Kumagai H & Saruta T (2002). Altered renal microvascular response in Zucker obese rats. *Metabolism* **51,** 1553–1561.

Heistad DD & Baumbach GL (1992). Cerebral vascular changes during chronic hypertension: good guys and bad guys. *J Hypertens Suppl* **10,** S71-5.

Humphrey JD (2008). Mechanisms of arterial remodeling in hypertension coupled roles of wall shear and intramural stress. *Hypertension* **52,** 195–200.

Iadecola C & Davisson RL (2008). Hypertension and Cerebrovascular Dysfunction. *Cell Metab* **7,** 476–484.

Iadecola C & Gottesman RF (2019). Neurovascular and Cognitive Dysfunction in Hypertension: Epidemiology, Pathobiology, and Treatment. *Circ Res* **124,** 1025–1044.

Ivanova N, Liu Q, Agca C, Agca Y, Noble EG, Whitehead SN & Cechetto DF (2020). White matter inflammation and cognitive function in a co-morbid metabolic syndrome and prodromal Alzheimer's disease rat model. *J Neuroinflammation* **17,** 1–18.

Jaggar JH, Porter VA, Lederer WJ & Nelson MT (2000). Calcium sparks in smooth muscle. *Am J Physiol - Cell Physiol* **278,** C235-256.

Jarajapu YPR, Guberski DL, Grant MB & Knot HJ (2008). Myogenic tone and reactivity of cerebral arteries in Type II diabetic BBZDR/Wor rat. *Eur J Pharmacol* **579,** 298–307.

Johnson FK, Johnson RA, Durante W, Jackson KE, Stevenson BK, Peyton KJ & Johnson FK (2006). Metabolic syndrome increases endogenous carbon monoxide production to promote hypertension and endothelial dysfunction in obese Zucker rats. *Am J Physiol Regul Integr Comp Physiol* **290,** 601–608.

Jones CJ, Kuo L, Davis MJ & Chilian WM (1993). Myogenic and flow-dependent control mechanisms in the coronary microcirculation. *Basic Res Cardiol* **88,** 2–10.

de Jong J., de Jonge R, Keijzer E & Bradamante S (2000). The role of adenosine in preconditioning. *Pharmacol Ther* **87,** 141–149.

Kasemsri T & Armstead WM (1997). Endothelin production links superoxide generation to altered opioid- induced pial artery vasodilation after brain injury in pigs. *Stroke* **28,** 190–197.

Kayyali US, Donaldson C, Huang H, Abdelnour R & Hassoun PM (2001). Phosphorylation of Xanthine Dehydrogenase/Oxidase in Hypoxia. *J Biol Chem* **276,** 14359–14365.

Kazuyama E, Saito M, Kinoshita Y, Satoh I, Dimitriadis F & Satoh K (2009). Endothelial dysfunction in the early- and late-stage type-2 diabetic Goto-Kakizaki rat aorta. *Mol Cell Biochem* **332,** 95–102.

Koller A & Toth P (2012). Contribution of flow-dependent vasomotor mechanisms to the autoregulation of cerebral blood flow. *J Vasc Res* **49,** 375–389. Available at: www.karger.com [Accessed June 4, 2019].

Kozora E & Filley CM (2011). Cognitive dysfunction and white matter abnormalities in systemic lupus erythematosus. *J Int Neuropsychol Soc* **17,** 385–392.

Kurtz TW, Morris RC & Pershadsingh HA (1989). The zucker fatty rat as a genetic model of obesity and hypertension. *Hypertension* **13,** 896–901.

Kusano Y, Echeverry G, Miekisiak G, Kulik TB, Aronhime SN, Chen JF & Winn HR (2010). Role of adenosine A2 receptors in regulation of cerebral blood flow during induced hypotension. *J Cereb Blood Flow Metab* **30,** 808–815.

Lee S et al. (2016). White matter hyperintensities are a core feature of Alzheimer's disease: Evidence from the dominantly inherited Alzheimer network. *Ann Neurol* **79,** 929–939.

Levit A, Regis AM, Garabon JR, Oh SH, Desai SJ, Rajakumar N, Hachinski V, Agca Y, Agca C, Whitehead SN & Allman BL (2017). Behavioural inflexibility in a comorbid rat model of striatal ischemic injury and mutant hAPP overexpression. *Behav Brain Res*; DOI: 10.1016/j.bbr.2017.07.006.

Levit A, Regis AM, Gibson A, Hough OH, Maheshwari S, Agca Y, Agca C, Hachinski V, Allman BL & Whitehead SN (2019). Impaired behavioural flexibility related to white matter microgliosis in the TgAPP21 rat model of Alzheimer disease. *Brain Behav Immun*; DOI: 10.1016/j.bbi.2019.02.013.

Li H & Förstermann U (2013). Uncoupling of endothelial NO synthase in atherosclerosis and vascular disease. *Curr Opin Pharmacol* **13,** 161–167.

Li Q & Puro DG (2001). Adenosine activates ATP-sensitive K+ currents in pericytes of rat retinal microvessels: role of A1 and A2a receptors. *Brain Res* **907,** 93–99.

Li X, Ma C, Sun X, Zhang J, Chen Y, Chen K & Zhang Z (2016). Disrupted white matter structure underlies cognitive deficit in hypertensive patients. *Eur Radiol* **26,** 2899–2907.

Li XL, Aou S, Hori T & Oomura Y (2002). Spatial memory deficit and emotional

abnormality in OLETF rats. *Physiol Behav* **75,** 15–23.

Van Lieshout JJ, Wieling W, Karemaker JM & Secher NH (2003). Syncope, cerebral perfusion, and oxygenation. *J Appl Physiol* **94,** 833–848.

Liu JQ & Folz RJ (2004). Extracellular superoxide enhances 5-HT-induced murine pulmonary artery vasoconstriction. *Am J Physiol - Lung Cell Mol Physiol*; DOI: 10.1152/ajplung.00006.2004.

Liu Q & Flavahan NA (1997). Hypoxic dilatation of porcine small coronary arteries : role of endothelium and K ATP -channels. *Br J Pharmacol* **120,** 728–734.

Loftin CD, Trivedi DB, Tiano HF, Clark JA, Lee CA, Epstein JA, Morham SG, Breyer MD, Nguyen MT, Hawkins BM, Goulet JL, Smithies O, Koller BH & Langenbach R (2001). Failure of ductus arteriosus closure and remodeling in neonatal mice dificient in cyclooxygenase-1 and cyclooxygenase-2. *Proc Natl Acad Sci U S A* **98,** 1059–1064.

Lombard JH, Liu YP, Fredricks KT, Bizub DM, Roman RJ & Rusch NJ (1999). Electrical and mechanical responses of rat middle cerebral arteries to reduced Po-2 and prostacyclin. *Am J Physiol Hear Circ Physiol* **276,** H509–H516.

López-Farré A, Rodriguez-Feo JA, García-Colis E, Gomez J, López-Blaya A, Fortes J, De Andrés R, Rico L & Casado S (2002). Reduction of the soluble cyclic GMP vasorelaxing system in the vascular wall of stroke-prone spontaneously hypertensive rats: Effect of the α 1 -receptor blocker doxazosin. *J Hypertens* **20,** 463–470.

Lue LF, Kuo YM, Beach T & Walker DG (2010). Microglia activation and anti-inflammatory regulation in alzheimer's disease. *Mol Neurobiol* **41,** 115–128.

Lynch FM, Austin C, Heagerty AM & Izzard AS (2006). Adenosine and hypoxic dilation of rat coronary small arteries: roles of the ATP-sensitive potassium channel, endothelium and nitric oxide. *Am J Physiol Hear Circ Physiol* **290,** H1145–H1150.

Mandell DM, Han JS, Poublanc J, Crawley AP, Kassner A, Fisher JA & Mikulis DJ (2008). Selective Reduction of Blood Flow to White Matter During Hypercapnia Corresponds With Leukoaraiosis. *Stroke* **39,** 1993–1998.

Manso Y, Holland PR, Kitamura A, Szymkowiak S, Duncombe J, Hennessy E, Searcy JL, Marangoni M, Randall AD, Brown JT, McColl BW & Horsburgh K (2018). Minocycline reduces microgliosis and improves subcortical white matter function in a model of cerebral vascular disease. *Glia* **66,** 34–46.

Matsuo Y, Kuwabara M, Tanaka-Totoribe N, Kanai T, Nakamura E, Gamoh S, Suzuki A, Asada Y, Hisa H & Yamamoto R (2011). The defective protein level of myosin light chain phosphatase (MLCP) in the isolated saphenous vein, as a vascular conduit in coronary artery bypass grafting (CABG), harvested from patients with diabetes mellitus (DM). *Biochem Biophys Res Commun* **412,** 323–327.

Messina EJ, Sun D, Koller A, Wolin MS & Kaley G (1992). Role of Endothelium-Derived Prostaglandins in Hypoxia-Elicited Arteriolar Dilation in Rat Skeletal Muscle. *Circ Res* **71,** 790–796.

Michinaga S & Koyama Y (2015). Pathogenesis of brain edema and investigation into

anti-edema drugs. *Int J Mol Sci* **16,** 9949–9975.

Misiak B, Leszek J & Kiejna A (2012). Metabolic syndrome, mild cognitive impairment and Alzheimer's disease-The emerging role of systemic low-grade inflammation and adiposity. *Brain Res Bull* **89,** 144–149.

Morham SG, Langenbach R, Loftin CD, Tiano HF, Vouloumanos N, Jennette JC, Mahler JF, Kluckman KD, Ledford A, Lee CA & Smithies O (1995). Prostaglandin synthase 2 gene disruption causes severe renal pathology in the mouse. *Cell* **83,** 473–482.

Morii S, Ngai AC, Ko KR & Winn HR (1987). Role of adenosine in regulation of cerebral blood flow: Effects of theophylline during normoxia and hypoxia. *Am J Physiol - Hear Circ Physiol* **253,** H165–H175.

Murrant CL, Dodd JD, Foster AJ, Inch KA, Muckle FR, Ruiz DA, Simpson JA & Scholl JHP (2014). Prostaglandins induce vasodilatation of the microvasculature during muscle contraction and induce vasodilatation independent of adenosine. *J Physiol* **592,** 1267–1281.

Ng TP, Feng L, Nyunt MSZ, Feng L, Gao Q, Lim ML, Collinson SL, Chong MS, Lim WS, Lee TS, Yap P & Yap KB (2016). Metabolic syndrome and the risk of mild cognitive impairment and progression to dementia follow-up of the Singapore longitudinal ageing study cohort. *JAMA Neurol* **73,** 456–463.

Ngai AC & Winn HR (1993). Effects of Adenosine and Its Analogues on Isolated Intracerebral Arterioles Extraluminal and Intraluminal Application. *Circ Res* **73,** 448–457.

Nomoto S, Miyake M, Ohta M, Funakoshi A & Miyasaka K (1999). Impaired learning and memory in OLETF rats without cholecystokinin (CCK)-A receptor. *Physiol Behav* **66,** 869–872.

Nöth U, Kotajima F, Delchmann R, Turner R & Corfield DR (2008). Mapping of the cerebral vascular response to hypoxia and hypercapnia using quantutative perfusion MRI at 3T. *NMR Biomed* **21,** 464–472.

Ohta M, Toyama K, Gutterman DD, Campbell WB, Lemaître V, Teraoka R & Miura H (2013). Ecto-5′-nucleotidase, CD73, is an endothelium-derived hyperpolarizing factor synthase. *Arterioscler Thromb Vasc Biol* **33,** 629–636.

Olver TD, Mcdonald MW, Klakotskaia D, Richardson RA, Jasperse JL, Melling CWJ, Schachtman TR, Yang HT, Emter CA & Laughlin MH (2017). A chronic physical activity treatment in obese rats normalizes the contributions of ET-1 and NO to insulin-mediated posterior cerebral artery vasodilation. *J Appl Physiol* **122,** 1040–1050.

Osol G, Brekke JF, Mcelroy-Yaggy K & Gokina NI (2002). Myogenic tone, reactivity, and forced dilatation: a three-phase model of in vitro arterial myogenic behavior. *Am J Physiol Hear Circ Physiol* **283,** H2260–H2267.

Paisansathan C, Xu H, Vetri F, Hernandez M & Pelligrino DA (2010). Interactions between adenosine and K + channel-related pathways in the coupling of somatosensory activation and pial arteriolar dilation. *Am J Physiol - Hear Circ*

Physiol **299,** 2009–2017.

Paterno R, Heistad DD & Faraci FM (2000). Potassium channels modulate cerebral autoregulation during acute hypertension. *Am J Physiol Hear Physiol* **278,** H2003–H2007.

Patrono C (2016). Cardiovascular effects of cyclooxygenase-2 inhibitors: a mechanistic and clinical perspective. *Br J Clin Pharmacol*957–964.

Payne RA, Wilkinson IB & Webb DJ (2010). Arterial stiffness and hypertension: Emerging concepts. *Hypertension* **55,** 9–14.

Peterson EC, Wang Z & Britz G (2011). Regulation of cerebral blood flow. *Int J Vasc Med* **2011,** 8.

Phillips SA, Sylvester FA & Frisbee JC (2005). Oxidant stress and constrictor reactivity impair cerebral artery dilation in obese Zucker rats. *Am J Physiol Regul Integr Comp Physiol* **288,** R522–R530.

Piechnik SK, Chiarelli PA & Jezzard P (2008). Modelling vascular reactivity to investigate the basis of the relationship between cerebral blood volume and flow under CO 2 manipulation. *Neuroimage* **39,** 107–118.

Pires PW, Dams Ramos CM, Matin N & Dorrance AM (2013). The effects of hypertension on the cerebral circulation. *Am J Physiol Hear Circ Physiol* **304,** H1598–H1614.

Prentice DJ & Hourani SMO (2000). Characterisation of adenosine receptors mediating relaxation in hamster isolated aorta. *Naunyn Schmiedebergs Arch Pharmacol* **362,** 427–434.

Ramkumar V, Hallam DM & Nie Z (2001). Adenosine, Oxidative Stress and Cytoprotection. *Jpn J Pharmacol* **86,** 265–274.

Reich T & Rusinek H (1989). Cerebral Cortical and White Matter Reactivity to Carbon Dioxide. *Stroke* **20,** 453–457.

Rogers J, Churilov L, Hannan AJ & Renoir T (2017). Search strategy selection in the Morris water maze indicates allocentric map formation during learning that underpins spatial memory formation. *Neurobiol Learn Mem* **139,** 37–49.

Roman R & Dokkum R (2014). Commentary on the Special Issue on the Impact of Myogenic Tone in Health and Disease. *Curr Vasc Pharmacol* **12,** 779–780.

Rosenberg GA (2009). Inflammation and White Matter Damage in Vascular Cognitive Impairment. *Stroke* **40,** S20–S23.

Sachidanandam K, Hutchinson JR, Elgebaly MM, Mezzetti EM, Dorrance AM, Motamed K & Ergul A (2009*a*). Glycemic control prevents microvascular remodeling and increased tone in Type 2 diabetes: link to endothelin-1. *Am J Physiol Regul Integr Comp Physiol* **296,** 952–959.

Sachidanandam K, Hutchinson JR, Elgebaly MM, Mezzetti EM, Dorrance AM, Motamed K & Ergul A (2009*b*). Glycemic control prevents microvascular remodeling and increased tone in Type 2 diabetes: link to endothelin-1. *Am J Physiol Regul Integr*

Comp Physiol **296,** 952–959.

Sato A, Sakuma I & Gutterman DD (2003). Mechanism of dilation to reactive oxygen species in human coronary arterioles. *Am J Physiol - Hear Circ Physiol* **285,** 2345–2354.

Schubert R, Kalentchuk VU & Krien U (2002). Rho kinase inhibition partly weakens myogenic reactivity in rat small arteries by changing calcium sensitivity. *Am J Physiol Hear Circ Physiol* **283,** H2288–H2295.

Shin JA, Lee JH, Lim SY, Ha HS, Kwon HS, Park YM, Lee WC, Kang M Il, Yim HW, Yoon KH & Son HY (2013). Metabolic syndrome as a predictor of type 2 diabetes, and its clinical interpretations and usefulness. *J Diabetes Investig* **4,** 334–343.

Smith BA, Clayton EW & Robertson D (2011). Experimental Arrest of Cerebral Blood Flow in Human Subjects: the Red Wing studies revisited. *Perspect Biol Med*; DOI: 10.1353/pbm.2011.0018.

Smith EE (2017). Clinical presentations and epidemiology of vascular dementia. *Clin Sci* **131,** 1059–1068.

Sofroniew M V. & Vinters H V. (2010). Astrocytes: Biology and pathology. *Acta Neuropathol* **119,** 7–35.

Sohn HY, Krotz F, Gloe T, Keller M, Theisen K, Klauss V & Pohl U (2003). Differential regulation of xanthine and NAD(P)H oxidase by hypoxia in human umbilical vein endothelial cells. Role of nitric oxide and adenosine. *Cardiovasc Res* **58,** 638–646.

Sylvester FA, Stepp DW, Frisbee JC & Lombard JH (2002). High-salt diet depresses acetylcholine reactivity proximal to NOS activation in cerebral arteries. *Am J Physiol Heart Circ Physiol* **283,** H353-63.

Tabrizchi R & Bedi S (2001). Pharmacology of adenosine receptors in the vasculature. *Pharmacol Ther* **91,** 133–147.

Thorin-Trescases N & Bevan JA (1998). High Levels of Myogenic Tone Antagonize the Dilator Response to Flow of Small Rabbit Cerebral Arteries. *Stroke* **29,** 1194–1201.

Tilo G, Susanne F & Garret AF (2006). Biological basis for the cardiovascular consequences of COX-2 inhibition: therapeutic challenges and opportunities. *J Clin Invest* **116,** 4–15.

Toblli JE, Cao G, DeRosa G, Di Gennaro F & Forcada P (2004). Angiotensin-Converting enzyme inhibition and angiogenesis in myocardium of obese Zucker rats. *Am J Hypertens* **17,** 172–180.

Tsai C-K, Kao T-W, Lee J-T, Wu C-J, Hueng D-Y, Liang C-S, Wang G-C, Yang F-C & Chen W-L (2016). Increased risk of cognitive impairment in patients with components of metabolic syndrome. *Medicine (Baltimore)* **95,** e4791.

Ungvari Z, Pacher P, Kecskemeti V, Papp G, Szollár L & Koller A (1999). Increased myogenic tone in skeletal muscle arterioles of diabetic rats. Possible role of increased activity of smooth muscle Ca2+ channels and protein kinase C. *Cardiovasc Res* **43,** 1018–1028.

Vaziri ND, Xu ZG, Shahkarami A, Huang KT, Rodríguez-Iturbe B & Natarajan R (2005). Role of AT-1 receptor in regulation of vascular MCP-1, IL-6, PAI-1, MAP kinase, and matrix expressions in obesity. *Kidney Int*; DOI: 10.1111/j.1523-1755.2005.00750.x.

Vorhees C V. & Williams MT (2014). Assessing spatial learning and memory in rodents. *ILAR J* **55,** 310–332.

Wang Y, Liu G, Hong D, Chen F, Ji X & Cao G (2016). White matter injury in ischemic stroke. *Prog Neurobiol* **141,** 45–60.

Von der Weid PY (2013). Lymphatic myogenic constriction - how lymphatic vessels pump lymph uphill. *J Physiol* **591,** 391–392.

Wendler O, Landwehr P, Bandner-Risch D, Georg T & Schäfers HJ (2001). Vasoreactivity of arterial grafts in the patient with diabetes mellitus: Investigations on internal thoracic artery and radial artery conduits. *Eur J Cardio-thoracic Surg* **20,** 305–311.

Willie CK, Macleod DB, Shaw AD, Smith KJ, Tzeng YC, Eves ND, Ikeda K, Graham J, Lewis NC, Day TA & Ainslie PN (2012). Regional brain blood flow in man during acute changes in arterial blood gases. *J Physiol* **590,** 3261–3275.

Willie CK, Smith KJ, Day TA, Ray LA, Lewis NCS, Bakker A, Macleod DB & Ainslie PN (2014*a*). Regional cerebral blood flow in humans at high altitude: gradual ascent and 2 wk at 5,050 m. *J Appl Physiol* **116,** 905–910.

Willie CK, Tzeng Y-C, Fisher JA & Ainslie PN (2014*b*). Integrative regulation of human brain blood flow. *J Physiol* **592,** 841–859.

Wilson MH, Edsell ME, Davagnanam I, Hirani SP, Martin DS, Levett DZ, Thornton JS, Golay X, Strycharczuk L, Newman SP, Montgomery HE, Grocott MP & Imray CH (2011). Cerebral artery dilatation maintains cerebral oxygenation at extreme altitude and in acute hypoxia-an ultrasound and MRI study. *J Cereb Blood Flow Metab* **31,** 2019–2029.

Winocur G & Gagnon S (1998). Glucose treatment attenuates spatial learning and memory deficits of aged rats on tests of hippocampal function. *Neurobiol Aging* **19,** 233–241.

Winocur G, Greenwood CE, Piroli GG, Grillo CA, Reznikov LR, Reagan LP & Mcewen BS (2005). Memory Impairment in Obese Zucker Rats: An Investigation of Cognitive Function in an Animal Model of Insulin Resistance and Obesity. *Behav Neurosci* **119,** 1389–1395.

de Wit C, Schäfer C, von Bismarck P, Bolz S-S & Pohl U (1997). Elevation of plasma viscosity induces sustained NO-mediated dilation in the hamster cremaster microcirculation in vivo. *Pflugers Arch Eur J Physiol* **434,** 354–361.

Yates KF, Sweat V, Yau PL, Turchiano MM & Convit A (2012). Impact of metabolic syndrome on cognition and brain: A selected review of the literature. *Arterioscler Thromb Vasc Biol* **32,** 2060–2067.

Yokota A, Gamoh S, Tanaka-Totoribe N, Shiba T, Kuwabara M, Nakamura E, Hayase T,

Hisa H, Nakamura K & Yamamoto R (2016). Angiotensin II, as well as 5-hydroxytriptamine, is a potent vasospasm inducer of saphenous vein graft for coronary artery bypass grafting in patients with diabetes mellitus. *Biochem Biophys Reports* **6,** 82–87.

Yu YN, Li M-L, Xu Y-Y, Meng Y, Trieu H, Villablanca JP, Gao S, Feng F, Liebeskind DS & Xu W-H (2018). Middle cerebral artery geometric features are associated with plaque distribution and stroke. *Neurology* **00,** 1–10.

Appendices

Appendix 1: Normalization analysis: automatic selection from HKG Panel

Groups	Samples	Actb	Rplp1	Ldha	Hprt1	B2m	Geometric Mean	Average Geometric Mean
Control Group	LZR1	17.48	18.97	20.72	20.95	19.61	19.50	19.61
Control Group	LZR2	17.85	18.91	21.01	21.34	19.70	19.72	
Control Group	LZR3	17.59	19.10	20.67	21.21	19.89	19.65	
Control Group	LZR4	17.57	19.10	20.54	20.99	19.82	19.57	
Group 1	OZR7	17.64	19.19	20.69	21.17	20.23	19.74	19.68
Group 1	OZR8	17.96	19.38	21.45	21.78	19.70	20.00	
Group 1	OZR9	17.98	18.92	20.76	20.83	19.56	19.58	
Group 1	OZR10	17.35	18.75	20.84	20.96	19.27	19.39	

In the Automatic Selection from HKG Panel method, the software automatically selected the listed optimal set of housekeeping / reference genes with the most stable expression across the Samples based on the results of the PCR Array's housekeeping / reference gene set. The geometric mean of the genes' assays' data was used as the normalization factor.

Appendix 2: Genes over-expressed in OZR vs LZR

Position	Gene Symbol	Fold Regulation	p-Value	Comments	RT² qPCR Assay Catalog #
A03	Agt	1.21	0.317886		PPR43580A
A04	Agtr1b	1.10	0.573063	B	PPR44499A
A05	Angpt1	1.25	0.298240		PPR57511C
A12	Casp1	1.10	0.163435		PPR06427A
B01	Casp3	1.10	0.463398		PPR06384B
B04	Ccl5	1.21	0.400732		PPR06854F
B07	Col18a1	1.11	0.470221		PPR45565A
B09	Cxcl1	1.18	0.876882	B	PPR06663A
B11	Cxcr5	1.67	0.003089		PPR06524A
C01	Edn2	1.74	0.185719	B	PPR44969B
C02	Ednra	1.29	0.251393		PPR45119A
C06	Fas	1.21	0.239055		PPR47870F
C08	Fgf1	1.81	0.135555		PPR06631C
D05	Il3	9.46	0.150014	B	PPR06385A
D06	Il6	1.36	0.231956	B	PPR06483B
E02	Mmp1	3.46	0.295453	B	PPR52149A
E04	Mmp9	1.11	0.590681		PPR44728C
E06	Nppb	1.24	0.672689	B	PPR43251A
E07	Npr1	1.25	0.419813		PPR57579A
E11	Pf4	2.06	0.009704		PPR06698A
E12	Pgf	1.12	0.342771		PPR43735A
F02	Plau	1.55	0.167521	A	PPR43507F
F04	Ptgis	1.41	0.214316		PPR51929B
G04	Thbs1	1.42	0.268712		PPR63321D
G07	Tnfsf10	1.12	0.431657		PPR06735B
G11	Vwf	1.15	0.378679		PPR48855B
G12	Xdh	1.59	0.040661		PPR44571F

Appendix 3: Genes under-expressed in OZR vs LZR

Position	Gene Symbol	Fold Regulation	p-Value	Comments	RT² qPCR Assay Catalog #
A02	Adam17	-1.21	0.233619		PPR06414A
A06	Anxa5	-1.12	0.035680		PPR43047A
A07	Apoe	-1.19	0.134939		PPR48524A
A10	Bcl2l1	-1.12	0.496529		PPR06491A
A11	Calca	-1.24	0.458700		PPR52808B
B03	Ccl2	-1.10	0.572092	A	PPR06714B
B08	Cx3cl1	-1.17	0.410493		PPR06433F
C03	Eng	-1.17	0.304149		PPR57754B
D04	Il1b	-1.21	0.532942	A	PPR06480B
D12	Kdr	-1.13	0.607145		PPR06671F
E09	Pdgfra	-1.11	0.365687		PPR06696A
F05	Ptgs2	-1.82	0.017020		PPR49747F
F07	Sele	-1.23	0.630772	B	PPR44808A
F09	Selp	-5.87	0.692473	B	PPR44614E
F12	Tek	-1.11	0.524279		PPR44285B
G06	Tnf	-1.48	0.001417		PPR06411F
G09	Vcam1	-1.12	0.497575		PPR45334A

Appendix 4: Curve fits used for vascular reactivity statistical comparison

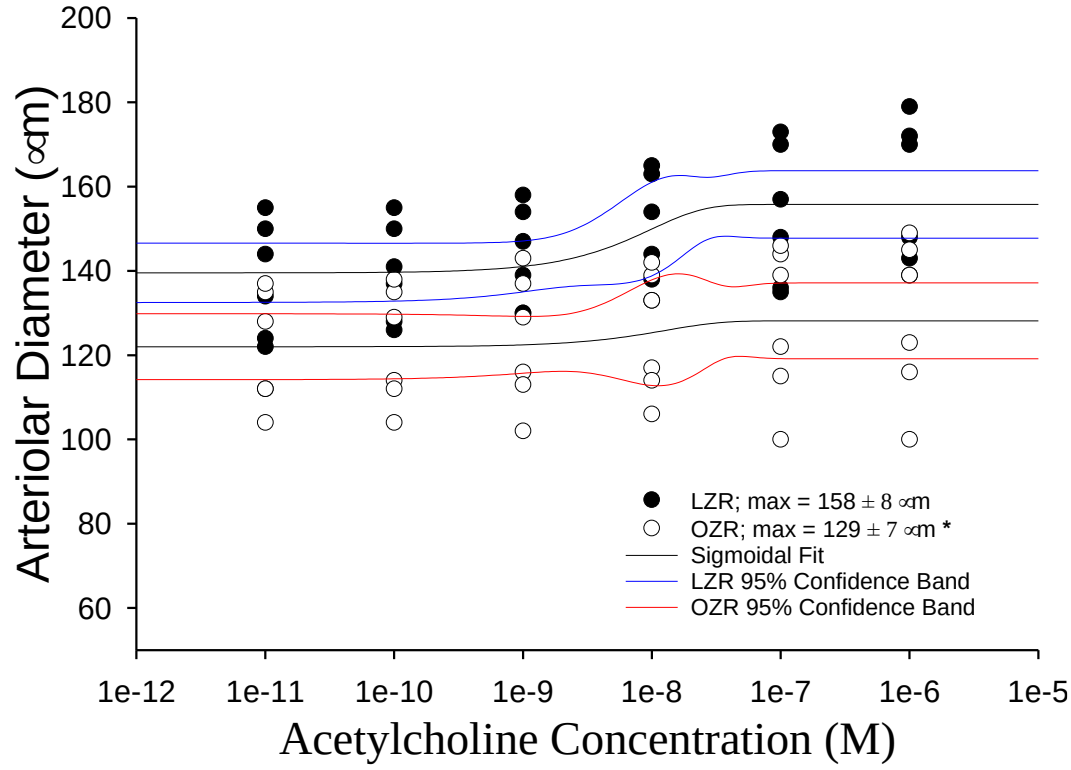

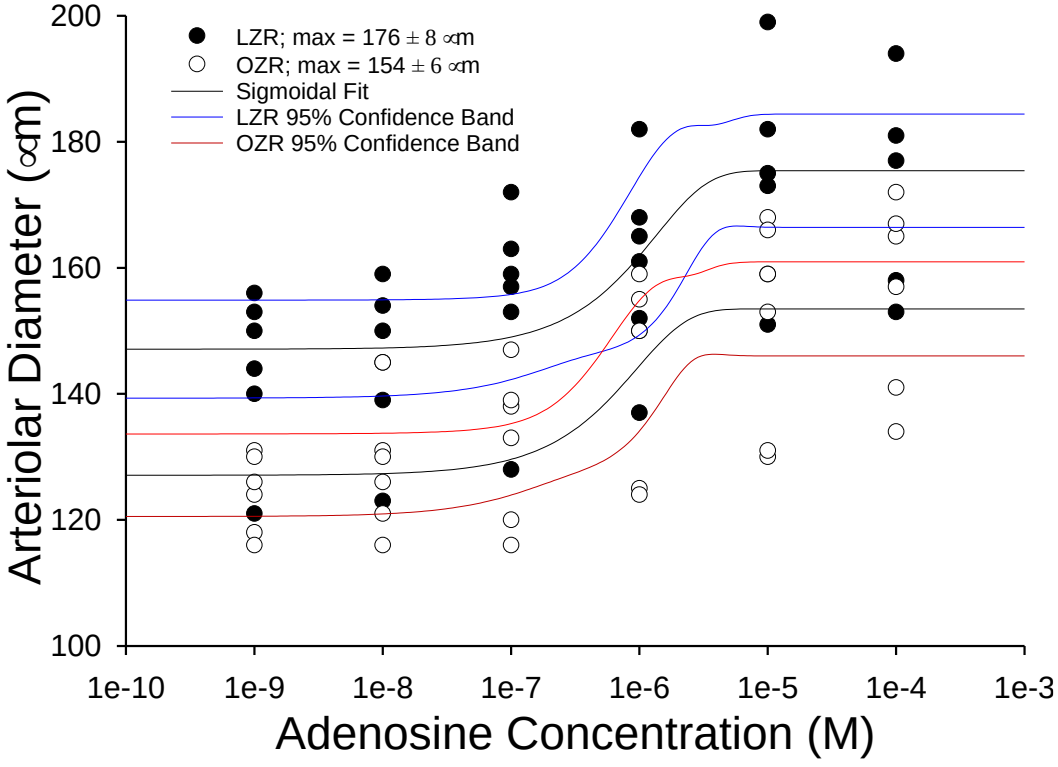

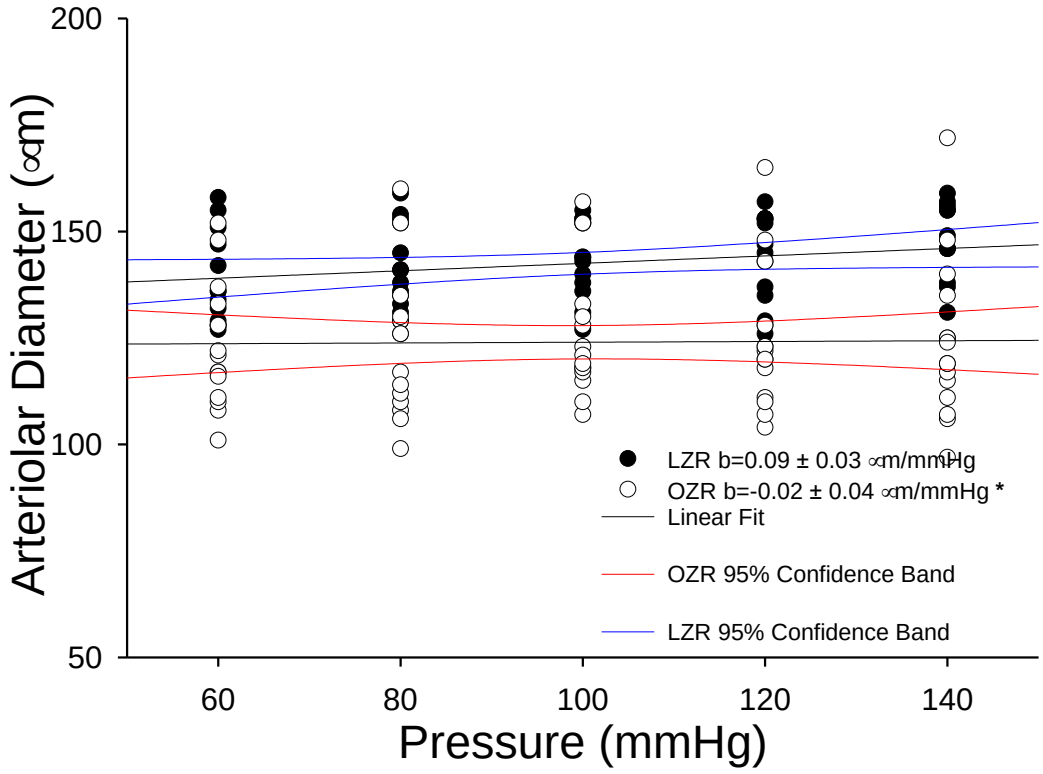
200
150
100
50
Arteriolar Diameter (∝m)
60
80
100
120
140
Pressure (mmHg)
LZR b=0.09 ± 0.03 ∝m/mmHg
OZR b=-0.02 ± 0.04 ∝m/mmHg *
Linear Fit
OZR 95% Confidence Band
LZR 95% Confidence Band

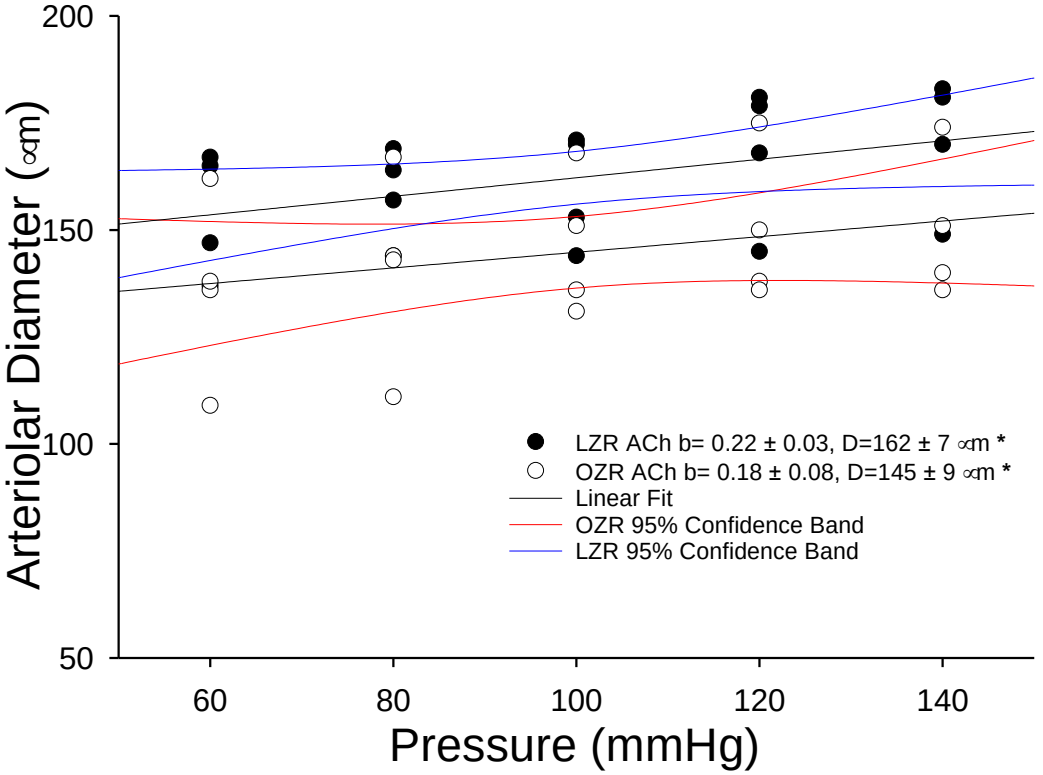
200
150
100
50
Arteriolar Diameter (∝m)
60
80
100
120
140
Pressure (mmHg)
LZR ACh b= 0.22 ± 0.03, D=162 ± 7 ∝m *
OZR ACh b= 0.18 ± 0.08, D=145 ± 9 ∝m *
Linear Fit
OZR 95% Confidence Band
LZR 95% Confidence Band

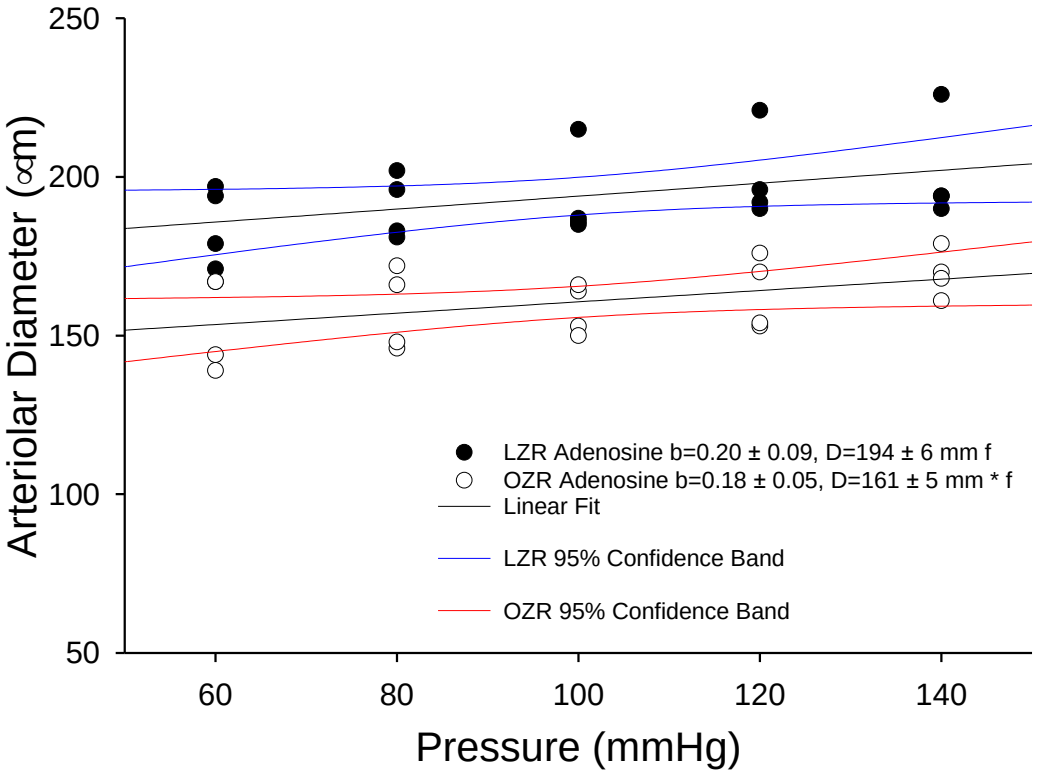
250
200
150
100
50
Arteriolar Diameter (∝m)
60
80
100
120
140
Pressure (mmHg)
LZR Adenosine b=0.20 ± 0.09, D=194 ± 6 mm f
OZR Adenosine b=0.18 ± 0.05, D=161 ± 5 mm * f
Linear Fit
LZR 95% Confidence Band
OZR 95% Confidence Band

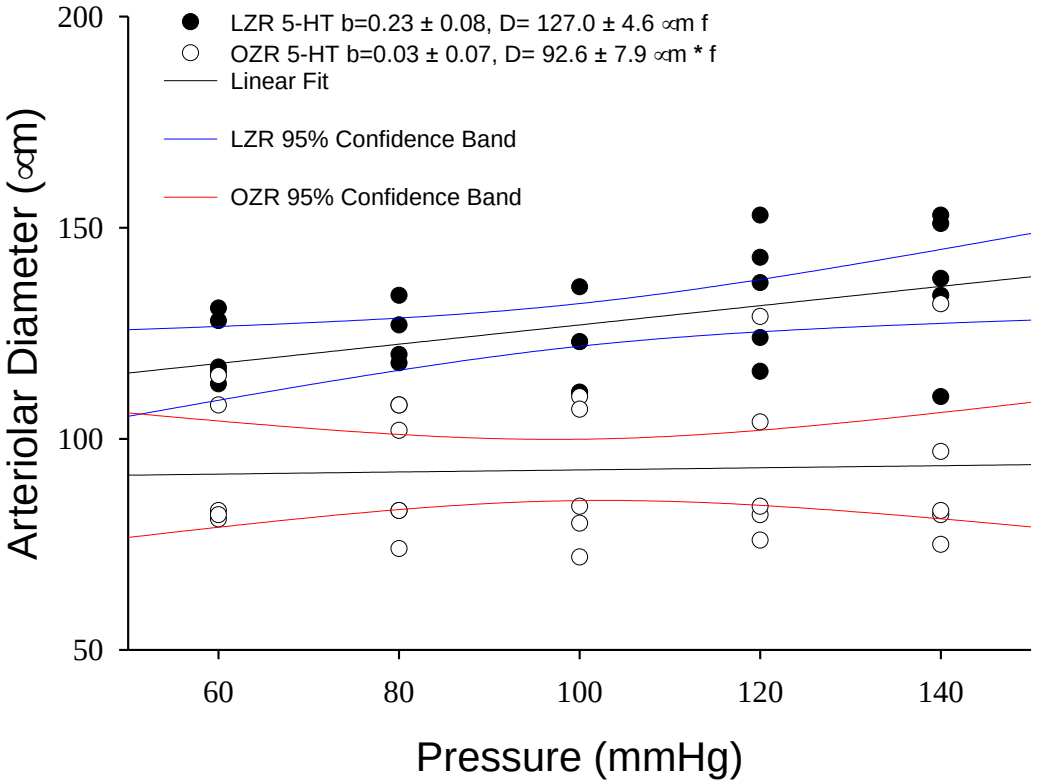
200
150
100
50
Arteriolar Diameter (∝m)
60
80
100
120
140
Pressure (mmHg)
LZR 5-HT b=0.23 ± 0.08, D= 127.0 ± 4.6 ∝m f
OZR 5-HT b=0.03 ± 0.07, D= 92.6 ± 7.9 ∝m * f
Linear Fit
LZR 95% Confidence Band
OZR 95% Confidence Band

Appendix 5: Animal Use Protocol

PI :	Frisbee, Jefferson
Protocol #	2017-029
Status :	Approved (w/o Stipulation)
Approved :	09/01/2017
Expires :	09/01/2021
Title :	Vascular Dysfunction with Elevated CVD Risk

Table of Contents

Animal Holding/Housing and Use Location Information

Animal Holding within Extra Vivarial Spaces (EVSs)

Acclimatization Period & Quarantine

Veterinary Drugs

Experimental Agents Information

SOP List

Procedures Checklist for Reporting and Training

Procedures Narrative

Procedural Consequences & Monitoring

Endpoint Method Information

Animal Numbers Requested

Protocol Attachments

Protocol Introduction

The questions on this page activate specific sections within the AUP form.

Note that species selection is part of this introductory page

Does this AUP involve teaching?

Yes ○ No ◉

Is the animal work on this project shared by another Animal Care Committee?

Yes ○ No ◉

Will you be using hazards?

Yes ◉ No ○

Will live animals be moved outside of their housing facility?

Yes ◉ No ○

Will field studies be conducted?

Yes ○ No ◉

Add/Update/Remove Species Used on this Protocol

Species	Agents	Drugs	Restraint	Breeding
Rat	Yes	Yes	No	No

Animal Use Protocol Overview

Animal Use Protocol Title

Vascular Dysfunction with Elevated CVD Risk

Application Type. If this is a post-pilot project, please attach the Pilot Report to this section, below.

New

Provide Associated Previous Protocol Number

Please provide a report detailing the previous AUP's use of Animals

Replacement: rodent models of elevated CVD risk have long been considered to be the gold standard for biomedical research and represent the optimal species from the perspective of replacement. There are no other "simpler" models that would be appropriate and there are no models or simulations that can be substituted appropriately.

Reduction: based on our extensive experience with these species and models, this is the minimum number of animal usage to satisfactorily address the hypotheses and aims of the project. In fact, we have developed a "parallel use" infrastructure in the laboratory to get maximum possible information from any individual animal in an attempt to use as few animals as possible.

Refinement: all techniques are well established and the PI is considered to be expert in each of them. There is no further refinement that is possible while still adequately addressing the experimental questions proposed.

Using non-scientific language, please describe the project's purpose, expected benefit, and a brief summary of your work with the animal model(s).

Public health research has identified that the presence of chronic stress and clinical depression is a severe risk factor for poor health outcomes, particularly with regard to cardiovascular disease. For future treatment, it is important that we acquire an accurate understanding of how chronic stress/depression causes poor cardiovascular health. The most appropriate rodent model for the effects of chronic stress/depression is 'Unpredictable Chronic Mild Stress' (UCMS), as it causes the animals to show all of the major symptoms of human clinical depression. We will expose rats and mice to the UCMS protocol and will determine its impact on depressive symptom severity and on

vascular function (which is the start of overt cardiovascular disease). While the UCMS protocol is neither painful nor requires restraint, it is based on a chronic, unpredictable change in their environment to cause constant stress. This can include altering light/dark cycles, the temporary use of wet bedding, cage tilts, etc. Both genders will be used as female rodents appear to be better protected (versus males) from vascular problems despite greater susceptibility to the UCMS protocol. The reasons for this protection are unknown and require investigation. The major benefits from this research effort will be the determination of how chronic stress/depressive symptoms causes vascular problems (providing guidance for how we can prevent this) and why females are protected from vascular problems in a way that males are not (also providing insight for future treatments).

It is important to emphasize that we are NOT measuring depression. "Depression" is a clinical diagnosis that cannot be applied to animal research. We are measuring "depressive symptoms" (as outlined above) as a model for the human condition. We use the UCMS model as this has been highly effective in behavioral and metabolic research to mimic the human condition.

Further, we are not measuring "cardiovascular disease", but are measuring vascular dysfunction as a contributing element for cardiovascular disease risk. "CVD" is a clinical condition and should not be applied to animals. Vascular dysfunction (measured as outlined in the proposal) is a contributing factor to CVD, but should not be considered as CVD itself -it is a condition that increases the risk for developing the overt pathology.

GLOSSARY OF TERMS - Identify each individual scientific term and abbreviation using *CAPITAL LETTERS*, and then briefly define each term to be referenced in any section of this protocol.

e.g. ALLELE - The genetic variant of a gene responsible for the different traits of certain characteristics and genetic diseases.

UCMS - Unpredictable Chronic Mild Stress

Here is the link to CCAC's Policy on Scientific Merit and Ethical Review of Animal-based Research:

http://www.ccac.ca/Documents/Standards/Policies/Scientific_merit_and_ethical_review_of_animal-based_research.pdf (http://www.ccac.ca/Documents/Standards/Policies/Scientific_merit_and_ethical_review_of_animal-based_research.pdf) **Has the work outlined in this AUP received favourable scientific peer review?**

Yes ○ No ◉

Do you wish to provide a funding peer review assessment, which may be considered in lieu of internal scientific peer review? If 'YES', please attach the funding assessment.

Yes ○ No ◉

If this is a RESEARCH AUP, please provide a list of one to three publications relevant to the work outlined in this AUP.

1: Frisbee JC, Brooks SD, Stanley SC, d'Audiffret AC. An Unpredictable Chronic Mild Stress Protocol for Instigating Depressive Symptoms, Behavioral Changes and Negative Health Outcomes in Rodents. J Vis Exp. 2015 Dec 2;(106). doi:

10.3791/53109. PubMed PMID: 26650668.

2: Stanley SC, Brooks SD, Butcher JT, d'Audiffret AC, Frisbee SJ, Frisbee JC. Protective effect of sex on chronic stress- and depressive behavior-induced vascular dysfunction in BALB/cJ mice. J Appl Physiol (1985). 2014 Nov 1;117(9):959-70. doi:

10.1152/japplphysiol.00537.2014. Epub 2014 Aug 14. PubMed PMID: 25123201; PubMed Central PMCID: PMC4217050.

3: d'Audiffret AC, Frisbee SJ, Stapleton PA, Goodwill AG, Isingrini E, Frisbee JC. Depressive behavior and vascular dysfunction: a link between clinical depression and vascular disease? J Appl Physiol (1985). 2010 May;108(5):1041-51. doi: 10.1152/japplphysiol.01440.2009. Epub 2010 Feb 18. PubMed PMID: 20167667; PubMed Central PMCID: PMC2867547.

++++++++++++++++++++++++++++

The most concise outline would be provided in reference #1 above, a peer-reviewed publication with describes all stages to the protocol, the applications, rationale, objectives, etc. This reference is also associated with an on-line video that fully describes all aspects of the protocol. In brief:

Background: the UCMS protocol is based in the recognition that many conditions of depression are associated with an environment of chronic stressors that cannot be accommodated or predicted. This results in behavioral, endocrine and inflammatory alterations to the animal that are highly comparable to that in the human subject. One of the health outcomes associated with chronic depressive states in both humans and animal subjects is elevated CVD risk and the development of states of overt CVD and vascular failure. One of the striking previous observations from our group is that female rodents, while suffering the depressive symptoms more severely, are protected from the vasculopathy as compared to responses in males. The purpose of the present studies is to determine the basis of this protection and how it can be used to improve future therapuetic approaches to treating health and disease.

Rationale: Animal models experiencing UCMS develop depressive symptoms that are very similar to those determined in human subjects dealing with chronic depression in terms of their behavioral responses, alterations to endocrine profiles, systemic patterns of inflammatory biomarkers, etc. They also develop overt vasculopathies that are extremely consistent with those determined in human subjects as well, and demonstrate the sex-disparity that has been long identified through public health data. These experiments will use rat models (of both sexes) to determine the impact of chronic unresolvable stresses on both behavioral outcomes as well as vascular (dys)function.

Hypotheses: the broad hypotheses of the proposal state that, when exposed to chronic unresolvable stresses in their environment, female rats, although suffereing the behavioral responses more severely than males, exhibit a protection to the vascular structure and function, and show a superior maintenance of organ perfusion. This is based in the anti-oxidant and anti-inflammatory defense afforded by circulating sex hormones.

Objectives: to determine the mechanistic bases of the sex-based protection in female as opposed to male rats subject to the unpredictable chronic mild stresses. This knowledge can then be used to better target interventional strategies to improve outcomes.

Experimental Procedures: please see reference #1 (above) for a full presentation of all procedures.

If this is a resarch AUP, attach an OUTLINE for scientific merit reviewers that provides sufficient information that another scientist working in the same field of study could effectively review this AUP's scientific merit, below. PIs may utilize whichever format best describes its scientific merit, e.g. background, rationale, hypothesis, objectives, experimental procedures

Using only key words, specify the animal models and procedures described within this AUP.

fundamental research, chronic, rat, chronic stress, behavioral tests, UCMS - Unpredictable Chronic Mild Stress model, euthanasia

Funding Source List

Fund Source Grant Holder	Grant Title	Funded?	Grant Number	Start Date
Internal Research Fund		Yes		/ /

Funding Source Name

Internal Research Fund

Proposal Title

Is this award currently funded?

Please provide the associated GRANT #

Funding START date *mm/dd/yy*

/ /

PI on Grant (if different than PI on Protocol)

Purpose of Animal Use

Identify PRIMARY purpose of

animal use 1-Fundamental Research

Hazardous Materials

Microorganism, Biological Agent or Hazardous Species Used?

Yes No

Institute Biosafety Committee #

Recombinant DNA or Viral Vector Directly into Animals Used?

Yes No

Experimental Agents or Veterinary Drug Used?

Yes No

Hazardous Chemicals Registration #

Nuclear Substance, Radiation, or Imaging Device Used?

Yes No

Radiation Permit #

Animal Movement Outside of Animal Facilities

Will live animals move to or from laboratory animal facilities or external sites?

Yes ○ No ◉

Will live animals leave the laboratory animal facility?

◉ ○

Yes No

Per area outside of Animal Facility, list the room #, the specific procedures to be performed per room, and justify why these procedures cannot be performed within an Animal Facility.

Animals will be aged/exposed to the UCMS procedures in the institutional vivarium. They will be removed from the vivarium ONLY for terminal usage as outlined in subsequent sections. This movement will be from the vivarium to the PI laboratory (MSB 496) and animals will not be returned to the vivarium.

Will either CW-443 Rodent Transport Containment Level 1, or CW-444 Non-Rodent Animal Transport be followed?

Yes ◉ No ○

Outline the method(s) used to transport animals between sites: Detail in chronological order the transfer route, including all Citywide 'Source' and 'Destination' sites, transport duration and frequency, and animal containment used.

Animal Groups and Experimental Timelines Overview

'C', 'D' and 'E'-level AUPs

Using simple diagrams the following must be attached:

- Animal Groups - names the animal groups (with unique identifiers) as well as the number of animals requested

and

- Experimental Timelines - names, in chronological order, ALL procedures that animals undergo (note that the description of each of these procedures is detailed in the *Procedure Narrative* section of the AUP

'B'-level AUPs

- Attach Animals Groups and Experimental Timeline diagrams as described above

Attach a document that describes the same information in paragraph format.

In the textbox below, please list file names of the most recent attachments

See attached 08.24.17

Please attach your Groups and Timelines documents above.

Rat Tissue Collection

Will live animals be used in this study?

Yes

Will this species be used exclusively for tissue collection?

Yes ○ No ◉

Justification for Choice of Species

Justify the choice of species by stating why a) this is the most appropriate species, and

b) a species lower on the phylogenic scale is not appropriate.

This model calls of chronic stress and CVD in rats. While rats and mice can be used in the UCMS protocol, rat models are well established and allow for a more sophisticated physiological and pharmacological interrogation than is possible for mice, with the added benefit that the study of non-atherosclerotic peripheral vascular disease is much more robust in rats than in mice. Additionally, the Obese Zucker rat strain is a well-established model of metabolic syndrome to the Lean Zucker background, allowing for the investigation of comorbid CVD on the effects of the stress protocol, stroke outcomes and efficacy of treatments.

the 3Rs: Replace, Reduce, Refine

The Three Rs concept originated from the scientific community and is a widely accepted cornerstone of policies on animal-based science around the world.

Ethical animal use requires consideration of animal welfare needs http://3rs.ccac.ca (http://3rs.ccac.ca)

Prior to any animal-based science, the 3 Rs should be considered.

Replacement refers to methods which avoid or replace the use of animals in an area where animals would otherwise have been used

Please show how you've considered the tenet of Replacement in your AUP.

For more information, please see Western's Alternative Use Guide (https://guides.lib.uwo.ca/animalalternatives).

Replacement Consideration

Replacement: rodent models of elevated CVD risk have long been considered to be the gold standard for biomedical research and represent the optimal species from the perspective of replacement. There are no other "simpler" models that would be appropriate and there are no models or simulations that can be substituted appropriately.

Reduction refers to any strategy that will result in fewer animals being used.

Please show how you've considered the tenet of Reduction in your AUP.

For more information, please see Western's Alternative Use Guide (https://guides.lib.uwo.ca/animalalternatives).

Reduction Consideration

Reduction: based on our extensive experience with these species and models, this is the minimum number of animal usage to satisfactorily address the hypotheses and aims of the project. In fact, we have developed a "parallel use" infrastructure in the laboratory to get maximum possible information from any individual animal in an attempt to use as few animals as possible.

Refinement refers to the modification of husbandry or experimental procedures to minimize pain and distress in your animals.

Please show how you've considered the tenet of Refinement in your AUP.

For more information, please see Western's Alternative Use Guide (https://guides.lib.uwo.ca/animalalternatives).

Refinement Consideration

Refinement: all techniques are well established and the PI is considered to be expert in each of them. There is no further refinement that is possible while still adequately addressing the experimental questions proposed.

Species Strains

Species Strain	Age/Weight	Vendor Stock#
Sprague Dawley	7-20 Weeks	Envigo
ZDF-Leprfa (lean)	7-20 Weeks	Envigo
ZDF-Leprfa (obese)	7-20 Weeks	Envigo
ZUC-Lepr^fa (lean)	200-350g	Charles River or Envigo
ZUC-Lepr^fa (obese)	300-700g	Charles River or Envigo

Strain Name

Sprague Dawley

Is this strain acquired commercially?

Yes (●) No ( )

Are the animals coming from a non-commercial source or another AUP?

Provide 'supplier name' and stock #, if available

Envigo

Age or weight at procurement

7-20 Weeks

Provide phenotype detail for non-genetically altered strains

Is this strain genetically altered?

Yes ( ) No (●)

If Genetically Altered Animals are COMMERCIALLY AVAILABLE, insert VENDOR STRAIN INFO URL.

If Genetically Altered Animals are from a NON-COMMERCIAL SOURCE, PROVIDE the Original Source of Animal(s)

Describe the NATURE of the genetic modification in heterozygous and homozygous animals. Identify the SYSTEMS AFFECTED and SPECIAL CARE required.

Strain Name

ZDF-Leprfa (lean)

Is this strain acquired commercially?

Yes (●) No ( )

Are the animals coming from a non-commercial source or another AUP?

Provide 'supplier name' and stock #, if available

Envigo

Age or weight at procurement

7-20 Weeks

Provide phenotype detail for non-genetically altered strains

Is this strain genetically altered?

Yes ( ) No (●)

If Genetically Altered Animals are COMMERCIALLY AVAILABLE, insert VENDOR STRAIN INFO URL.

If Genetically Altered Animals are from a NON-COMMERCIAL SOURCE, PROVIDE the Original Source of Animal(s)

Describe the NATURE of the genetic modification in heterozygous and homozygous animals. Identify the SYSTEMS AFFECTED and SPECIAL CARE required.

Strain Name

ZDF-Leprfa (obese)

Is this strain acquired commercially?

Yes (●) No ( )

Are the animals coming from a non-commercial source or another AUP?

Provide 'supplier name' and stock #, if available

Envigo

Age or weight at procurement

7-20 Weeks

Provide phenotype detail for non-genetically altered strains

Is this strain genetically altered?

Yes ○ No ◉

If Genetically Altered Animals are COMMERCIALLY AVAILABLE, insert VENDOR STRAIN INFO URL.

If Genetically Altered Animals are from a NON-COMMERCIAL SOURCE, PROVIDE the Original Source of Animal(s)

Describe the NATURE of the genetic modification in heterozygous and homozygous animals. Identify the SYSTEMS AFFECTED and SPECIAL CARE required.

Strain Name

ZUC-Lepr^fa (lean)

Is this strain acquired commercially?

Yes ◉ No ○

Are the animals coming from a non-commercial source or another AUP?

Provide 'supplier name' and stock #, if available

Charles River or Envigo

Age or weight at procurement

200-350g

Provide phenotype detail for non-genetically altered strains

Fawn Hooded background, male and females, these are the healthy control for the obese Zucker rat. **Is this strain genetically altered?**

Yes ○ No ◉

If Genetically Altered Animals are COMMERCIALLY AVAILABLE, insert VENDOR STRAIN INFO URL.

If Genetically Altered Animals are from a NON-COMMERCIAL SOURCE, PROVIDE the Original Source of Animal(s)

Describe the NATURE of the genetic modification in heterozygous and homozygous animals. Identify the SYSTEMS AFFECTED and SPECIAL CARE required.

Strain Name

ZUC-Lepr^fa (obese)

Is this strain acquired commercially?

Yes ◉ No ○

Are the animals coming from a non-commercial source or another AUP?

Provide 'supplier name' and stock #, if available

Charles River or Envigo

Age or weight at procurement

300-700g

Provide phenotype detail for non-genetically altered strains

This is the rat model for metabolic disease that we need to use moving forward. Severe leptin resistance, steady development of obesity, insulin resistance (leading to T2DM), dyslipidemia and hypertension. Based on the Fawn Hooded parental strain, the OZR still has the similar coat appearance. We need both males and females over the course of the protocol. Thanks.

Is this strain genetically altered?

Yes ○ No ◉

If Genetically Altered Animals are COMMERCIALLY AVAILABLE, insert VENDOR STRAIN INFO URL.

If Genetically Altered Animals are from a NON-COMMERCIAL SOURCE, PROVIDE the Original Source of Animal(s)

Describe the NATURE of the genetic modification in heterozygous and homozygous animals. Identify the SYSTEMS AFFECTED and SPECIAL CARE required.

Animal Transfers

Will animals originate from a DIFFERENT CITYWIDE PROTOCOL NUMBER?

Yes ○ No ◉

Are any animals being transferred from another AUP that have previous use?

Yes ○ No ◉

List AUP number and PI name from which animals will be transferred

Describe the previous use of animals sourced from different citywide AUPs.

Environmental Enrichment

Will all animals be group housed?

Yes ○ No ◉

Justify why group housing is not planned and specify which experimental animals will be singely housed

Animals in the UCMS protocol must be single housed to prevent social support (which would defeat the purpose of the protocol). This is the only modification necessary.

May Animal Care staff provide ENVIRONMENTAL ENRICHMENT to all animals of this species, as per its facility-specific Environmental Enrichment SOPs?

Yes ○ No ◉

May FOOD TREATS be given to all animals of this species by animal care staff as per its facility-specific Environmental Enrichment SOPs?

Yes ○ No ◉

Explain why additional enrichment and/or food treats may not be provided by Animal Care staff

This protocol requires chronic stress to be successful. Food treats and environmental enrichment undermine this for the UCMS animals.

Will any animals of this species undergo fasting at any point in the project?

Yes (●) No ( )

Provide justification and duration of fasting.

Simple overnight fast prior to final usage to ensure data quality and to consistently assess endocrine status at time of tissue harvest.

Trainees from the PIs laboratory will remove food at 8PM on the day prior to final animal usage. Rats will still retain access to water during this period, and yes - only bedding and water will be provided for the 12 hour period prior to usage. **If this species has other specialized caging, dietary or environmental requirements that you wish the animal facility manager(s) to be aware of, please identify them here.**

.

Animal Holding/Housing and Use Location Information

Location/Building	Room	Type
*Health Sciences Animal Care Facility	*Housing Room	HOUSING

Location/Building	Room	Type
*West Valley Animal Care Facility	*Housing Room	HOUSING
MEDICAL SCIENCES - OTHER	498	USE

ANIMAL LOCATION

*Health Sciences Animal Care Facility *Housing Room

Location Type

HOUSING

Identify the Procedure Location PURPOSE

ANIMAL LOCATION

*West Valley Animal Care Facility *Housing Room

Location Type

HOUSING

Identify the Procedure Location PURPOSE

ANIMAL LOCATION

MEDICAL SCIENCES - OTHER 498

Location Type

USE

Identify the Procedure Location PURPOSE

Anesthesia;Blood Collection;Euthanasia;Non-recovery Surgery

Animal Holding within Extra Vivarial Spaces (EVSs)

Will animals be held outside a laboratory animal facility for more than 12 hours and/or overnight?

Yes ○ No ◉

Per EVS locattion, list the room #, the specific procedures to be performed per room, and justify why animals must be held outside an Animal Facility for more than 12 hours and/or overnight.

Per area, provide the maximum duration and timeframe that live animals will be held, and estimate the number of cohorts anticipated per year.

Acclimatization Period & Quarantine

Will this species be held for the species-appropriate holding period prior to any form of USE, as per SOP 310?

Yes ◉ No ○

Provide Justification for this exemption

Will this species require quarantine?

Yes ○ No ◉

If quarantine requirements differ from the animal holding/housing facility's standard practice, please outline the requested QUARANTINE DETAIL.

Veterinary Drugs

Add all veterinary drugs to be used for therapeutic purposes in this AUP - planned veterinary treatments, e.g. anaesthesia, analgesia, post-op care, and euthanasia.

Note: Agents, materials, drugs and devices that are included in the experimental design of this AUP for this species should be added to the next **Experimental Agents** web page.

Drug	Dosage	Route of Administration	Frequency	Justification of Divergence	Pharma Grade
Alphachloralose					
Pentobarbital Sodium	40-60 mg/kg	IP;IV	1X initial anesthesia (IP), +10 mg/kg (IV or IP) as needed	No divergence	Yes
Urethane					

Drug Generic Name

Alpha-choloralose

Drug Type

Drug Dosage

Frequency of Administration

Route of Administration

Please justify any divergence from the standard dosage

Is this a Pharmaceutical Grade Drug?

Yes ○ No ○

Please justify the use of this drug and indicate how it is sterilized or determined to be pathogen-free.

Drug Generic Name

Pentobarbital Sodium

Drug Type

Drug Dosage

40-60 mg/kg

Frequency of Administration

1X initial anesthesia (IP), +10 mg/kg (IV or IP) as needed

Route of Administration

IP;IV

Please justify any divergence from the standard dosage

No divergence

Is this a Pharmaceutical Grade Drug?

Yes ◉ No ○

Please justify the use of this drug and indicate how it is sterilized or determined to be pathogen-free.

Drug Generic Name

Urethane

Drug Type

Anesthetic, Sedative

Drug Dosage

Frequency of Administration

Route of Administration

Please justify any divergence from the standard dosage

Is this a Pharmaceutical Grade Drug?

Yes No

Please justify the use of this drug and indicate how it is sterilized or determined to be pathogen-free.

Experimental Agents Information

Select all agents, materials, drugs and devices that are included in the experimental design of this AUP for this species.

Note: Veterinary drugs to be used for planned veterinary treatments, e.g. anaesthesia, analgesia, post-op care, and euthanasia, are to be included on the previous **Veterinary Drugs** web page.

Agent Name	Common /trade name	Class	Category	Pharma Grade
Urethane (ethyl Carbamate)	Urethane	Health Hazard (ghs) - Complete Safety Form	Chemical	Yes
Alpha-chloralose	Chloralose	Exempt From Safety Review	Chemical	Yes

Pentobarbital Sodium	Euthanyl	Controlled Drug, Exempt From Safety Review	Yes
		Pharmaceutical	

Agent

Urethane (ethyl Carbamate)

Category

Chemical

Common /trade name

Urethane

Concentration of agent

Dose administered

750mg/kg

Volume administered

As per animal weight

Route of Administration

IP

Other Route of Administration

Frequency of administration

Once, only used for terminal experiments

Will this agent be modified?

Yes ○ No ◉

Please list all modifications to the agent

Is this a Pharmaceutical Grade Agent?

Yes ◉ No ○

Please justify the use of this agent and indicate how it is sterilized or determined to be pathogen-free.

Agent

Alpha-chloralose

Category

Chemical

Common /trade name

Chloralose

Concentration of agent

Dose administered

80 mg/kg

Volume administered

As per animal weight

Route of Administration

IP

Frequency of administration

Once -used for terminal experiments only

Will this agent be modified?

Yes ○ No ◉

Please list all modifications to the agent

Is this a Pharmaceutical Grade Agent?

Yes ◉ No ○

Please justify the use of this agent and indicate how it is sterilized or determined to be pathogen-free.

Agent

Pentobarbital Sodium

Category

Pharmaceutical

Common /trade name

Euthanyl

Concentration of agent

240 mg/ml

Dose administered

50 mg/kg

Volume administered

50 mg/kg concentration (between 0.3-0.7 ml total volume)

Route of Administration

IP;IV

Other Route of Administration

Frequency of administration

1X initially (50 mg/ kg, IP), +
10mg/kg IP or IV as needed **Will this agent be modified?**

Yes ○ No ◉

Please list all modifications to the agent

Is this a Pharmaceutical Grade Agent?

Yes ◉ No ○

Please justify the use of this agent and indicate how it is sterilized or determined to be pathogen-free.

Please attach all requested documentation, as applicable, including:

Hazardous Materials Safety Questions Documents - If the classification of the agent selected requires it, please fill out and append the appropriate safety review sheet:

- Biological (http://www.uwo.ca/animal-research/doc/biological-questions.doc)
- Chemical/Pharmaceutical (http://www.uwo.ca/animal-research/doc/chem-pharm-questions.doc)

Imaging & Laser (http://www.uwo.ca/animal-research/doc/imaging-laser-questions.doc)

Nuclear/Radiation (http://www.uwo.ca/animal-research/doc/nuclear-radiation-questions.doc)

Material Safety Data Sheet (MSDS) or Equivalent - Occupational Health & Safety requires that you attach the current MSDS for each newly added agent as this is an essential element of safety review.

SOP List

Add all Standard Operating Procedures that will be followed within this AUP.

Go to the ACVS SOPs web page for SOP details - http://uwo.ca/animal-research/sops/index.html (http://uwo.ca/animalresearch/sops/index.html)

SOP Name	Divergences
Cln-310 - Holding Period Post-admission	

Select an SOP

Cln-310 - Holding Period Post-admission

Are you following the SOP exactly?

Yes No

If you are not following the SOP exactly, please list and justify all divergences from the SOP

Procedures Checklist for Reporting and Training

Use the checklist below to identify all AUP elements to be used **with this species**. If none of the listed AUP elements pertain to this species, select *Not Applicable.

Entries selected here will be linked to other AUP pages, including Personnel Training Requirements and the eSirius Training Module where animal user training records are maintained. Therefore, please ensure that this list is complete. **Procedure Name**

06. Injections - Ip

17. Anesthetics - Injectable

20. Surgery - Non-recovery

I. Behavioral Testing

Procedures Narrative

In view of the live animal activities identified within this AUP and listed below, provide a concise description of the procedural events identified within the **Groups and Timelines** page associated with this specific species.

The intent is to name and briefly describe the procedural events and associate them with each experimental group within this species.

Specific detail pertaining to drug dosage, monitoring, euthanasia/endpoint method, breeding, and physical restraint methods have been captured within other AUP sections, so they do not need to be described in detail here.

Species	**Description**

Use the following formatting method to complete **each procedure listed** within this section:

1. **Bold Font for Procedure Name - e.g. Anesthesia**
2. *Italicized Font for Group Identifiers - e.g. Groups 1, 2, and 6*

3. Regular Font for Procedure Description - e.g. Animals will be placed in a clean cage for transport to the OR

Please note that the AUP will be returned for updates if this section does not align with the above formatting method.

Procedures Narrative

Unpredictable Chronic Mild Stress Procedure

UCMS

Control animals will be maintained in their home cages at all times, while UCMS groups will be exposed to the series of challenges within that protocol. All stressors will be imposed during the working day and, unless specifically noted, will be terminated by 5PM. At that point, the animals will be returned to a normal home cage with fresh bedding overnight. The earliest a new stress will be applied is 8AM on the successive day. These stressors will be varied on a daily basis and will include: a. Damp bedding 10 oz. of water will be added to each standard cage for the next 3 hours. After this time, the wet bedding will be replaced with normal dry bedding until the stress protocol on the following day. This will use warm water (30 C) to minimize the potential for temperature problems. b. Water all bedding will removed and ~0.5 inches (rat) of water added to empty cage for the next 3 hours. To prevent the development of hypothermia, all water will be maintained at between 30-35 degrees C and animals will be briefly dried with a towel prior to placement back in cages with normal dry bedding. c. Each cage tilted to 45 degrees with or without bedding for 3 hours, and will be locked in place with a block and clamps. At the conclusion of this step, normal bedding will be replaced and the cage restored to its normal orientation. d. Social stress each rat is switched (i.e., replaced) into a cage of a neighboring animal for 3 hours. As this step involves replacing the animals in a cage with animals from neighboring cages, the potential for fighting is not present. This does NOT involve adding an animal from one cage into a different cage with the original animal still present. Animals will be returned to new cages with clean dry bedding after the 3 hour period. e. No bedding lasting for 3 hours or, on two occasions each week, overnight. Immediately following the 3 hour period or immediately following the overnight period (i.e., at 8AM), clean, dry bedding will be replaced into the cages. f. Alternating light/dark periods, lasting 30 minutes, for 8 hours, within a day. This will begin at 8AM during the day in question and terminate at 4PM on that same day, at which time the animal will be returned its normal light/dark cycle. g. Exposure to predator smells (e.g., tufts of fur, 10-20 ml urine from cats) added to the cage for 3 hours. Usually, this step is assisted by the veterinary/maintenance staff in the animal housing facility by a collection procedure from housed cats. At the conclusion of this exposure, fresh bedding will be replaced in the cage. If cat urine/fur are not available, this step in the UCMS protocol is generally eliminated.

Anesthesia

UCMS and Control (all animals)

Acute anesthesia via intraperitoneal injection of urethane/chlorolose OR pentobarbital sodium. Animals will be anesthetized for no more than 15-20 minutes prior to surgical tissue recovery. No ventilator will be used for these procedures. ***while this is essentially a very deep anesthesia followed by tissue harvest, we have elected to consider this as non-survival surgery in order to ensure full compliance for ourselves and the institution. Animals are terminated within 15 minutes of full anesthesia. ***we have utilized nembutal previously for our work and this amendment is to provide us with the ability to use it in the future. However, we request the flexibility of maintaining our use of urethane/chlorolose as well for novel collaborations here at Western.

Tissue Recovery

UCMS and Control (all animals)

While fully anesthetized, full tissue recovery will be performed. This will include blood, aorta and other vessels and heart, thus resulting in the death of the animal while deeply anesthetized.

Behavioral Testing and Analyses

UCMS and Control (all animals)

On a weekly basis, all animals will undergo a depressive symptom severity screening . In this, established indices of depressive symptoms in rodents will be evaluated. These tests include: a. Coat Status: This evaluation is done in the home cage. This evaluation is done weekly throughout the duration of the UCMS protocol. The total cumulative score is computed by giving an individual score of 0 (clean) or 1 (dirty) to eight body parts (head, neck, dorsal coat, ventral coat, tail, forelimb, hind-limb, and genital region). b. Splash Test: This test is done on iso pads to prevent bedding from adhering to the animal. This test is used to evaluate acute grooming behavior, defined as cleaning of the fur by licking or scratching. A 10% sucrose solution is sprayed on the dorsal coat of each rat and grooming activity was recorded for five minutes. The viscosity of the sucrose solution will dirty the coat and induce grooming behavior, with depressive symptoms characterized by an increased latency (idle time between spray and initiation of grooming) and decreased frequency (number of times grooming a particular body part). A. Locomotor activity: Locomotor activity will be measured as an index of the degree of symptom severity by neurological impairment using an automated activity monitoring system (San Diego Instruments, San Diego, CA). The rats will be given 30 60 min to acclimate to the testing room before being habituated to the testing chambers for an additional 30 min. Each testing chamber consists of two 16 16 photobeam arrays to detect movements of the animals. Ambulatory, fine, and rearing movements will be quantified to give an overall activity score. The animals will be returned to the testing chambers and their activity was quantified for the next 30 min. B. Elevated-plus Maze: The elevated-plus maze is well accepted for assessing anxiety-like behavior of rats and we will use this assay as described in the literature. The plus-maze consists of two open arms (50 cm x 10 m) and two enclosed arms (50 cm x 10 cm) with 30-cm high walls. The four arms meet at a central platform (10 cm x 10 cm) that opens to all arms, forming a + shape. The entire apparatus will be elevated 60 cm above the floor and surrounded by a padded surface. The apparatus will be illuminated with a ceiling lamp placed 90100 cm above the maze. The rat will be placed on the central platform facing an open arm. The number of entries and time spent in each of the arms will be recorded over a period of 5 minutes. Following testing, the rat will be placed back into its original cage.

Procedures

Behaviour Testing –

The current tests (outlined aboved) are used for assessing indices of chronic stress and depressive symptoms. While those are valuable, they really do not give much of an indication of cognitive impairments. The new tests (Morris Water Maze and Set Shifting) that will be performed with Dr. Whitehead's assistance will provide for a more robust understanding of the cognitive impairments that accompany the development of the metabolic syndrome. At present, we will only use these tests in control LZR and OZR (i.e., rats that have NOT undergone the UCMS procedures).

MORRIS WATER MAZE: Rats will be trained to swim to a platform in the spatial learning/working memory version of the Morris Water Maze, consisting of 4 trials/day for 4 consecutive days. Rats will then be subjected to two 30s probe trials where the platform is removed to assess rats spatial reference memory. To complete the task rats are placed in a circular pool (146cm diameter, 58cm high) and trained to escape from the water by swimming to a hidden platform. The water is maintained at a temperature of 21 1 C. Rats are allowed to swim in search of the platform for 90s. If the rat is unable to locate the platform in that time, they are guided to the platform and allowed to remain on it for 15s or 30s before being removed from the pool. If rats are not immediately re-introduced into the pool, they are dried off after each trial with a towel and then placed back in their cages and kept under a heat lamp to stay warm until their next trial (approximately 15-20 min). Following the final trial rats are toweled dry and kept in their cage under a heat lamp for 15 min before being returned to the animal housing facility. There is no food or weight restriction required for this test.

SET SHIFTING – Rats will be placed into an operant chamber box and will be trained to press a level corresponding to a light. A sucrose pellet will be released upon the correct choice. Up to 160 trials will be performed for each rat. A mild food restriction will be enacted to provide additional incentive to perform the task (please see food restriction details below).

Food Restriction for Set Shifting Behaviour -

Rats in both of these Animal Groups will be trained to perform an appetitive operant conditioning behavioural task which involves food pellet reinforcement. Thus, while housed in their home cage, these rats will be on a food-restricted diet as this is a well-established procedure to optimize behavioural performance. This food restriction involves a limited amount of food to be available to the animal throughout the day, instead of food being available for continuous consumption. To ensure that the animals remain healthy and that the food restriction is not excessive, at the end of each behavioural testing session (less than 2 hours per day), the animals will be weighed and provided with supplemental food to maintain body weight at greater than 85% of normal body weight (as per Principal Investigator’s recent publication, Schormans et al., Frontiers in Behavioral Neuroscience, 2017). Trainees will be informed that the goal is to maintain the food-restricted animals above this 85% level (e.g., ideally >90%), as this degree of weight reduction is the endpoint weight that guides our early euthanasia. Effort will be made to keep the rats at >90% of weight reduction as long as our outcomes (animals that are performing behavioral tasks) are achieved. Rats are maintained on this food-restricted diet up to a maximum of 14 days. Trainees will account for weekly weight gain in the rats so that they do not rely on using a single weight (15% less of the pre procedure weight) as their target or maximum allowable weight loss. Monitoring charts for the animals on food restriction include a column that addresses the "target weight". This is expected to change weekly as we know the animals will gain weight as they age. To that end, growth charts from the animal supplier will be used to gauge specified weight range as well as the animal’s short term running average weight.

Procedural Consequences & Monitoring

From both the project overview & detail perspectives, identify and describe specific procedural or other/combined elements of this AUP that may produce pain, distress, or impairment - and identify all possible consequences Behavioural, Physical, Biochemical, Physiological, and Reproductive - for this species.

The UCMS procedures, by definition, cause chronic stress to the animal. These are not painful, damaging or cause any impairment, they simple are chronic stresses to the system. The behavioral outcomes can include lack of movement, failure to groom, anhedonia, learned helplessness, among others. There should be no physical consequences. Biochemical and physiological consequences are consistent with chronic stress and metabolic disease and can include elevated cortisol, oxidant radicals, inflammatory biomarkers, etc. Reproductive consequences are not relevant for this protocol.

There may be a minor weight loss (or reduction to the rate of increase) for rats as a result of the food restriction prior to the behavioral testing. This is not expected to result in a loss of more than 3-5% of animal mass (at the most) and is anticipated that it will most likely result in no change in mass over the week. If weight loss (monitored daily) exceeds 5%, this will result in the immediate termination of the behavioral testing due to unanticipated impacts on behavioral, metabolic and cardiovascular outcomes.

Modification March 2019 - Morris Water Maze and Set Shifting

There will be no procedural consequences as a result of these tests, and they will not have any lasting impact on an animal prior to final usage

Detail relief to be provided for each of the above-stated potential consequences, and, if relief is not planned, offer scientific justification for not doing so.

There is no relief provided to the UCMS animals during the protocol, as this inherently undermines the purpose of the procedures.

As stated above, no relief is planned as impacts on weight are anticipated to be minimal, if present. However, if weight loss exceeds 5%, all procedures will be terminated and the animal will be returned to normal ad libitum diet.

The CCAC and OMAFRA require that all AUPs include:

- a 'Monitoring Plan' to minimize animal pain, distress, or discomfort, and a plan for 'Early Euthanasia' for the purpose of emergency intervention in advance of the experimental endpoint.

As per UCAC's *Animal Care and Use Records Policy*, http://uwo.ca/animal-research/doc/ACU_Records.pdf (http://uwo.ca/animal-research/doc/ACU_Records.pdf) Animal

Records, e.g. scoring sheets, procedure logs, anaesthetic and surgery records (except those involved in Field Studies) must be kept with the animals at all times.

Has a monitoring sheet used for determining interventions and early euthanasia endpoints been developed for this species, e.g. scoring sheets, anaesthetic record, surgery record. If YES, please attach the monitoring sheet(s) below.

If NO, please complete the following checklist

Yes ◉ No ○

Weight -*When checked, this indicates that weights will be recorded*

☑

Food/Water Intake

☐

Behaviour

☑

Fecal/Urine Output

☐

Body Condition Score

☑

Appearance

☐

Other Monitoring

☐

Please Specify Other Monitoring Type.

For every individual monitoring element checked above:

Describe the frequency, Specify the intervention points including criteria for early euthanasia, Provide other relevant detail. If attached monitoring sheets capture this information, then indicate this here.

Daily, if non healing wounds and injuries are present (even after treatment) animals will be euthanized. Body mass will be determined 3X/week, with appropriate end points. Lethargy and deteriorating grooming behavior will be assessed regularly (daily), although this is a part of the UCMS outcomes so must be assessed appropriately All other aspects will not result in early euthanasia as these can be outcomes of the procedures.

If an unforeseen animal welfare condition arises, we will discuss appropriate options with the vivarium staff/veterinarian. Please attach your monitoring sheets.

Endpoint Method Information

Endpoint Method

Drug-Agent Overdose

Endpoint Method

Drug-Agent Overdose

CCAC Classification

Acceptable

This method is conditionally acceptable. Please provide sufficient justification for using this method. Please note that conditionally acceptable methods may require additional training prior to use.

Provide Additional experimental endpoint detail, as required

Animals will be given an acute overdose of the urethane/chloralose anesthetic followed by a bilateral pneumothoracotomy and destruction of the heart to ensure euthanasia.

Provide endpoint detail for animals not euthanized

For endpoint methods selected above that use drugs, please list them below, and include the dosage.

Drug	Dosage

Drug	Dosage
	>200 mg/kg

Urethane	>1000 mg/kg

Animal Numbers Requested

With a view to the animal numbers disclosed on the **Groups and Timelines** web page, please provide your requested total four- and first-year animal numbers by Category of Invasiveness as well as justification for these numbers.

Please consider the activities selected for this species in the list below with a view to their combined impact upon an animal.

Species	Type	Description

Please select the top Category of Invasiveness for this species and, for AUPs containing breeding colonies, please separate these numbers into the 'Z' category.

Categories of Invasiveness – Levels assigned to AUPs in accordance with CCAC policy. Experiments involving:

- **B** - Little or no discomfort or stress
- **C** - Minor stress or pain of short duration
- **D** - Moderate to severe distress or discomfort
- **E** - Procedures causing severe pain at or above the pain tolerance threshold of unanaesthetized conscious animals

Z - Animals used for breeding purposes (internal letter designation to separate out breeding from research numbers - a CCAC requirement) For more detail go to the CCAC Website:

http://www.ccac.ca/en_/standards/policies/policy-categories_of_invasiveness (http://www.ccac.ca/en_/standards/policies/policy-categories_of_invasiveness)

CCAC Category	4 YR #	1st YR #
B	0	0
C	0	0
D	320	0

E	0	0
Z	0	0

Justification for Number of Animals Requested

Sample size has been determined based on historical numbers and experience based on animal phenotype, specific physiological outcome, and differences in health and disease outcomes. Additional numbers are included to determine mechanistic underpinnings of physiological observations. The numbers used are the minimum number required to provide for statistically validated outcomes.

https://www.dssresearch.com/KnowledgeCenter/toolkitcalculators/statisticalpowercalculators.aspx

These are determined based on two-tailed tests, with an alpha = 0.5, and 25% differences between groups.

Curriculum Vitae

Name: Brayden Davis Halvorson, BSc

Title: M.Sc. Graduate Student and Graduate Research Assistant, Department of Medical Biophysics University of Western Ontario; Schulich School of Medicine and Dentistry

Other Appointments: Graduate Research Assistant, Department of Medical Biophysics University of Western Ontario; Schulich School of Medicine and Dentistry

Birth Date Location: May 11, 1996; Thunder Bay, Ontario

Citizenship: Canada

Education:
2014-2018 University of Western Ontario B.Sc. (Honours Kinesiology, Scholar's Electives Program)
2018-present University of Western Ontario M.Sc. (Medical Biophysics) *Supervisor: Jefferson Frisbee*

Previous Academic Positions:
Pre-Graduate Student Researcher, Department of Medical Biophysics, University of Western Ontario
Cardiorespiratory Undergraduate Student Researcher, Canadian Centre for Activity and Aging, School of Kinesiology, University of Western Ontario
Community Engaged Learner, Middlesex County Department of Economic Development

Professional Society Memberships:
Microcirculation Society
American Physiological Society

Academic Honors and Professional Recognition:
Zweifach Student Travel Award, Microcirculatory Society ($475 USD) 2020
Alfred Jay Award for Cellular and Cardiovascular Research ($2 000) 2020
CIHR National Graduate Scholarship - Masters ($17 500) 2019-2020
Extraordinary Mustang Gala Award ($380) 2017
All-OUA Academic 2015-2018
Dean's Honor List 2014-2018
J. Howard Crocker School of Kinesiology Entrance Scholarship ($30 000) 2014-2018

PUBLICATION HISTORY

Book Chapters and Reviews:

Brayden Halvorson and Jefferson Frisbee (May 29th 2020). Cerebral Vascular Tone Regulation: Integration and Impact of Disease, Basic and Clinical Understanding of Microcirculation, Kaneez Fatima Shad, Seyed Soheil Saeedi Saravi and Nazar Luqman Bilgrami, IntechOpen, DOI: 10.5772/intechopen.90404. Available from: https://www.intechopen.com/books/basic-and-clinical-understanding-of-microcirculation/cerebral-vascular-tone-regulation-integration-and-impact-of-disease

Peer-Reviewed Manuscripts:

B.D. Halvorson, S.N. Whitehead, J.J. McGuire, J.C. Frisbee. Endothelium-dependent impairments to cerebral dilator reactivity with type II diabetes mellitus in the Goto-Kakizaki rat. *Am. J. Physiol. Reg. Integr. Comp. Physiol.* 317(1):R149-159, *2019*

J.C. Frisbee, **B.D. Halvorson**, M. T. Lewis, R.W. Wiseman. Shifted vascular optimization: the emergence of a new arteriolar behaviour with chronic metabolic disease. *Exp. Physiol.* (In Press)

Published Abstracts:

B.D. Halvorson, S.N. Whitehead, J.J. McGuire, J.C. Frisbee. Impaired Dilator Reactivity of Middle Cerebral Arteries in Goto-Kakizaki Rats with Type II Diabetes Mellitus. (Experimental Biology 2019)

J.C. Frisbee, **B.D. Halvorson**, M.T. Lewis, J.D. Kasper, P.D. Chantler, R.W. Wiseman. Type II Diabetes Mellitus In The Goto-Kakizaki Rat Impairs Microvascular Function And Contributes To Premature Skeletal Muscle Fatigue (Experimental Biology 2019)

B.D. Halvorson, J. Williamson, J.C. Frisbee. Myogenic Activation and Endothelial Function in Cerebral Arteries with Metabolic Disease: Is Increased Myogenic Tone Protective for the Endothelium? (Experimental Biology 2020)

B.D. Halvorson, S.N. Whitehead, J.C. Frisbee. Mild Cognitive Impairment in the Presence of Depressive Symptoms Related to Impaired Cerebrovascular Function in the Obese Zucker Rat. (Experimental Biology 2020)

Internal Poster Presentations:

B.D. Halvorson, S.N. Whitehead, J.J. McGuire, J.C. Frisbee. Impaired Dilator Reactivity of Middle Cerebral Arteries in Goto-Kakizaki Rats with Type II Diabetes Mellitus. (presented at London Health Research Day and Friends of Médecins Sans Frontières/Doctors Without Borders 2019)

Seminars

“Endothelium-dependent impairments to cerebral dilator reactivity with type II diabetes mellitus”. Department of Medical Biophysics, University of Western Ontario, London, ON, 2020